NUREG/CR-6810
SAND2003-0840P

Overpressurization Test of a 1:4-Scale Prestressed Concrete Containment Vessel Model

Sandia National Laboratories

U.S. Nuclear Regulatory Commission
Office of Nuclear Regulatory Research
Washington, DC 20555-0001

Nuclear Power Engineering Corporation
Tokyo 105, Japan

AVAILABILITY OF REFERENCE MATERIALS IN NRC PUBLICATIONS

NRC Reference Material

As of November 1999, you may electronically access NUREG-series publications and other NRC records at NRC's Public Electronic Reading Room at http://www.nrc.gov/reading-rm.html. Publicly released records include, to name a few, NUREG-series publications; *Federal Register* notices; applicant, licensee, and vendor documents and correspondence; NRC correspondence and internal memoranda; bulletins and information notices; inspection and investigative reports; licensee event reports; and Commission papers and their attachments.

NRC publications in the NUREG series, NRC regulations, and *Title 10, Energy*, in the Code of *Federal Regulations* may also be purchased from one of these two sources.

1. The Superintendent of Documents
   U.S. Government Printing Office
   Mail Stop SSOP
   Washington, DC 20402–0001
   Internet: bookstore.gpo.gov
   Telephone: 202-512-1800
   Fax: 202-512-2250
2. The National Technical Information Service
   Springfield, VA 22161–0002
   www.ntis.gov
   1–800–553–6847 or, locally, 703–605–6000

A single copy of each NRC draft report for comment is available free, to the extent of supply, upon written request as follows:

Address: Office of the Chief Information Officer,
Reproduction and Distribution
Services Section
U.S. Nuclear Regulatory Commission
Washington, DC 20555-0001
E-mail: DISTRIBUTION@nrc.gov
Facsimile: 301–415–2289

Some publications in the NUREG series that are posted at NRC's Web site address http://www.nrc.gov/reading-rm/doc-collections/nuregs are updated periodically and may differ from the last printed version. Although references to material found on a Web site bear the date the material was accessed, the material available on the date cited may subsequently be removed from the site.

Non-NRC Reference Material

Documents available from public and special technical libraries include all open literature items, such as books, journal articles, and transactions, *Federal Register* notices, Federal and State legislation, and congressional reports. Such documents as theses, dissertations, foreign reports and translations, and non-NRC conference proceedings may be purchased from their sponsoring organization.

Copies of industry codes and standards used in a substantive manner in the NRC regulatory process are maintained at—

The NRC Technical Library
Two White Flint North
11545 Rockville Pike
Rockville, MD 20852–2738

These standards are available in the library for reference use by the public. Codes and standards are usually copyrighted and may be purchased from the originating organization or, if they are American National Standards, from—

American National Standards Institute
11 West 42nd Street
New York, NY 10036–8002
www.ansi.org
212–642–4900

Legally binding regulatory requirements are stated only in laws; NRC regulations; licenses, including technical specifications; or orders, not in NUREG-series publications. The views expressed in contractor-prepared publications in this series are not necessarily those of the NRC.

The NUREG series comprises (1) technical and administrative reports and books prepared by the staff (NUREG–XXXX) or agency contractors (NUREG/CR–XXXX), (2) proceedings of conferences (NUREG/CP–XXXX), (3) reports resulting from international agreements (NUREG/IA–XXXX), (4) brochures (NUREG/BR–XXXX), and (5) compilations of legal decisions and orders of the Commission and Atomic and Safety Licensing Boards and of Directors' decisions under Section 2.206 of NRC's regulations (NUREG–0750).

NUREG/CR-6810
SAND2003-0840P

Overpressurization Test of a 1:4-Scale Prestressed Concrete Containment Vessel Model

Manuscript Completed: March 2003
Date Published: March 2003

Prepared by
M.F. Hessheimer, E.W. Klamerus,
L.D. Lambert, G.S. Rightley,
R.A. Dameron*

Sandia National Laboratories
Operated by Sandia Corporation for the
U.S. Department of Energy
Albuquerque, NM 87185

*ANATECH Corporation
5435 Oberlin Drive
San Diego, CA 92121

Prepared for

Nuclear Power Engineering Corporation
Systems Safety Department
Tokyo 105, Japan
under Fia DE-F104-91-AL73734

NUPEC Project Manager: S. Shibata

Division of Engineering Technology
Office of Nuclear Regulatory Research
U.S. Nuclear Regulatory Commission
Washington, DC 20555-0001
NRC Job Code Y6131

NRC Project Manager: J.F. Costello

ABSTRACT

The Nuclear Power Engineering Corporation (NUPEC) of Japan and the U.S. Nuclear Regulatory Commission (NRC), Office of Nuclear Regulatory Research, cosponsored and jointly funded a Cooperative Containment Research Program at Sandia National Laboratories (SNL) from July, 1991 through December, 2002. As part of this program, a 1:4 scale model of a prestressed concrete containment vessel (PCCV) was constructed and pressure tested to failure. The prototype for the model is the containment building of Unit 3 of the Ohi Nuclear Power Station in Japan. The design accident pressure, P_d, of both the prototype and the model is 0.39 MPa (57 psi). The objectives of the PCCV model test were to simulate some aspects of the severe accident loads on containment vessels, observe the model failure mechanisms, and obtain structural response data up to failure for comparison with analytical models.

The PCCV model was designed and constructed by NUPEC and its Japanese contractors, Mitsubishi Heavy Industries, Obayashi Corp., and Taisei Corp. SNL designed and installed the instrumentation and data acquisitions systems and conducted the overpressurization tests. ANATECH Consulting Engineers conducted the pre- and posttest analyses of the model under contract to SNL.

Nearly 1500 transducers were installed on the PCCV model to monitor displacements, liner, rebar, concrete and tendon strains and tendon anchor forces. This instrumentation suite was augmented by the Soundprint® acoustic monitoring system, video, and still photography.

Low pressure testing, including a Structural Integrity Test to 1.125 P_d, and an Integrated Leak Rate Test at 0.9 P_d, was conducted in September, 2000. The Limit State Test (LST) of the model was conducted on September 27-28, 2000 by slowly pressurizing the model using nitrogen gas. A leak, presumably through a tear in the liner, was first detected at a pressure of 2.5 P_d and a leak rate of 1.5% mass/day was estimated. The test was terminated when the model reached a pressure of 3.3 P_d. At this pressure, the leak rate was nearly 1000% mass/day, exceeding the capacity of the pressurization system. Posttest inspections revealed 26 tears in the 1.6mm (1/16") steel liner as the source of the leaks.

Since only limited damage and inelastic response occurred during the LST, the interior was resealed with an elastomeric membrane. The PCCV was then filled nearly full with water and repressurized on November 14, 2001. This Structural Failure Mode Test reached a maximum pressure of 3.6 P_d when the model ruptured violently by failure of the prestressing tendons and then the reinforcing steel.

The resulting data from all the tests are provided for comparison with pretest and posttest analyses.

CONTENTS

FIGURES

TABLES

EXECUTIVE SUMMARY

Introduction

The Nuclear Power Engineering Corporation (NUPEC) of Japan and the U.S. Nuclear Regulatory Commission (NRC), Office of Nuclear Regulatory Research co-sponsored and jointly funded a cooperative containment research program at Sandia National Laboratories[1] (SNL). Tests of two containment models were authorized under this program. The first model, a mixed-scale model of an Improved Mark-II type steel containment vessel (SCV) for a Boiling Water Reactor (BWR), was tested in December 1996. The second model tested was a 1:4-scale model of the prestressed concrete containment vessel (PCCV) of an actual nuclear power plant in Japan, Ohi-3. Ohi-3 is an 1127 MWe Pressurized Water Reactor (PWR) unit, one of four units comprising the Ohi Nuclear Power station located in Fukui Prefecture, owned and operated by Kansai Electric Power Company. The scale of the PCCV model was a uniform 1:4, with minor exceptions to accommodate fabrication and construction concerns. This was judged to be the minimum scale that would allow the steel liner to be constructed from prototypical materials and fabricated with details and procedures that were representative of the prototype.

By definition, the scope of this program was limited to addressing the capacity of containment vessels to loads beyond the design basis, the so-called severe accident loads. Design accident loads for light water reactor containment vessels are typically based on the loss-of-coolant accident (LOCA) and are defined by bounding pressure and temperature transients. The design accident pressure, P_d, of both the prototype and the model is 0.39 MPa (57 psi). The term "severe accidents" is used to describe an array of conditions that could result in loads, in excess of the design basis loads, on the containment. The definition of severe accident loads, which is not as rigorous as the design basis loads definition, results from a consideration of various postulated failure scenarios of the primary nuclear system, up to and including a complete core meltdown and breach of the reactor pressure vessel. The resulting pressure and thermal loading characteristics depend on the unique features of the nuclear steam supply (NSS) system and the containment structure in addition to the postulated accident.

For this test program, it was necessary to decide whether both thermal and pressure loads would be applied to the model, either separately or simultaneously, what the pressurization medium should be, and whether the transient characteristics of these loads should be considered. Programmatically, the decision to perform a *static pneumatic* overpressurization test at *ambient temperature* was dictated by risk and cost considerations and previous experience.

Design and Construction

Within the cooperative framework agreed on by NUPEC and the NRC, NUPEC and its Japanese contractors designed and constructed the PCCV model at SNL's Containment Technology Test Facility-West (CTTF-W). This test facility was specially constructed by SNL on land temporarily permitted for this purpose on Kirtland Air Force Base (KAFB), Albuquerque, New Mexico, USA. The prime contractor to NUPEC for the construction of the PCCV model was Mitsubishi Heavy Industries (MHI), who also designed and constructed the prototype plant, Ohi-3. In addition to overall design and construction, MHI designed, fabricated and erected the steel liner and all primary steel pressure-retaining components. Supporting MHI for the reinforced concrete portions of the model and ancillary structures were several subcontractors. Obayashi Corp., a large Japanese Architect/Engineer (A/E) and construction company, performed the detailed design of the PCCV model and Taisei Corp, another large A/E/Contractor, was the construction manager. Taisei retained the U.S. construction firm, Hensel Phelps Construction Co., Greeley, CO for general construction work and management of day-to-day construction operations. MHI pre-fabricated portions of the steel liner and the penetrations at their Kobe Shipyard and transported these components to the CTTF-W for final erection. The balance of the model was constructed on-site.

---

[1] This work is jointly sponsored by the Nuclear Power Engineering Corporation and the U.S. Nuclear Regulatory Commission. The work of the Nuclear Power Engineering Corporation is performed under the auspices of the Ministry of Economy, Trade and Industry, Japan. Sandia is a multiprogram laboratory operated by Sandia Corporation, a Lockheed Martin Company, for the U.S. Department of Energy under Contract Number DE-AC04-94AL85000

Instrumentation and Data Acquisition

NUPEC funded SNL to provide programmatic and model design support, instrument the model, and design and assemble the data acquisition system. The PCCV model instrumentation suite was designed to measure the global behavior in free-field locations of the model and the local structural response of the model near discontinuities. Global response measurements included both displacements referenced to a global or fixed reference and strain measurements at a regular pattern of azimuths and elevations to characterize the overall shape of the model. Local response measurements consisted of strain measurements of individual structural elements (i.e. liner, rebar, tendons, concrete) to characterize the force distribution near structural discontinuities. In areas absent of structural discontinuities or where membrane behavior was expected to dominate the response, relatively simple arrays of transducers were specified. Where structural discontinuities were judged to be significant more complex arrays of strain gages were utilized. Both hoop and meridional strains were measured.

Pressure measurement requirements included careful measurement of the PCCV interior pressure for purposes of leak detection, and to a lesser extent, leak rate measurement, characterization of the mechanical response as a function of pressure and to control the pressurization rate. It should be noted, that while measurement of leak rates was not a primary objective, detection of the onset of leakage requires the calculation of very small leak rates with relatively high accuracy.

As implied by the name, the unique feature of the PCCV model is the prestressing system, comprised of the vertical and hoop tendons and associated hardware. Special efforts were made to monitor the response of the prestressing system, both prior to and during pressure testing. An extensive effort was undertaken to develop and demonstrate the reliability of the tendon instrumentation. The resulting system was comprised of two types of strain gages to monitor the strain, and by calculation, the force distribution along the length of selected tendons along with load cells to measure the forces at the tendon anchors. Since the behavior of the tendons and the overall response of the model to the pressure load would be directly affected by the initial prestressing forces, the response of the PCCV model was monitored continuously from the start of prestressing through the subsequent pressure tests.

While these force, strain and displacement measurements provide accurate information on the response of the model at discrete locations, it was desirable to have some method to monitor the overall response of the model in the (likely) event that some significant response occurs at locations remote from any transducer. The displacement transducers reflect, to a greater extent than the strain or force transducers, the overall response of the model but might still miss other local response modes. This deficiency was addressed by including an extensive array of acoustic and, to a lesser degree, video/photographic monitoring of the PCCV model. While more qualitative in nature than the discrete response measurements, some quantitative information could be obtained from these monitoring systems. The acoustic system, in particular, was designed to detect the onset of liner tearing and leakage, along with concrete cracking and rupture of tendon wires or rebar. Similarly, video and still photography was used to document the development and distribution of concrete cracking, detect liner tearing at discrete locations during pressure testing and capture any unanticipated response modes.

Analysis

NRC funded SNL to perform preliminary, pre- and posttest analyses of the model. This analytical work was subcontracted by SNL to ANATECH Consulting Engineers, San Diego, CA. The preliminary analyses supported design studies, identified critical response modes and assisted in locating instrumentation. The pretest analysis consisted of the development and analysis of detailed numerical models in an attempt to predict the response of the PCCV to the test pressures and predict the capacity and most probable failure mode. The posttest analysis compared the test results to the pretest predictions, investigated and demonstrated changes in the modeling methods to improve the comparison with the test results and provided insights into the response observed during the pressure tests. The pre- and posttest analyses have been reported separately and are not included in this report.

NUPEC and NRC also jointly provided funding to share the costs associated with organizing and conducting a pretest Round Robin analysis. The Round Robin analysis euphemistically refers to an activity where a number of nuclear safety research organizations from government, industry and academia in the United States, Japan and other countries are provided with a common set of data on the model test (design drawings, material properties, test specifications, etc.) and then complete independent predictions of the model response, failure mode and pressure capacity. SNL was the focal point for this effort in terms of disseminating and consolidating the work of the participating organizations. Seventeen independent organizations, including NUPEC and SNL, participated in this effort, performing pretest analyses and meeting before and after the PCCV model test to discuss and compare analysis results. The efforts of these Round Robin participants are documented in separate NUREG Contractor Reports. While a formal posttest Round Robin exercise was not conducted for the PCCV, most of the participants attended a posttest workshop and have reported the results of their posttest analyses independently.

Testing

NRC funded the planning and conduct of test operations. After extensive discussions between NUPEC, the NRC and SNL, a detailed Test Plan was developed by SNL to describe the conduct of the pressurization tests of the PCCV model. A final series of three tests were agreed upon:

- A leak check and System Functionality Test (SFT) @ 0.5 P_d (2.0 kg_f/cm^2 or 28.4 psig)
- A Structural Integrity Test (SIT) @1.125 P_d followed by an Integrated Leak Rate Test (ILRT) @ 0.9 P_d
- A Limit State Test (LST) to the static pressure capacity of the PCCV model (or the pressurization system, whichever comes first)

The *pneumatic* Limit State Test was the final test in the original program plan. This test was terminated following a functional failure, i.e. a leak, in the PCCV model, with only limited structural damage occurring. Subsequently, it was decided to re-pressurize the PCCV model, prior to demolition, in an attempt to observe larger inelastic response and, possibly, a global structural failure. This Structural Failure Mode Test (SFMT) was a combined *pneumatic-hydrostatic* test, where the PCCV model was filled nearly full with water, to reduce the volume of gas to be pressurized, and nitrogen gas was used to generate the overpressure.

The SFT was conducted beginning approximately 9:00 AM, July 18, 2000. The model was pressurized using nitrogen to 0.5 P_d (0.2 MPa or 28.4 psig) in three increments holding pressure for one hour or longer at each step, depending on the duration needed to perform all system functionality and leak checks. The model was then isolated and a leak rate check was performed by monitoring the model pressure and temperature for approximately 18 hours. After 18 hours, the calculated leak rate was 0.15% mass/day, which was interpreted as confirming that the model was leak-tight. After the model leak rate check, the model was allowed to depressurize through a pair of orifice plates calibrated to leak rates of 1% and 10% mass/day to perform a calibration test on the leak rate measurement instrumentation. The calculated leak rates for each test were 0.87% and 7.86%, respectively, indicating that the leak rate instrumentation was capable of accurately detecting a leak of 1% mass per day, which is the goal specified for the ILRT. The SFT was concluded on July 20 by opening the vent valve, allowing the model to depressurize.

The Structural Integrity Test and the Integrated Leak Rate Test were conducted on September 12-14, 2002 as a combined test, with the ILRT following immediately after the SIT. The SIT/ILRT reproduced the pre-operational tests conducted at the prototype plant and allows for a comparison of the model's elastic response characteristics and leak behavior with the prototype and pretest analyses. The SIT test pressure, P_{SIT}, was 1.125 P_d. After the SIT pressure was maintained for one hour, the PCCV model was depressurized to the ILRT pressure, 0.9 P_d. The calculated leakage rate at P_{ILRT}, L_{tm}, after 24 hours at 0.9 P_d, was 0.06% mass/day.

The Limit State Test (LST) was designed to fulfill the primary objectives of the PCCV test program, i.e. to investigate the response of representative models of nuclear containment structures to pressure loading beyond the design basis accident and to compare analytical predictions to measured behavior. The LST was conducted after the SIT and ILRT were completed and the data from these tests evaluated. The PCCV model was depressurized between the SIT/ILRT and the LST. The LST began at 10:00 AM, Tuesday, September, 26, 2000 and continued, without depressurization, until the test was terminated just before 5:00 PM on Wednesday, September 27. The model was pressurized in increments of approximately 0.2P_d to 1.5 P_d when a leak check was conducted yielding a leak rate of 0.48% mass/day. Pressurization of the model continued in increments of approximately 0.1P_d to 2.0P_d when a second leak check resulted in a calculated leak rate of 0.003%, i.e. essentially zero. Pressurization of the model resumed in increments of 0.1P_d to 2.5P_d. At 2.4P_d the acoustic system operator reported hearing a change in the acoustic output which might indicate that "something had happened". The model was isolated for a third leak check and after approximately 1-1/2 hours, a fairly stable leak rate of 1.63% mass per day was calculated, indicating that the model was leaking, most likely from a tear in the liner in the vicinity of the E/H. The average hoop strain at $2.5P_d$, coinciding with the onset of liner tearing and leakage was 0.18%.

After concluding that the model had functionally failed between 2.4 and 2.5 P_d, the next goal was to continue to pressurize the model as high as possible to collect data on the inelastic response of the structure and to observe, if possible, a structural failure mode. Pressurization continued in increments of 0.05 P_d. The pressure was increased to slightly over 3.3 P_d before the leak rate exceeded the capacity of the pressurization system and the test was terminated. After the model had completely depressurized, it was purged with fresh air, the E/H was removed and a detailed inspection of the inside of the model revealed 26 discrete tears in the liner, all located at vertical field welds. Extensive examination and metallurgical analysis of the liner after the test revealed that fabrication defects contributed to nearly all of the liner tears.

Almost immediately after the completion of the LST, there was a recognition that while the PCCV model had demonstrated it's capacity to resist pressures well above the design pressure and had exhibited liner tearing and leaking as the functional failure mode, the test objectives were not fully met with respect to observing large inelastic deformations, for comparison with analyses. NUPEC and NRC approved a concept proposed by SNL to seal the interior surface of the liner with an elastomeric membrane, fill the model with water to 1.5m (5') from the dome apex, approximately 97% of the interior, and repressurize the remaining gas pocket with nitrogen until the model failed or pressure could not be maintained.

The Structural Failure Mode Test (SFMT) began shortly after 10:00 AM on Wednesday, November 14, 2001. The model was continuously pressurized at a rate of approximately 0.035 MPa/min (5 psi/min). All active sensors were continuously scanned at intervals of approximately 30 seconds and the video cameras were continuously recording the response of the model. As the pressure was increased, evidence of leakage was visible by increasing wetting of the concrete surface. At 10:38 AM, the effective pressure in the model equaled the peak pressure achieved during the LST, 3.3 P_d. At approximately 10:39 AM, the acoustic system recorded a very high noise level event which was interpreted as the breaking of a tendon wire. At this point in the test, events occurred very quickly. Shortly after detecting the wire break, a small spray of water was observed at approximately 0° azimuth and additional tendon wire breaks were detected by the acoustic system with increasing frequency. The rate of pressurization was decreasing and the nitrogen flow rate was increased to maintain the pressurization rate. Pressurization of the model continued until a second spray of water was observed and then, suddenly, at 10:46:12.3, at an effective pressure of 3.63 P_d (1.42 MPa or 206.4 psig) the PCCV model ruptured violently at ~6° azimuth near the mid-height of the cylinder. The maximum average hoop strain at the peak pressure of 3.63 P_d was 1.02%. The model continued to expand after reaching the peak pressure and the maximum hoop strain recorded just prior to rupture was 1.65%.

Conclusions

The over-pressurization tests of the 1:4-scale PCCV model represent a significant advance in understanding the capacity of nuclear power plant containments to loads associated with severe accidents. The data collected during the tests, as well as the response and failure modes exhibited, will be used for many years to come to benchmark numerical simulation methods used to predict the response of concrete containment structures. While lessons for actual plants can and should be drawn from this and previous large scale containment model tests, these insights are beyond the scope of this report and will be addressed in a future effort. The reader is cautioned *not* to draw direct conclusions regarding the pressure capacity of actual plants from these tests or interpret these results as a demonstration of the prototype capacity. The PCCV model tests have demonstrated the importance of the unique details and as-built characteristics of the model on the ultimate capacity. Any efforts to estimate the capacity of an actual containment must address the unique features of the plant under consideration.

With the completion of the PCCV tests, restoration of the test site and submittal of the test reports, the NUPEC/NRC Cooperative Containment Research Program was formally concluded on December 31, 2002.

ACKNOWLEDGMENTS

No one person was responsible for the success of the PCCV Test Project. Without the dedicated efforts of a team including the project sponsors, partners and contractors and supporting organizations, the outcome of this project would have been far less successful than it has proven to be. It is, however, difficult to acknowledge everyone who contributed to this project without unconsciously omitting some individuals. I would like to begin therefore by apologizing to those anonymous, but no less important contributors I may have overlooked.

But the contributions of some individuals are too significant to overlook. I would like to begin, therefore, by acknowledging the program managers of the sponsoring organizations, NUPEC and the U.S. NRC. Dr. James F. Costello, U.S. NRC, has been the guiding force behind the containment integrity research conducted at SNL for over 25 years, including this project. His perseverance, support, and guidance has been invaluable and it is no overstatement to say that this project may never happened without his involvement. Similarly, the NUPEC project directors: Dr. Kenji Takumi, Dr. Hideo Ogasawara and Dr. Takshi Kiguchi; and the project managers: Mr. Akira Nonaka, Mr. Tomoyuki Matsumoto, Mr. Masaki Iriyama and Mr. Satoru Shibata ensured that this program had the financial and technical resources to meet the program objectives in order to make a significant contribution to the international nuclear power industry.

There were many Japanese colleagues who, as primary contractors or subcontractors to NUPEC, contributed to the planning, design, and construction of the PCCV model. These included, from Mitsubishi Heavy Industries: Toshisada Kato, Kaoru Nagata, Kazutoshi Hayashi, Nozumo Watanabe, Tomoyuki Kitani, Hiroshi Urakawa, Ryuichi Oshima, and Hiroshi Matsuoka; from Obayashi Corporation: Katsuhiko Umeki, Katsuyoshi Imoto, and Takako Kashiwase; and from Taisei Corporation: Yasuyuki Murazumi, Yutaka Kobayashi, and Shiro Mitsugi. General Construction of the model was managed by Hensel Phelps Construction Company whose on-site staff included: Guy Mills, Tina Connelly, Subba Padmendra and Norman 'Butch' Brackett.

SNL management support was provided by Walter von Riesemann and Dennis Berry. I am especially indebted to Brad Parks who was the initial program manager responsible for the planning and organization of an excellent project team. The dedication and professionalism exhibited by the SNL project team was unsurpassed in my experience and I am fortunate and proud to have had the opportunity to work with such an outstanding group of individuals. The primary project team included Dave Pace (PCCV Lead Engineer), L. Dwight Lambert (Site Manager and Instrumentation Leader), Eric Klamerus (Instrumentation and Pressurization System Engineer), Gina Rightley (DAS Lead Engineer), Mike Rightley (DAS and Instrumentation Design), Mike Luker (DAS and Instrumentation Engineer), Vincent Luk (Analysis and Round Robin Coordinator), Ken Eckelmeyer (Liner Inspection and Metallurgical Analysis) and a team of outstanding technicians consisting of Mike Ramirez, Bob Smyth, Ed Baynes, Bob Eyers, Raymond Davis, Roy Morgan, John Mulder, Richard Padilla, Jack Pantuso, Ed Vieth, Richard Klingler, and Larry Yellowhorse. Kimberly Brower assisted in the posttest data processing and analysis. Management and Administrative support was provided by Berlinda Gonzalez, Yolanda Aragon, Viola Madrid, Mary Campos, Rebecca Campbell, Linda Flores, Barbara Meloche and Barbara Hawkins. Site support was provided by SNL's Facilities Department members Walter Heimer, Paul Schlavin, George Greer, Ed Sanchez and Dave Hendrix. Nadine Williams was responsible for all permits and land-use issues. Dave Sparks and Russ Adams from SNL's Video Services Department taped the construction and testing of the model. Environmental, Safety and Health support was provided by Daniel 'Mac' MacLaughlin.

In addition to SNL's in-house staff, vital support was provided by several key sub-contractors, especially from ANATECH Consulting Engineers: Bob Dameron (Lead Analyst), Yusef Rashid, Jason Maxwell and Brian Hanson; from Pure Technologies, Ltd. Peter Paulson and Monroe Thomas; and from the University of New Mexico's ATR Institute, Lary Lenke. Faith Puffer (Tech Reps) was the technical editor responsible for producing this report.

The direction and planning of the project was greatly assisted by special advisors to the project. In Japan, NUPEC's Structural Advisory Committee included Prof. Hiroshi Akiyama, Prof. Katsuki Takiguchi and Prof. Noriyuki Miyazaki. The NRC's Peer Review Panel consisted of Tom Ahl, Bryan Erler, Ted Johnson, Richard Orr, Mete Sozen, John Stevenson, H.T. Tang, Walt von Riesemann, Richard White, Lyle Gerdes, Harold Townsend and Joseph Ucifferro.

It is very difficult to adequately describe the contribution of all these individuals in this short space, but to each of them, I would like to express my heartfelt thanks.

Thank you.

Michael F. Hessheimer, P.E.

Project Manager
NUPEC/NRC Cooperative Containment Program
Sandia National Laboratories

December 2002

ABBREVIATIONS

A/L	air lock
A/E	Architect/Engineer
AO	Acoustic System Operator
ASME	American Society of Mechanical Engineers
BWR	Boiling Water Reactor
CE	fiber optic gages
CONV	converted data
COR	corrected data
CPOT	Cable Potentiometer
CTTF	Containment Technology Test Facility
CVDT	converted
DA	data analyst
DAS	Data Acquisition System
DET	Division of Engineering Technology
DISP	displacement
DO	Data Acquisition System Operator
DOE	Department of Energy
DOR	data of record
DT	displacement
DYN	dynamic
E/H	equipment hatch
EPRI	Electric Power Research Institute
ES&H	Environmental Safety and Health
F/W	feedwater
GBST	gage bar strains
GFAC	gage-specific factors
ILRT	Integrated Leak Rate Test
KAFB	Kirtland Air Force Base
LI	liner strain gage
LINST	liner strains
LOCA	loss-of-coolant accident
LST	Limit State Test
LVDT	Linear Variable Differential Transformer
M/S	main steam
METI	Ministry of Economy, Trade and Industry
MHI	Mitsubishi Heavy Industries
NO	Nitrogen Supply Operator
NRC	U.S. Nuclear Regulatory Commission
NSS	nuclear steam supply
NUPEC	Nuclear Power Engineering Corporation
PCCV	prestressed concrete containment vessel
PLC	Programmable logic controller
PRES	pressure
PWR	Pressurized Water Reactor
REBST	rebar strain
RES	Office of Nuclear Regulatory Research
RS	rebar strain gages
RTD	Resistance Temperature Detectors
SCV	steel containment vessel
SFMT	Structural Failure Mode Test
SFT	System Functionality Test
SIT	Structural Integrity Test
SNL	Sandia National Laboratories
SOL	Standard Output Location

T/C	thermocouple
TC	test conductor
TEMP	temperature
UTS	ultimate strength
YS	yield strength

1. INTRODUCTION

The Nuclear Power Engineering Corporation (NUPEC) of Japan and the U.S. Nuclear Regulatory Commission (NRC), Office of Nuclear Regulatory Research have cosponsored and jointly funded a cooperative containment research program at Sandia National Laboratories (SNL). NUPEC was founded in 1976 as the Nuclear Power Engineering Center under the initiative of academia and private corporations. Supported by the Agency for Natural Resources and Environment of the Ministry of Economy, Trade and Industry (METI), NUPEC is mandated to advance the performance and public acceptance of commercial nuclear power plants through engineering tests, safety analyses, information acquisition and analyses, and public relations activities. Within NUPEC, the Systems Safety Department is conducting research on the integrity of reactor containment vessels during severe accidents. Containment integrity tests include experiments and analyses of debris cooling phenomena, hydrogen combustion behavior, fission products transport behavior, and containment structural behavior. In addition, the department coordinates the cooperative containment program with the NRC and manages program activities with SNL and other subcontractors.

The Office of Nuclear Regulatory Research (RES) at U.S. NRC plans, recommends, and implements programs of nuclear regulatory research, standards development, and resolution of safety issues for nuclear power plants and other facilities regulated by the NRC. Within RES, the Division of Engineering Technology (DET) plans, develops, and directs comprehensive research programs and standards development for nuclear and materials safety. In the nuclear safety area, there are programs for the design, qualification, construction, maintenance, inspection, and testing of current and advanced nuclear power plants. For materials safety, program activities include material characteristics, aging, and seismic and engineering aspects of these facilities and materials. Within DET, the Engineering Research Applications Branch has the lead for determining adequacy of structures and systems and for the coordinating and interfacing activities associated with the American Society of Mechanical Engineers (ASME) Code Section III. This branch coordinates the cooperative containment program with NUPEC and manages SNL activities.

SNL is a multi-program national security laboratory, operated by Sandia Corporation, a subsidiary of Lockheed Martin Company, for the National Nuclear Security Administration, U.S. Department of Energy (DOE). SNL's Nuclear Energy Technology Center has provided engineering and scientific support in the areas of reactor safety and safeguards to the NRC and the DOE for more than 20 years. A significant area of support has included analytical and experimental efforts to address issues related to severe accidents and containment integrity.

This cooperative containment program builds on the combined expertise of these organizations and continues to advance the understanding of nuclear containment structure's response to pressure loading beyond the design basis accident and the ability to predict, analytically, the structural behavior. This is accomplished by conducting static, pneumatic overpressurization tests at ambient temperature of scale models of actual containment vessels for nuclear power plants in Japan. NUPEC and the NRC formulated the overall scope of the program, and NUPEC, under contract with METI, is responsible for designing and constructing the models. SNL is funded by NUPEC to develop and operate a facility for conducting these tests, review the model designs and provide design support, instrument the models and collect data during the pressure tests, and report the results of the test. The NRC is funding SNL to perform pre- and posttest analyses of the models and to conduct the pressure tests. All funding is directed to SNL through agreements with the DOE's Work-for-Others Office in the Science and Technology Transfer Division.

Tests of two containment models were authorized under this program. The first model, a mixed-scale model of an Improved Mark-II type steel containment vessel (SCV) for a Boiling Water Reactor (BWR), was tested in December 1996. The results of the SCV tests and analyses have been published [1-5]. The second model tested was a 1:4-scale model of the prestressed concrete containment vessel (PCCV) of an actual nuclear power plant in Japan, Ohi-3 (Figure 1.1). Ohi-3 is an 1127 MWe Pressurized Water Reactor (PWR) unit, one of four units comprising the Ohi Nuclear Power station located in Fukui Prefecture and owned and operated by Kansai Electric Power Company.

This report describes the design, construction, and instrumentation of the PCCV model, the conduct of the pressure tests, and the results of those tests. The pre- and posttest analyses performed by ANATECH Corp (San Diego, CA) under contract to SNL are reported separately [6, 7]. Independent pretest analyses, conducted by a number of international organizations, were also conducted and presented in a summary report [8].

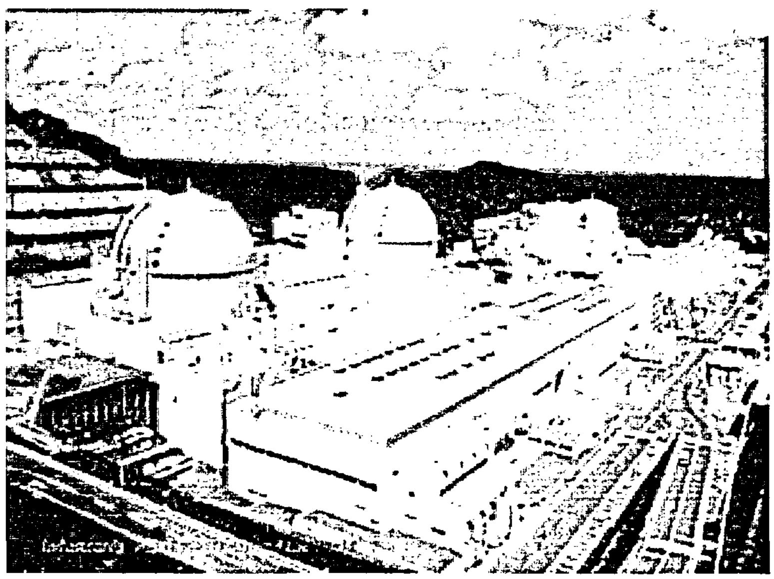

Figure 1.1. Ohi Nuclear Power Station, Ohi-cho, Fukui, Japan

1.1 Background

Containment vessels in nuclear power plants comprise, with the penetrations and other pressure boundary components, the final barrier between the environment and the nuclear steam supply system. The functions of the containment are to:

- contain any radioactive material that might be released from the primary system (reactor vessel, steam generators, piping) in the event of an accident;
- act as a supporting structure for operational equipment.

Containment buildings have been an integral part of commercial nuclear power plants in Japan and the United States since the first units were constructed in the 1960s. For U.S. containments, the design loads and their combinations, as well as the response limits, are specified in the ASME Boiler and Pressure Vessel Code [9]. Initially, severe accidents were not part of the design basis due to their perceived low probability of occurrence, and pressure relief valves were not required. In Japan, METI Directives control the design of nuclear power plants, and the design standards for containments are specified in the METI Notification No. 501 and in JEAG4601.

After the accident at Three Mile Island in the United States in 1979, attention turned to the capacity of containment systems beyond their design basis. SNL conducted a preliminary study [10], commissioned by the NRC, to identify experiments conducted to investigate this issue, but concluded that the scope of the tests and the data did not provide sufficient insight into the problem. As a result, a program, including scale model tests coupled with detailed structural analysis, was formulated by the NRC to investigate the integrity of containment systems beyond their design basis. The primary objective of the NRC program was, and continues to be, the validation of analytical methods used to predict the performance of light water reactor containment systems when subjected to loads beyond those specified in the design codes. While some insights could be gained into structural response and failure mechanisms of actual containments, it was also recognized that the capacity of actual containments could not be determined solely from tests of simplified scale models. The results of this program, as summarized by Parks [11], concluded that there was significant reserve capacity in the containment vessels to resist loads above the design basis and that although the analytical efforts were encouraging, uncertainties remained about structural response and failure mechanisms.

Remaining uncertainties regarding the response of containment structures led to discussions among NUPEC, the NRC, and SNL that culminated in a 1991 agreement to start the NUPEC/NRC Cooperative Containment Program. In parallel with this cooperative program, there are independent efforts sponsored and conducted by both NRC and NUPEC. These efforts include investigating the response of penetrations [12,13], the effects of aging on containment structure capacity [14], and the seismic capacity of containment structures [15, 16].

1.2 Scope

Nuclear power plants in Japan and the U.S. generally utilize one of two types of light water reactor systems; BWR and PWR. The containment vessels for the pressurized water reactors in Japan and the U.S. are typically free-standing reinforced concrete shells with an integral steel liner. A few have only regular steel reinforcing bars (rebar); however, the majority use both regular and posttensioned reinforcing. (For this report, the terms prestressed and posttensioned are used synonymously, even though the reinforcing is, technically, posttensioned; i.e. tensioning of the reinforcing is conducted after the concrete has been placed and cured to the specified minimum strength.) A variety of prestressed reinforcing or tendon configurations are represented in the fleet of PWR containments. However, the evolution of prestressed containment designs has been toward the use of longer, continuous tendons, culminating in the two-buttress containment with meridonal 'hairpin' tendons and 360-degree hoop tendons, represented by the Ohi-3 design. No two-buttress prestressed concrete containments were constructed in the U.S. (although some were planned prior to the TMI-2 accident); however, many of the features of the Ohi-3 containment are similar to features in existing U.S. plants and the design philosophy is similar. As a result, NUPEC and the NRC agreed on a scale model of the Ohi-3 containment for the second test subject in the Cooperative Containment Program.

1.2.1 Model Features and Scale

The Ohi-3 containment is a thin prestressed concrete cylindrical shell with a hemispherical dome and a continuous steel liner anchored to a reinforced concrete basemat that extends beyond the containment to support other plant structures. Consistent with the objectives of the sponsoring organizations, the features and scale of the PCCV model were chosen so that the response of the model would mimic the global behavior of the prototype, and local details, particularly those around penetrations, would be represented. One of the primary considerations in determining the scale of the model was the desire to utilize nearly identical construction materials to the material used in the construction of the prototype. Preliminary design studies, conducted to determine the appropriate scale of the model, initially focused on a mixed scale model where the scale on the overall geometry would be 1:6, while the scale on the liner thickness would be 1:3. These preliminary studies indicated, however, that use of this mixed scale might upset the relationship between failure modes that might be expected in the prototype. In particular, the use of a steel liner, which was twice as thick, relative to the prestressed concrete shell, as the prototype, might retard the onset of liner tearing (leakage) failure modes and increase the likelihood of a structural failure mode occurring. As a result, it was decided that the scale of the model would be a uniform 1:4, with minor exceptions to accommodate fabrication and construction concerns. This was judged to be the minimum scale that would allow the steel liner to be constructed from prototypical materials and fabricated with details and procedures representative of the prototype. The overall geometry and dimensions of the PCCV model are shown in Figure 1.2.

Although both NUPEC and SNL (under NRC sponsorship) had conducted component tests of both full-size and scaled penetrations [12-13, 17], the PCCV model included both a functional representation of the major penetrations, namely the equipment hatch (E/H) and the personnel air lock (A/L), and nonfunctional representation of the main steam (M/S) and feedwater (F/W) penetrations. The E/H and A/L penetrations were fully-functional, one-fourth scale models of the penetrations in the prototype, while only the penetration sleeves of the M/S and F/W penetrations, terminated with pressure seating blind flanges, were included in the model. The liner and concrete reinforcing details around these penetrations were also retained in the model.

During construction and instrumentation of the model, primary access to the interior was through the E/H, while the A/L was used to provide heating, cooling, and ventilation for personnel working inside the model. The M/S and F/W penetrations provided portals for interior instrumentation cabling, power and, during testing, the pressurization medium. Prior to testing, after the E/H cover was installed and sealed, the A/L provided the means for final egress and sealing of the model with a specially-designed pressure seating cover that could be closed from the outside.

Details of the design and fabrication of the PCCV model are described in Chapters 2 and 3.

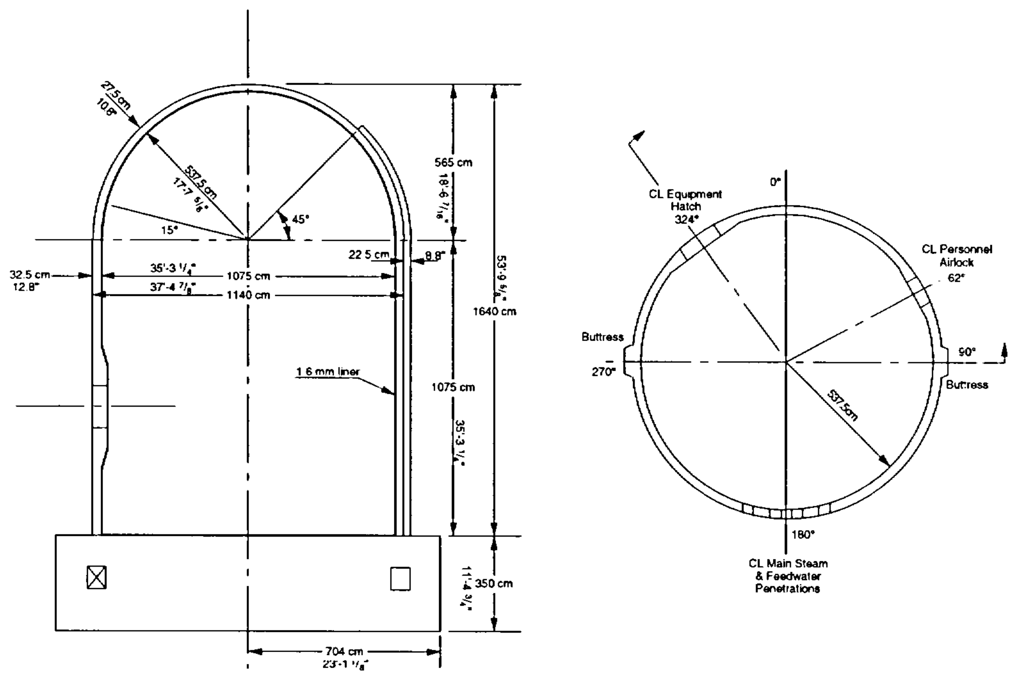

Figure 1.2 PCCV Model Elevation and Cross-Section

1.2.2 Loading

By definition, the scope of this program was limited to addressing the capacity of containment vessels to loads beyond the design basis, the so-called severe accident loads. Design accident loads for light water reactor containment vessels are typically based on the loss-of-coolant accident (LOCA) and are defined by a "bounding" pressure and temperature transients. The term "severe accidents" is used to describe an array of conditions that could result in loads exceeding the design basis on the containment. The definition of severe accident loads, which is not as rigorous as the design basis loads definition, results from considering of various postulated failure scenarios of the primary nuclear system, up to and including a complete core meltdown and breach of the reactor pressure vessel. The resulting pressure and thermal loading characteristics depend on the unique features of the nuclear steam supply (NSS) system and the containment structure, in addition to the postulated accident.

For this test program, it was necessary to decide whether both thermal and pressure loads would be applied to the model, either separately or simultaneously; what the pressurization medium should be; and whether the transient characteristics of these loads should be considered. Programmatically, the decision to perform a *static, pneumatic* overpressurization test at *ambient temperature* was dictated by risk and cost considerations and previous experience.

The effects of severe accident *temperature* loads on the structural response of the containment building are primarily limited to (1) the effects of elevated temperatures on the mechanical properties of the materials and (2) the mechanical loads resulting from differential or constrained thermal expansion. The effects of temperature on the material properties can be determined from standard material tests methods. These test results could be incorporated into the evaluation of the prototypical containment vessels without adding this complexity and cost (in terms of generating the thermal environment and protecting the instrumentation) to the PCCV model test. Regarding the stresses imposed by differential thermal expansion, there are only a few locations in a steel and/or concrete containment building where these effects are significant, notably at the junction of the containment wall and the basemat or, in the case of the PCCV model, the differential thermal expansion between the steel liner and the concrete shell under non-steady-state thermal conditions. Again, the added complexity and cost of simulating the thermal environments to reproduce these local effects was judged not justified for the PCCV model. It was further concluded that the effects of temperature could be addressed using analytical methods that had been benchmarked against the pressure tests. Therefore, the decision was made to conduct the PCCV model test at *ambient temperature.*

The containment atmosphere during a severe accident consists of air, steam, and other by-products of the accident, including hydrogen and particulates (aerosols). The program's primary interest is in observing and measuring the structural response of the containment to pressure loads, and identifying failure modes. Containment failure (see Section 1.2.3) includes both functional failure, i.e. leakage, and structural failure, i.e., rupture of the pressure-resisting elements. There is not a rigorous distinction between functional and structural failure, and it is conceivable that they might occur simultaneously. Conventional wisdom holds, however, that local, limited structural failure (i.e. liner tearing) and leakage will occur prior to, and at pressures well below those required to cause extensive structural failure. As a result, *detection* of leakage, which indicates a tear in the steel liner or failure of a penetration seal, not *measurement* of actual leak rates for real containment atmospheres (see Section 1.2.3), is the objective of the test. Hence, there is no need to reproduce the containment atmosphere resulting from a severe accident. The choice of a pressurization medium, then, becomes somewhat arbitrary and is dictated by safety and operational considerations. Hydrostatic testing is preferable from a safety viewpoint; however, it raises operational problems and requires protection of sensitive electronics and wiring from the water under high pressure. *Pneumatic* testing, while more dangerous, does not present any risks that cannot be managed cost-effectively and does not require any unusual measures to protect the instrumentation. Nitrogen gas was chosen as the pressurization medium for the PCCV model tests primarily for operational considerations. Fairly large quantities could be delivered at the test site in liquid form with a limited amount of fixed equipment. Nitrogen gas also has the advantage of being dry for instrumentation considerations, and it allows simpler and more accurate calculations to detect a small leak.

The test plan and conduct of the pressure tests, along with the design and operation of the pressurization system, are described in Chapter 5.

It should be noted that the *pneumatic* Limit State Test (LST) was the final test in the original program plan. This test was terminated following a functional failure, i.e. a leak, in the PCCV model, with only limited structural damage occurring. Subsequently, it was decided to repressurize the PCCV model, prior to demolition, in an attempt to observe larger inelastic response and, possibly, a global structural failure. This test was a combined *pneumatic-hydrostatic* test, where the PCCV model was sealed inside with an elastomeric membrane and filled nearly full with water to reduce the volume of gas to be pressurized, and nitrogen gas was used to generate the overpressure. The rationale and design of this Structural Failure Mode Test (SFMT) are also described in Chapter 5.

1.2.3 Response

One important aspect of the PCCV model response in the high pressure tests is the concept of *failure*. In the U.S., the functional failure for the prototypical containment is defined in the regulations as containment leak rates exceeding 0.1 to 0.5% of the containment mass per day [18], considering maximum offsite dose rates due to fission product released to the environment. In Japan, the functional failure is defined in design specifications made by the utility company, not the regulations. (The specified leak rate for the PCCV prototype is 0.1% mass/day.) The functional failure criteria are not particularly useful to test the structural capacity of a containment vessel model, especially when one of the objectives is to generate large inelastic response modes for comparison with analytical predictions, which may be well beyond the levels required to cause functional failure; and secondly to gain some insight into design margins, i.e. the functional and structural capacity beyond the specified design load conditions. In the case of the PCCV model test, the pressurization system allows the model to be pressurized to levels significantly above those expected to cause local strains in the model to exceed the ultimate strain limits of the materials. The test(s) were terminated when the model and the pressurization system were incapable of maintaining or increasing the model pressure due to excessive leakage or gross rupture. In this report, the maximum pressure achieved prior to the termination of the tests will *not* be identified as the *failure pressure*, since failure is defined in terms of some acceptance criteria, not the operational inability to maintain pressure in the model.

The PCCV model instrumentation suite was designed to measure the global behavior in free-field locations of the model and the local structural response of the model near discontinuities. Global response measurements included both displacements referenced to a global or fixed reference, and strain measurements at a regular pattern of azimuths and elevations to characterize the overall shape of the model. Local response measurements consisted of individual structural element (i.e. liner, rebar, tendons, concrete) strain measurements to characterize the force distribution in the free field and near structural discontinuities. In areas without structural discontinuities or where membrane behavior was expected to dominate the response, relatively simple arrays of transducers were specified. Where structural discontinuities were judged to be significant, more complex arrays of strain gages were utilized. Both hoop and meridonal strains were measured.

Pressure measurement requirements included careful measurement of the PCCV interior pressure for leak detection (to a lesser extent); leak rate measurement; characterization of the mechanical response as a function of pressure; and controlling the pressurization rate. Note that while measurement of leak rates was not a primary objective, detecting the onset of leakage requires calculating very small leak rates with relatively high accuracy.

While there was no attempt to simulate severe accident temperature conditions, a fairly extensive set of thermal measurements were taken to measure both the interior and exterior atmospheric temperature for accurate leak rate calculation. Given the large volume of the PCCV model, gas temperatures inside the model could vary significantly and multiple measurements were required to limit errors resulting from nonuniform gas temperatures. During pressurization steps, large thermal gradients could occur as the gas inside the model was compressed. Furthermore, since the model was exposed to the environment, ambient thermal variations, both spatial and temporal, affected the interior gas temperature and could affect the accuracy of the leak rate calculations if not considered. Similarly, ambient thermal effects could affect the model response measurements. Multiple measurements of the model temperature using both embedded and surface mounted temperature transducers were employed to account for this effect.

As implied by the name, the unique feature of the PCCV model is the prestressing system, comprised of the vertical and hoop tendons and associated hardware. Special efforts were made to monitor the response of the prestressing system, both prior to and during pressure testing. An extensive effort was undertaken to develop and demonstrate the reliability of the tendon instrumentation. The resulting system was comprised of two types of gages to monitor the strain, and, by calculation, the force distribution along the length of selected tendons along with load cells to measure the forces at the tendon anchors. Since the behavior of the tendons and the overall response of the model to the pressure load would be directly affected by the initial prestressing forces, the response of the PCCV model was monitored continuously from the start of prestressing through the subsequent pressure tests.

While these force, strain, and displacement measurements provide accurate information on the response of the model at discrete locations, it is desirable to monitor the overall response of the model in the (likely) event that some significant response occurs at locations remote from any transducer. The displacement transducers reflect, to a greater extent than the strain or force transducers, the overall response of the model, but might still miss other local response modes. This deficiency was addressed by including an extensive array of acoustic and, to a lesser degree, video/photographic monitoring of the PCCV model. While more qualitative in nature than the discrete response measurements, some quantitative information could be obtained from these monitoring systems. The acoustic system, in particular, was designed to detect the onset of liner tearing and leakage, along with concrete cracking and rupture of tendon wires or rebar. Similarly, video and still photography were used to document the development and distribution of concrete cracking, detect liner tearing at discrete locations during pressure testing, and capture any unanticipated response modes.

The design and implementation of the model instrumentation suite are described in Chapter 3. Performance requirements and features of the data acquisition system and data management are summarized in Chapter 4. A summary and discussion of the high pressure tests and posttest inspections are provided in Chapter 5. The test results are also summarized in Chapter 5 and the corrected test data, including a description of the corrections applied to the raw data, are included in the appendices.

1.3 Project Organization

As noted above, NUPEC and the NRC are the sponsoring organizations for this cooperative containment research program. Programmatic authorization to pursue this area of research is provided to these organizations by the ministerial or executive offices of their respective national governments, as dictated by statute. Technical guidance was provided by panels of expert advisers from academia and industry in each country. In Japan, the Structural Advisory Committee met regularly with NUPEC personnel to review the program plans and status, while in the U.S., a special Peer Review Panel provided the same support to NRC and SNL personnel.

Within the cooperative framework agreed to by NUPEC and the NRC, NUPEC and its Japanese contractors designed and constructed the PCCV model at SNL's Containment Technology Test Facility-West (CTTF-W). This test facility was specially constructed by SNL on land temporarily permitted for this purpose by Kirtland Air Force Base (KAFB), Albuquerque, New Mexico, USA. This 'West' facility is distinct from the CTTF used for the previous large-scale model tests conducted for the U.S. NRC in the 1980s. The 'East' facility was not considered suitable for continued large-scale model testing due to the identification of previous environmental contamination (not associated with the containment test operations) and subsequent clean-up operations that might interfere with the Cooperative program operations. The CTTF-West Land-Use Permit required NUPEC and the NRC, through their contracts with SNL, to remove all improvements within the permit boundaries and return the site to near its original condition at the conclusion of all test operations.

NUPEC and its Japanese contractors were authorized to construct the model at the CTTF-W under a specially negotiated Premise Access Agreement with SNL and the DOE. This agreement required NUPEC and its contractors to abide by all environmental health and safety regulations typically required for all capital construction activities managed by SNL, and authorized SNL to perform construction safety inspection to ensure that all requirements were being satisfied. The prime contractor to NUPEC for the construction of the PCCV model was Mitsubishi Heavy Industries (MHI), who also designed and constructed the prototype plant, Ohi-3. In addition to overall design and construction, MHI designed, fabricated, and erected the steel liner and all primary steel pressure-retaining components. Supporting MHI for the reinforced concrete portions of the model and ancillary structures were several subcontractors. Obayashi Corp., a large Japanese Architect/Engineer (A/E) and construction company, performed the detailed design of the PCCV model, and Taisei Corp, another large A/E/Contractor, was the construction manager. Taisei retained the U.S. construction firm, Hensel Phelps Construction Co., Greely, CO for general construction work and management of day-to-day construction operations. MHI prefabricated portions of the steel liner and the penetrations at their Kobe Shipyard and transported these components to the CTTF-W for final erection. The balance of the model was constructed on-site.

NUPEC also funded SNL to provide programmatic and model design support, instrument the model, and design and assemble the data acquisition system.

NRC funded SNL to perform preliminary, pre- and posttest analyses of the model. This analytical work was subcontracted by SNL to ANATECH Consulting Engineers, San Diego, CA. The decision to subcontract this work to ANATECH was based, in part, on a successful history of collaboration on previous containment model tests [19, 20] and ANATECH's experience in developing sophisticated concrete models and related efforts for the Electric Power Research Institute (EPRI), Palo Alto, CA [21]. The preliminary analyses supported design studies, identified critical response modes, and assisted in the locating instrumentation. The pretest analysis consisted of developing and analyzing detailed numerical models in an attempt to predict the response of the PCCV to the test pressures and predict the capacity and most probable failure mode. The posttest analysis compared the test results to the pretest predictions, investigated and demonstrated changes in the modeling methods to improve comparison with the test results, and provided insights into the response observed during the pressure tests. The pre- and posttest analyses are reported separately [6,7] and are not included in this report.

NRC also funded the planning and conduct of test operations.

NUPEC and NRC also jointly provided funding to share the costs associated with organizing and conducting a pretest Round Robin analysis. The Round Robin analysis euphemistically refers to an activity where a number of nuclear safety research organizations from government, industry, and academia in the U.S., Japan, and other countries, are provided with a common set of data on the model test (design drawings, material properties, test specifications, etc.) and complete independent predictions of the model response, failure mode, and pressure capacity. SNL was the focal point for this effort in terms of disseminating and consolidating the work of the participating organizations. Seventeen independent organizations, including NUPEC and SNL, participated in this effort, performing pretest analyses and meeting before and after the PCCV model test to discuss and compare analysis results. The efforts of these Round Robin participants are documented in separate NUREG Contractor Reports [8]. While a formal posttest Round Robin exercise was not conducted for the PCCV, most of the participants attended a posttest workshop and have reported the results of their posttest analyses independently.

Regular Technical Working Group meetings were held in both Japan and the U.S., involving program personnel from NUPEC, (including its contractors), the NRC, and SNL. These meetings planned and coordinated program activities and resolve technical issues. Separate meetings were held to discuss administrative issues related to cost and schedule.

1.4 Project Schedule

The NUPEC/NRC Cooperative Containment Research Program commenced in June 1991. The tests were conducted at the CTTF-W at SNL. Figure 1.3 illustrates the layout of the test site. A safety zone consisting of a circular area with

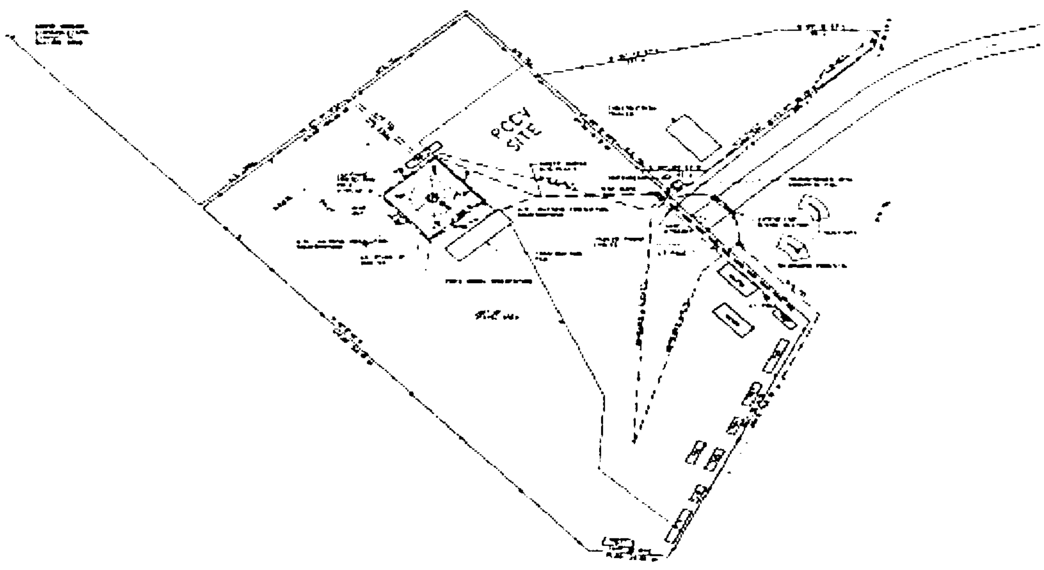

Figure 1.3 Plan of Containment Technology Test Facility-West

radius of 600 m (2000 ft) was maintained and monitored throughout the high-pressure test. The command center in Building 9950, located outside the exclusion zone, served as headquarters for conducting the high-pressure tests.

The high-pressure test of the SCV was completed on December 12, 1996. Construction of the PCCV model commenced January 3, 1997 with initial site preparation. Milestones in the construction and testing of the PCCV model included the following:

- 12 February 1997; First Basemat Pour (F1)
- 19 June 1997; First Liner Panel Installed
- 15 April 1999; Final Dome Pour (D3)
- 12-14 October 1999; Pretest Round Robin Meeting
- 8 March-3 May 2000; Prestressing
- 25 June 2000; PCCV Construction Completed
- 12-14 September 2000; Structural Integrity and Integrated Leak Rate Test
- 27-28 September 2000; Limit State Test
- 22 August 2001; Posttest Round Robin Meeting
- 14 November 2002; Structural Failure Mode Test
- 3 May 2002; PCCV Demolition and Site Restoration Completed

With the completion of the PCCV tests, restoration of the test site, and publication of the test reports, the NUPEC/NRC Cooperative Containment Research Program was formally concluded on December 31, 2002.

2. DESIGN AND CONSTRUCTION OF THE PCCV MODEL

2.1 Design

The PCCV model design was directed by NUPEC with overall responsibility for the design and construction contracted to MHI, Tokyo. Responsibility for the design of the liner and penetrations was assigned to MHI's Kobe Shipyard and Machinery Works while the concrete portions of the model were subcontracted to Obayashi Corp., Tokyo.

The basic philosophy guiding the design of the PCCV model was agreed upon very early in the program [22]. Key elements of this design philosophy included:

1. The PCCV model would be a uniform 1:4-scale model of the prototype or actual prestressed concrete containment vessel of Ohi Unit 3.
2. Elements of the model that would affect the ultimate strength would be equivalent to the prototype. The model liner would be one-fourth the thickness of the prototype liner. Reinforcing ratios would be maintained and the number and arrangement of the prestressing tendons would, to the extent possible, be identical to the prototype.
3. The model would be capable of reproducing the failure modes postulated for the prototype, including
   a. Hoop tensile failure of the cylinder wall
   b. Bending-shear failure at the junction of the cylinder wall with the basemat
   c. Shear failure in the basemat above the tendon gallery
   d. Bearing failure at the tendon anchors
   e. Bending-shear failure at the large penetrations
   f. Bending-shear at the small penetrations
   g. Liner tearing due to strain concentrations at local discontinuities (stiffeners/anchors, thickened reinforcing plates at penetrations and embedments)
   h. Leakage at penetration seals due to ovalization or distortion of the sealing surfaces.

Furthermore, to the extent possible, introduction of non-representative failure modes as a result of scaling or other modeling artifacts was to be avoided.

The general arrangement and representative failure mode locations are shown in Figure 2.1.

While the PCCV model was not 'designed' in the conventional sense, it's features were scaled directly from the Ohi-3 design with some simplifications to facilitate construction without compromising the objectives of the test. The prototype, Ohi-3, was designed in accordance with the "Draft Technical Code for Concrete Containment Vessels in Nuclear Power Plants" issued by Ministry of International Trade and Industry/Agency for Natural Resources and Energy (MITI/ANRE) in November, 1981 [23]. This draft code was formally adopted in 1993 as MITI Notification No. 452. The code is not identical to the American Society of Mechanical Engineers/American Concrete Institute (ASME/ACI) code [9], which governs the design of concrete containments in the U.S.; however, the basic design philosophies are similar, i.e., to ensure that all elements of the containment structure respond elastically (with some minor exceptions for secondary stresses) to the specified design loading conditions.

Construction of the prototype was also governed by Japanese Architectural Standard Specifications No. 5 and 5N for Reinforced Concrete Work at Nuclear Power Plants [24, 25]. Construction specifications for the PCCV model also followed these standards to the extent possible; however, modifications were made to adapt the specifications to U.S. construction practices.

The final design drawings for the PCCV model are provided in Appendix A. While it is beyond the scope of this report to include all the details of the design and construction specifications, a discussion of those features relevant to the model's response is appropriate and is included below.

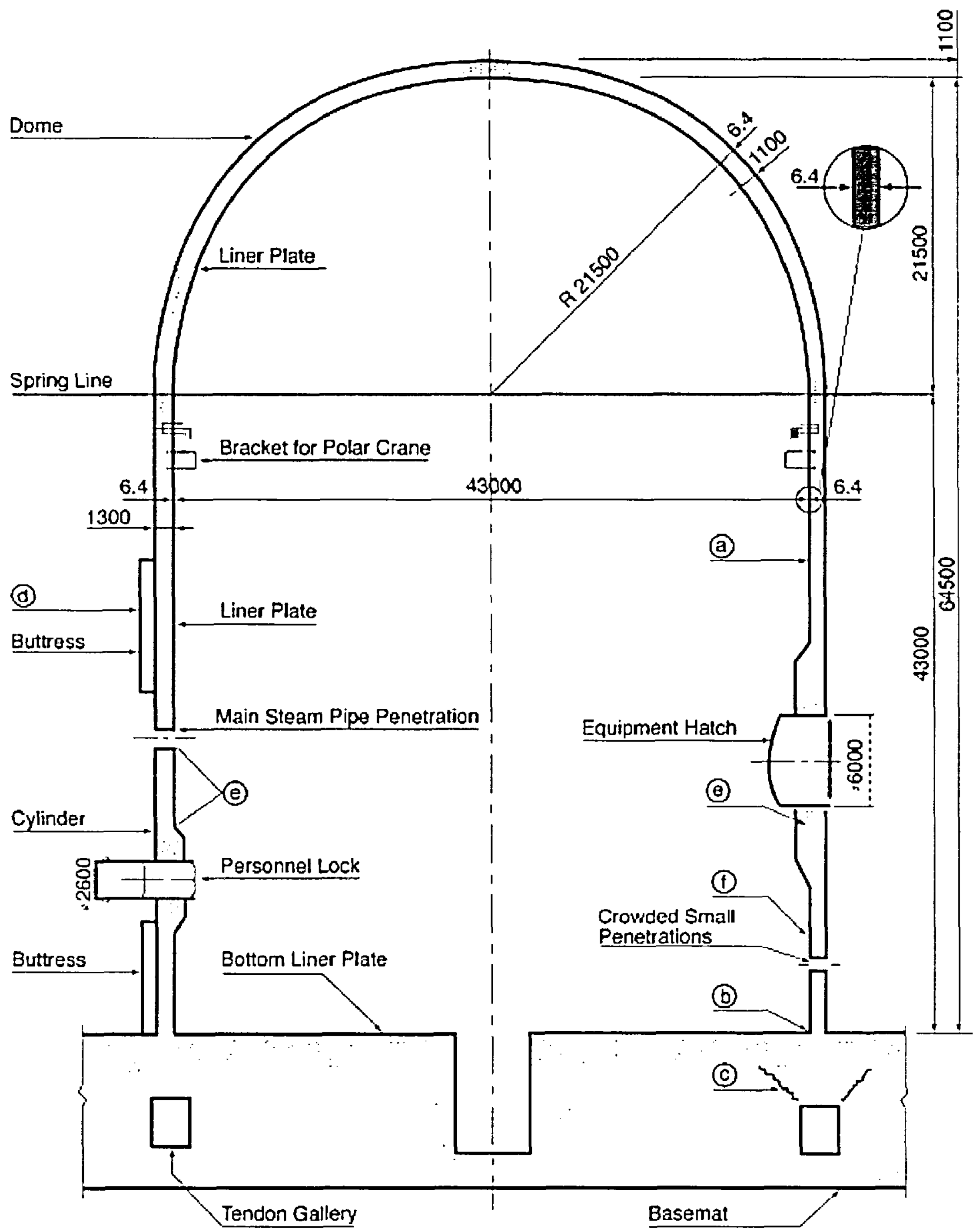

Figure 2.1. Elevation of PCCV Prototype and Potential Failure Locations

2.1.1 Liner Design Considerations

Design and fabrication/erection of the liner and penetrations was performed by MHI. The detailed specifications and practices are included in the project files. Essentially, the 1.6 mm (1/16") model liner was scaled from the 6.4 mm (~1/4") prototype liner. The as-built model liner thickness was 1.8 mm (0.070"), the extra 0.2 mm (0.008") providing a fabrication allowance. The model and prototype liner were both fabricated from SGV 410[1] carbon steel. JIS G3118 does not specify plate material under 6mm in thickness. The PCCV liner plate was fabricated to the same specifications as SGV410. Liner anchors and stiffeners were fabricated from SS 400[2]. Penetration assemblies were fabricated from SGV 410. The nominal properties of SGV 410 and SS 400 are given in Table 2.1. Miscellaneous non-structural components, e.g. back-up bars, were fabricated from U.S. common bar stock, typically ASTM A36 carbon steel.

Table 2.1 Properties of Liner Materials

Nominal Properties	Liner Plate	Liner Anchors
	SGV 410	SS 400
Yield Strength	225 Mpa (33 ksi)	235 Mpa (34 ksi)
Tensile Strength	410 MPa (59 ksi)	392 Mpa (57 ksi)

The liner material was procured in Japan, and liner panels were prefabricated and welded at MHI's Kobe Shipyard. Jigs, to support the liner panels and facilitate field erection and assembly, were attached to the liner panels prior to shipping them to the test site in Albuquerque, NM. Note that these jigs are unique to the construction of the model. The prototype liner is thick enough to be self-supporting without the use of any jigs. All vertical and horizontal liner weld seams in the prototype were reproduced in the model. Typically, the panel assemblies for the cylinder wall fabricated in Kobe encompassed three vertical rings of individual plate segments, resulting in assemblies approximately 3 m^2. Dome segments and penetration assemblies were typically smaller, individual plate segments. All welding of the assemblies in Kobe, including attachment of the anchors and stiffeners, was done by computer-controlled automatic welders. All shop welding was done without the use of back-up bars.

Standard coupons were made from the liner and liner anchor materials, and these specimens were tested for quality control purposes and to determine the actual material properties. The results of these tests are summarized in Appendix B.

The general arrangement of the liner anchors on the PCCV model is shown in the design drawings and is illustrated in Figure 2.2. The vertical liner anchors in the prototype consisted of 'T-anchors' spaced 600 mm (24") on-center throughout the cylinder wall and dome. These anchors are built-up sections, continuously welded to the liner plate with double-sided fillet welds. Horizontal bar stiffeners are provided above and below each horizontal weld seam to stiffen the liner during construction. The model liner anchors and stiffeners are 1:4-scale of the prototype. At 1:4-scale, the vertical anchor spacing would be 150 mm (6"); however, because the liner anchors are, in general, ineffective at resisting pressure and facilitating fabrication, the vertical anchor spacing was increased to 450 mm (18") except near discontinuities in the liner, such as the wall-base junction, around the E/H, A/L, M/S, and F/W penetrations and around the crane rail bracket embedments, as shown in Figure 2.2. Furthermore, the vertical liner anchors were not extended into the dome. T-stiffeners were used at the perimeter of the dome liner segments, but interior T-anchors were replaced with small stud-type anchors, as shown on the drawings. Again, since the strains in the dome were expected to be well below those experienced by the cylinder wall, this modification was not judged to affect the pressure capacity of the model.

As noted previously, the majority of the liner anchors were shop-welded to the liner using welding machines. One additional deviation from the prototype was the use of intermittent, staggered fillet welds to attach the anchors and stiffeners to the liner plate. There was a concern that these 'stitch' welds might generate additional local strain concentrations from the weld geometry itself. Therefore, anchors and stiffeners adjacent to other local liner discontinuities were continuously welded to reduce the possibility of premature liner tearing.

[1] Japanese Industrial Standard (JIS) G 3118, "Carbon Steel Plates for Pressure Vessels for Intermediate and Moderate Temperature Service," Japanese Standards Association.
[2] JIS G 3101, "Rolled Steel for General Structure," Japanese Standards Association.

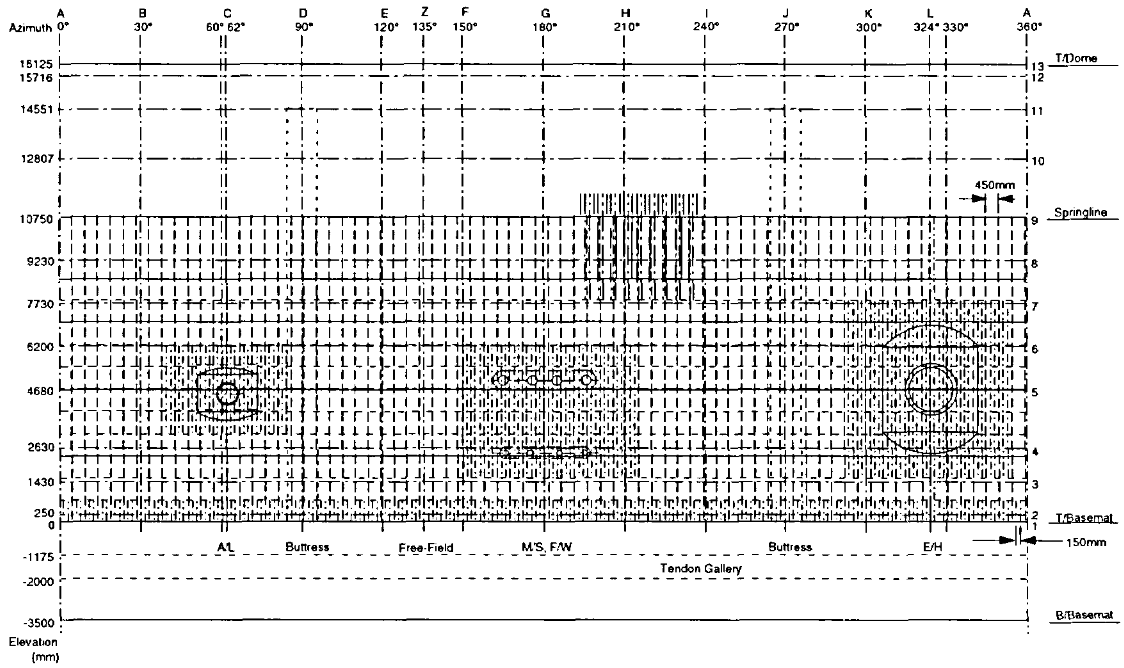

Figure 2.2 Liner Anchor Layout

While all the penetrations in the prototype were not included in the model, the major penetrations, consisting of the E/H, A/L, M/S, and F/W penetrations, were included in the model. These penetrations were representative of all the penetrations in the prototype and would be capable of reproducing the local strain concentrations in the structure and the liner. The E/H and A/L penetration assemblies in the model are 1:4-scale functional representations of the prototype assemblies, except that the A/L assembly includes only a single pressure seating cover and the interior doors are not reproduced. The model M/S and F/W penetration assemblies only included the penetration sleeve and reinforcing plates and were equipped with an interior flange and sealed with bolted pressure seating blind cover. No attempt was made to simulate the constraint conditions that might be imposed by the M/S or F/W piping. All the penetration sealing surfaces were milled and machined with groves for double O-ring gaskets. The prototype penetration assemblies are shown in Figures 2.3 to 2.6 for comparison to the model penetration assemblies shown in the design drawings. The model did not include the polar crane rail or brackets; however, a set of three adjacent bracket embedments were included to reproduce the local discontinuities in the liner.

The erection, field welding, and quality control of the liner are described in Section 2.2.

2.1.2 Concrete Design Considerations

2.1.2.1 Geometry

While the basic geometric scale of 1:4 was maintained throughout the PCCV model, some exceptions and modifications were required. Most significantly, the configuration of the model basemat had to be determined. The thickness of the model basemat at 1:4 scale is 3.5 m (11' 5-3/4"). The primary design consideration of the model basemat is that the rotational stiffness at the wall-base junction is equivalent to the prototype, since this affects the bending-shear failure mode at this location. The prototype containment basemat is continuous with the mat for the surrounding structures and includes a large reactor cavity at the center of the containment. Simplified three-dimensional finite element analyses of both the prototype and model subjected to pressure loading were performed to select the dimensions and reinforcement for the model basemat that would yield the desired response characteristics. The scaled basemat thickness of 3.5 m was maintained and, with the reactor cavity eliminated from the model, the radius of 7.2 m (23' 7 ½")and reinforcing were selected to match rotational stiffness of the prototype.

The location and size of the tendon gallery were scaled from the prototype. However, some modification of the construction sequence was required to accommodate this decision. Since the vertical prestressing tendons could not be inserted and tensioned inside a roughly 1-m^2 (2'-1" × 2'-8") tunnel, the portion of the basemat outside and below the tendon gallery was not constructed until after the tendons had been tensioned. This resulted in a somewhat different state of stress in the model basemat after prestressing; however, this difference was not significant and was unavoidable. Four access 'tunnels' to the tendon gallery were also included at 0 degrees, 90 degrees, 180 degrees, and 270 degrees to allow for visual inspection of the vertical tendon anchors and to ventilate the tendon gallery to minimize moisture that might affect the tendon anchors and the instrumentation.

Finally, some minor modifications in the geometry of the hoop tendon buttresses were required to accommodate the prestressing hardware. These were again judged to be insignificant with respect to the model's response to pressure.

2.1.2.2 Concrete Mix

The fundamental requirement of the PCCV model concrete was that it exhibit the same properties as the concrete used in the prototype. Based on prior experience with the construction and testing of a 1:6-scale reinforced concrete containment model at SNL, the approach to achieving this requirement was to specify a mix, using local (New Mexico) materials that would have the same 91-day[3] compressive strength (f_c') as the prototype concrete and then test the trial mix(es) to ensure they exhibited the same mechanical and chemical properties.

Two different concrete strengths were used in the prototype: 300 kg/cm^2 (4300 psi) for the majority of the basemat and 450 kg/cm^2 (6400 psi) for the cylinder wall, dome, and the portion of the basemat above the tendon gallery. The location of each mix, along with the lifts used in the construction of the model, are shown in Figure 2.7. Note that concrete lifts were not scaled from the prototype and are unique to the model.

The mix designs for the PCCV model consisted of Type I-II cement, air-entrained with 20% Class 2 Flyash and superplasticizer. Cement, aggregate, flyash, and water were all obtained locally and were batched by a supplier and mixed in transit. Maximum aggregate size was 10 mm (3/8"). Water/cement ratio for the 300 and 450 kgf/cm^2 mixes were 0.43% and 0.34%, respectively.

Corrosion due to the presence of chlorides and alkalis in the mix was a concern for the prototype due to the close proximity of the plant to the ocean; however, this was not judged to be a major concern for the model, although the chemical composition of the mix would be tested. Flyash was specified for the trial mix, since the use of flyash is standard practice in the construction of Japanese nuclear power plants and minimizes possible reaction and expansion of the aggregate. (Use of flyash is not permitted in construction of U.S. nuclear power plants). Superplasticizers were specified to facilitate placement of the concrete by pumping in congested areas. A maximum slump of 10 cm (4") before and 20 cm (8") after adding superplasticizers at the site was specified.

The trial mixes were batched and tested by Construction Technologies Laboratories, Skokie, IL to determine if they met the project specifications. The properties determined from trial mix specimens are summarized in Appendix B. In lieu of actual material property data, the trial mix properties were used for the pretest analysis of the PCCV model.

Quality control and material property test results for the concrete used to construct the model are described in Section 2.2 and summarized in Appendix B.

2.1.2.3 Reinforcing Steel (Rebar)

Normal, i.e. non-tensioned reinforcing steel for the prototype included grade SD490, SD390, and SD345 deformed bars[4]. The same grade steels were used to manufacture the rebar for the model in the U.S. (Cascade Steel, McMinnville, OR) in accordance with JIS Standards. The nominal properties for the rebar used in the model are summarized in Tables 2.2 and 2.3.

---

[3] JIS A 1108, "Method of Test for Compressive Strength of Concrete," allows specification of design strength at four weeks (28 days) or 13 weeks (91 days). Project specifications for the PCCV prototype and model specified the design strength f_c' at 91 days.

[4] JIS G 3112, "Steel Bars for Concrete Reinforcement."

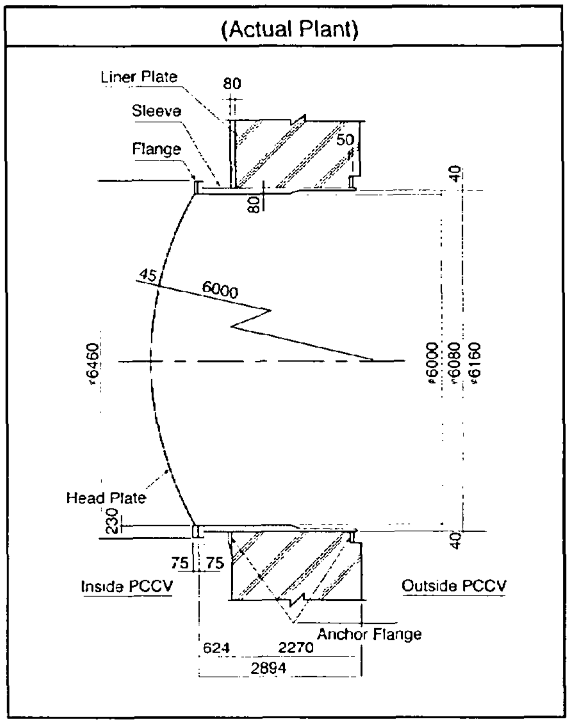

Figure 2.3 PCCV Prototype Equipment Hatch Arrangement

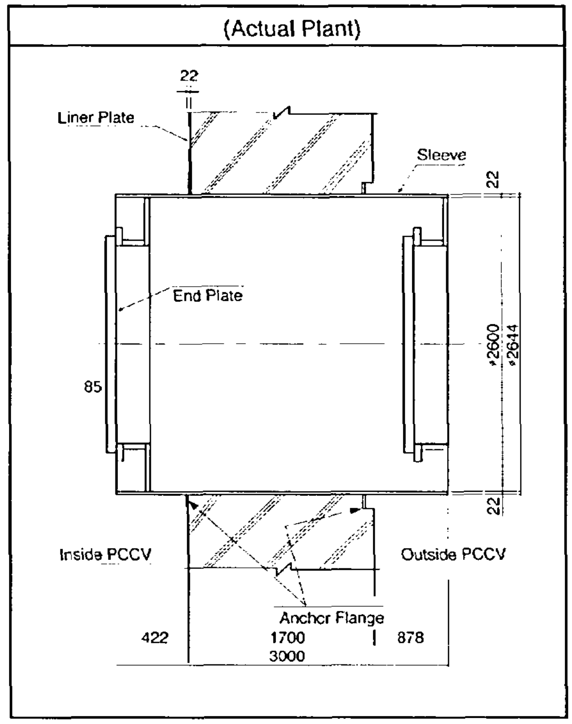

Figure 2.4 PCCV Prototype Personnel Airlock Arrangement

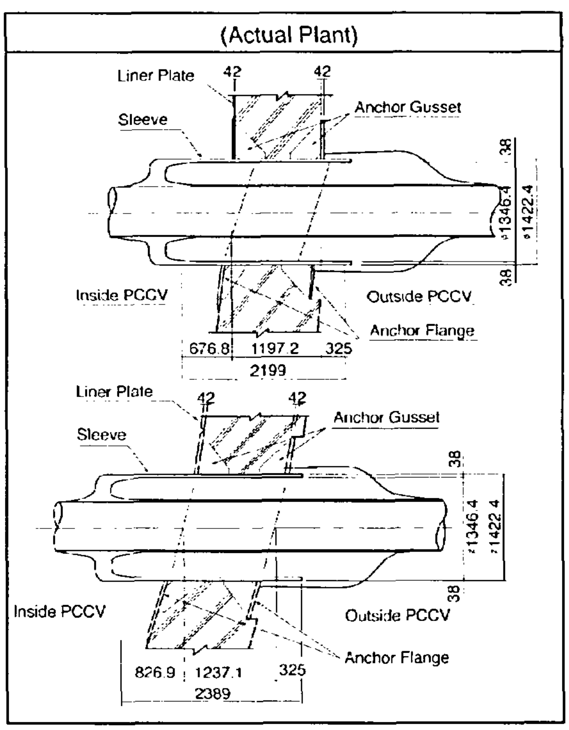

Figure 2.5 PCCV Prototype Main Steam Penetration Arrangement

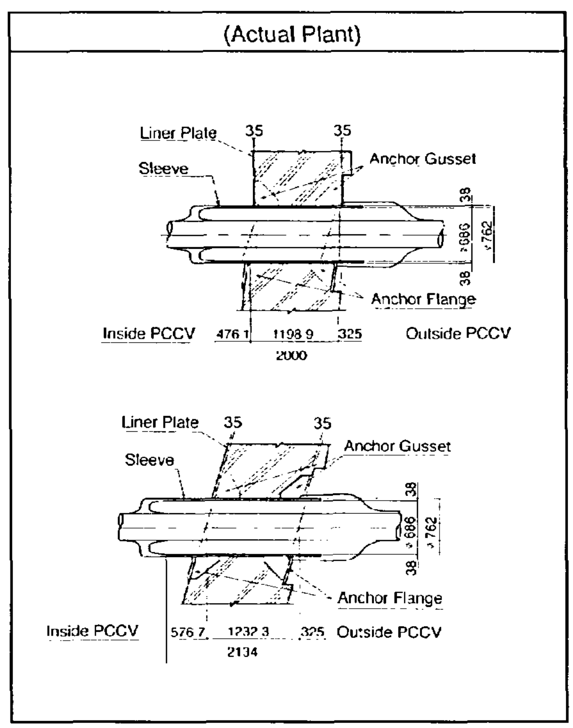

Figure 2.6 PCCV Prototype Feed Water Penetration Arrangement

In order to minimize rebar congestion in the model, all splices were originally intended to be made using swaged threaded couplers or position threaded couplers[5]. Swaged in-place couplers were not considered practical for the model due to limited clearance for the hand press. However, field considerations required some limited use of this type of coupler[6].

Samples of all the rebar used in the model were tested for quality control and to determine mechanical properties for analysis according to JIS and ASTM methods. Tests were also conducted of both the threaded and position-threaded couplers used in the model construction. (No tests were conducted of the swaged in-place couplers.) 'Dumbbell' specimens were machined from SD390 D16, and D22 bars to measure the basic material properties. Finally, a series of bars were tested with strain gages installed in the same manner as the instrumented bars in the model to calibrate the strains with a standard extensometer. The results of all these tests are summarized in Appendix B.

While the basic reinforcing ratios in the model were nearly the same as the prototype, the reinforcing in the model differed from the prototype. Individual bars in the model were not scaled directly from the prototype. Generally, in the containment shell (i.e. the cylinder wall and dome), the rebar was placed in one layer in each direction on each face. Figure 2.8 compares the arrangement of the reinforcing at the base of the cylinder wall in the prototype with the model. In-plane spacing of the rebar in the model is based on the arrangement of the prestressing tendons (2 degrees on center circumferentially and 112.5 mm (4.4") on center vertically). Bar sizes were then selected to reproduce as closely as possible, within the limits of the standard bar sizes available, the reinforcing ratio of the prototype.

Tolerances on formed surfaces and placement of rebar were developed by considering the 1:4-scaled tolerances for the prototype and then adjusting these to accommodate practical construction limitations, such as congestion and clearance for concrete placement. These tolerances are specified in the model construction specifications along with the as-built records. The deviations from the nominal design dimensions were not judged significant enough to affect the response of the model and, accordingly, are not included in this report.

Additional reinforcing was also provided around the penetrations in the model. However, where prototype penetrations were eliminated, no additional reinforcing was included in the model.

2.1.3 Prestressing Design Considerations

Since the unique feature of the PCCV model, compared to previous large-scale containment model tests, was the prestressing system, particular attention was paid to the design, construction, and instrumentation of this component. An unbonded, seven-wire strand prestressing system[7] was used in both the PCCV prototype and model. The tendons in the prototype consisted of 55, 12.7mm (½ in) diameter seven-wire strands[8]. The number and arrangement of the tendons in the model were kept the same as the prototype. The arrangement of the tendons is shown in Appendix A.

Both the prototype and model tendons were inserted in galvanized metal sheath or ducts after the concrete had been placed and allowed to cure, then tensioned. The model ducts were, generally, 35 mm (1-3/8") in diameter and were not 'greased' after tensioning. (The prototype tendon ducts were, as typical of most unbonded tendons, injected with a heavy grease after tensioning to protect the tendons from corrosion. Since the model tendons would only be in use for a relatively short time (< 2 years), they were not greased, although an anti-corrosion 'shop-coat' was brushed on prior to insertion in the ducts. Not greasing the tendons also facilitated the placement of instrumentation on selected tendons.)

In order to maintain the correct scaled cross-sectional area, the model tendons consisted of three, 13.7-mm (0.54") seven-wire strands. These model strands were custom-manufactured by the vendor for the model and nominal properties are not defined in the Japanese standard specifications, although the basic wire material was the same used for the prototype tendons[9]. The minimum properties of the model strands per the project specifications are given in Table 2.4. Extensive testing of individual strands as well as the tendon system were conducted for quality control and to determine the mechanical properties of the tendons. The results of these tests are summarized in Appendix B.

---

[5] Grip-Twist® System, manufactured by BarSplice Products Co., Dayton OH.
[6] Bar-Grip® System, ibid
[7] VSL Multistrand Posttensioning System®, VSL Corporation, Japan
[8] JIS G 3536, "Uncoated Stress-Relieved Steel Wires and Strands for Prestressed Concrete."
[9] JIS G 3502, "Piano Wire Rod."

	Concrete Pour Date	Specified Strength f_c' (kg/cm^2)
F1	2-12-97	300
F2	2-28-97	300
F3A	5-8-97	300
F3B	5-8-97	450
F4	7-2-97	450
C1	11-11-98	450
C2	12-10-98	450
C3	1-5-99	450
C4	1-28-99	450
D1	3-3-99	450
D2	4-12-99	450
D3	4-15-99	450
F5	5-24-00	300
F6	6-9-00	450

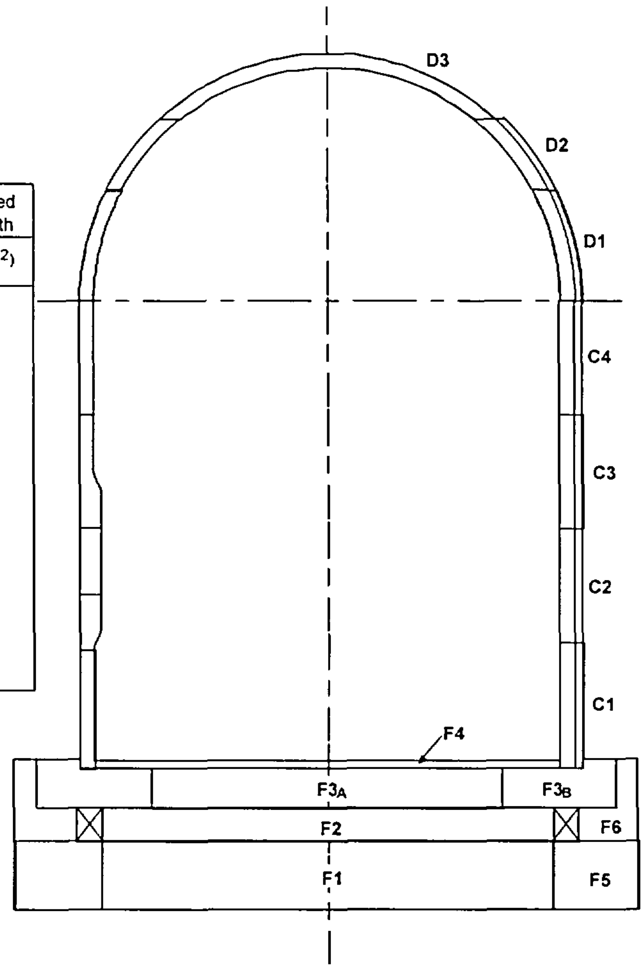

Figure 2.7 PCCV Concrete Lifts and Strengths

Table 2.2 JIS G 3112 Reinforcing Steel Properties

Grade	SD345	SD390	SD490
Model Location	Shell shear ties	Shell main bars, basemat shear bars	Basemat main bars
F_y min	343MPa ~50 ksi	392MPa ~57 ksi	490MPa ~71 ksi
F_t min	490MPa ~71 ksi	559MPa ~81 ksi	618MPa ~90 ksi
Elong.	18-20%	16-18%	12-14%

Table 2.3 JIS G 3112 Bar Properties
(Comparison with ASTM Standard Rebar)

	Nom. Diameter (d)		Nom. Area		Nom. Weight	
	millimeters	in	cm^2	in^2	kg/m	lb/ft
D6 (#2)	6.35	0.25	0.317	0.05	0.25	0.17
D10 (#3)	9.53	0.375	0.713	0.11	0.56	0.38
D13 (#4)	12.7	0.5	1.267	0.2	1	0.67
D16 (#5)	15.9	0.626	1.986	0.31	1.56	1.05
D19 (#6)	19.1	0.752	2.865	0.44	2.25	1.51
D22 (#7)	22.2	0.874	3.871	0.6	3.04	2.04

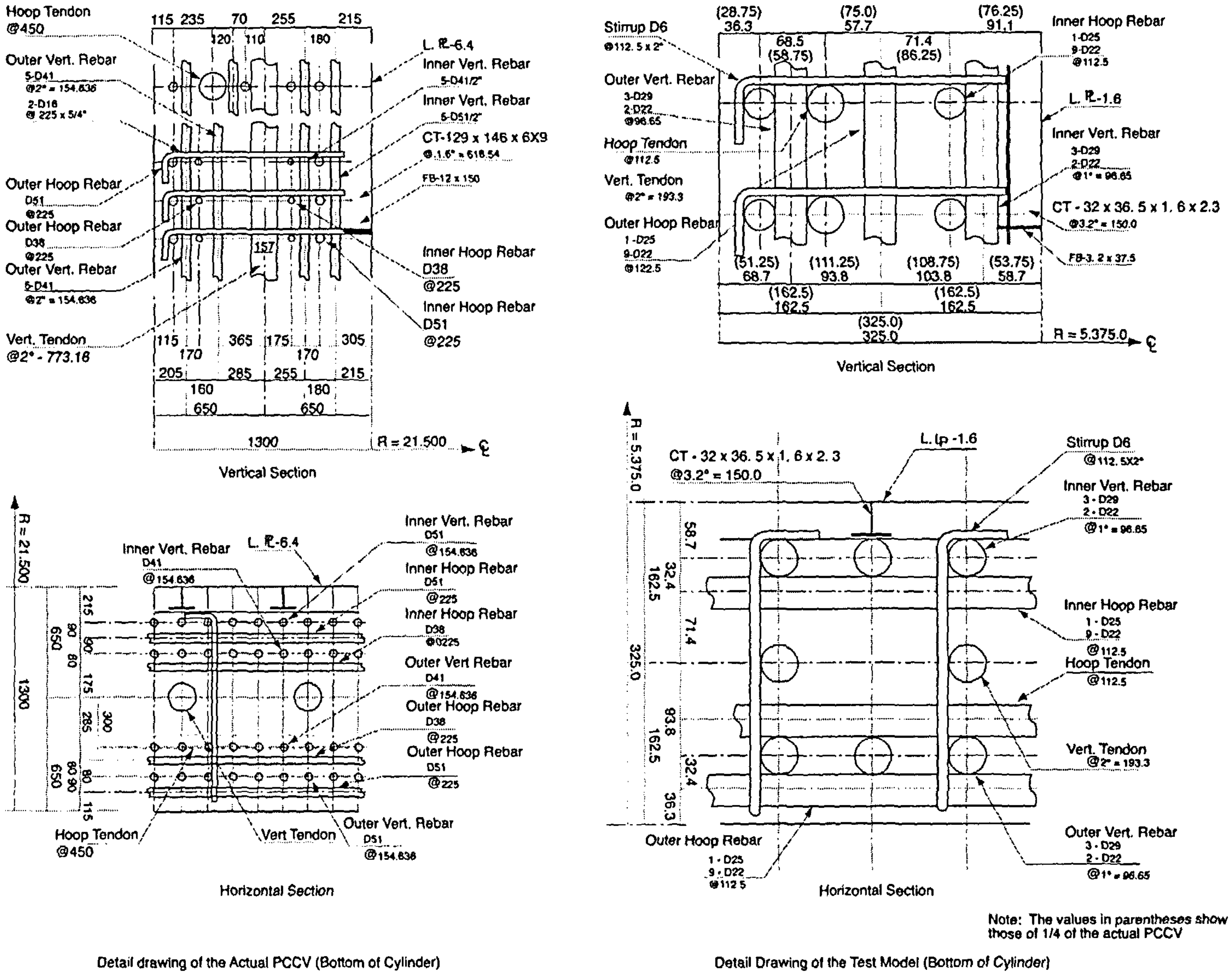

Figure 2.8 Arrangement of Reinforcing in the PCCV Prototype and Model at the Wall-Base Junction

Table 2.4 PCCV Model Tendon Strand Properties

Diameter:min nom max	13.5 millimeters 13.7 millimeters 14.1 millimeters	0.531 in 0.539 in 0.555 in
Area	1.131 cm^2	0.175 in^2
Yield Strength*	190 kN	42.7 kips
Tensile Strength	210 kN	47.2 kips
Min. Elongation	4.5%	4.5%

*Load at 0.2% elongation

Given the properties and arrangement of the tendons, the tensioning forces were specified to achieve the same effect in the model as the prototype, considering the unique features of the model prestressing system that do not scale. Three basic criteria were used to establish equivalence between the prototype and model prestressing.

1. First, the state of prestressing in the model should reflect the predicted state of stress in the prototype after reaching its 40-year design life. Since the model was tested approximately six months after tensioning the tendons, it was necessary to adjust the initial tensioning forces to account for the expected creep and relaxation losses in the prototype.
2. Second, the effective hoop compressive stress due to prestressing should be the same in the model as the prototype. This relates directly to the requirement that the hoop tensile response and failure mode in the cylinder wall be accurately modeled.
3. Third, the vertical compressive stress in the concrete at the base of the cylinder wall should be the same in the model and the prototype. This relates directly to the requirement that the bending/shear response and failure mode at the base of the cylinder wall be accurately modeled.

Given these criteria, the following factors were considered:

1. Tendon friction: Tendon stresses decrease from the point where the tension load is applied, i.e., the anchor, due to friction between the tendon and the sheath and between the strands themselves. Two components of friction are considered in the design; 'wobble' friction, λ, which results from the internal friction between the tendon strands and ducts, and angular friction, μ, which occurs as a result of sweeping the tendons around a curve. The tendon stress at any point, σ_x, along the length of the tendon is given by:

   $$\sigma_x = \sigma_o e^{-(\mu\alpha + \lambda l)}$$

   where s_o is the applied tension, α is the arc length, and l is the distance from the anchor along the tendon.

   The values of μ and λ used in the design of the prototype were 0.14 and 0.001, respectively. Since the model strands were actually larger in diameter than those used in the prototype (and therefore stiffer) and bent to a '4x' tighter radius, tests of the model tendons resulted in values for angular and wobble friction coefficients of

   $$\mu = 0.21, \lambda = 0.001$$

2. Setting Losses: After the tendons are tensioned, the tensioning forces are locked in by seating the strands in the anchor blocks using tapered wedges. During this process, there is some loss of anchor force due to slipping and settling of the anchor components. The tensioning hardware (anchors, wedges, jacks, etc.) cannot be scaled and as a result, the maximum setting loss specified for the model, 5 mm (0.2"), is larger than the scaled setting loss and nearly equal to the actual setting loss specified for the prototype. (The setting loss, specified in terms of length, is the measured change in length of the projecting tails of the tendons strands before and after anchoring.)

The larger setting loss, coupled with the higher friction coefficients for the model, result in stress profiles in the model tendons that are much less uniform than those in the prototype.

3. Gravity: For geometric scaling, mass densities are not scaled correctly if the same materials are used to construct the model and the prototype. For static tests, this only affects the dead load stresses, which, typically, are only a small percentage of the total stress. For the static overpressurization tests of the PCCV, this scaling artifact would not significantly affect on the model response, except, possibly, at the wall-base junction. Compressive stresses due to dead load are larger at the base of the cylinder wall than anywhere else in the model, and this stress may be an important response component for a bending/shear failure mode. Consequently, vertical tendon design loads were increased in the PCCV model to compensate for the reduced stress due to dead load at the wall-base junction.

The final tendon design stress profiles are shown in Figure 2.9. The profiles are given for a typical hoop tendon in the cylinder wall and for the longest and shortest vertical hairpin tendons. The stress distribution for the shorter hoop tendons in the dome and for both hoop and vertical tendons deflected around penetrations are not shown but can be calculated in a similar manner. (Note that the design tensioning and anchor forces for 'deflected' tendons are not adjusted in either the prototype or the model, to account for additional friction losses due to 'in-plane' curvature.) The corresponding design anchor forces are given in Table 2.5. These values were included in the model prestressing specifications. The as-built prestressing results are summarized in Section 2.2.3.

Table 2.5 PCCV Model Design Prestressing Anchor Forces

Tendons	Tensioning Force	Lift-Off Force	Losses (Creep and Relaxation)*	At Test
Vertical Tendons	49.6 tonnes (109.3 kips)	46.3 (102.1)	3.1 (6.8)	43.2 (95.3)
Hoop Tendons	44.4 tonnes (97.9 kips)	34.1 (75.2)	3.1 (6.8)	31 -68.4

*Losses evaluated at six months.

Considering the design tendon stress profiles, the prestressing design criteria can be satisfied. For the prototype, the average hoop tendon stress after 40 years is 85.3 kg_f/mm^2 (121.3 ksi). Calculating the equivalent pressure, p_{eqv}:

$$p_{eqv} = \frac{\sigma a}{R s} = \frac{(85.3\ kg_f/mm^2)(5429\ mm^2)}{(2150\ cm)(45\ cm)} = 4.8\ kg_f/cm^2\ (68\ psi)$$

where

a = the area of the tendon,
R = the inside radius of the containment, and
s = the hoop tendon spacing.

For the model, the average hoop stress after six months is 85.7 kg_f/mm^2 (121.8 ksi) and the equivalent pressure is:

$$p_{eqv} = \frac{\sigma a}{R s} = \frac{(85.7\ kg_f/mm^2)(339.3\ mm^2)}{(537.5\ cm)(11.25\ cm)} = 4.8\ kg_f/cm^2\ (68\ psi)$$

which is essentially identical to the prototype. Comparing the design pressure, P_d, the hoop prestressing is equivalent to applying a counterbalancing pressure of 120% of the design pressure.

$$\frac{P_{eqv}}{P_d} = \frac{4.8 kg_f/cm^2}{4.0 kg_f/cm^2} = 1.20$$

Comparing the concrete compressive stress at the base of the wall:

For the prototype after 40 years:

$$\sigma_c = \frac{\sigma a}{t\,s} = \frac{(106.3\ kg_f/mm^2)(5429\ mm^2)}{(130\ cm)(77.32\ cm)} = 57.4\ kg_f/cm^2\ (817\ psi)$$

Concrete compressive stress due to Dead Load 15.2 kg_f/cm^2 (216 psi)

Total compressive stress in Concrete 72.6 kg_f/cm^2 (1,033 psi)

where t is the thickness of the containment wall and s is the vertical tendon spacing.

For the model after 6 months:

$$\sigma_c = \frac{\sigma a}{t\,s} = \frac{(127.5\ kg_f/mm^2)(339.3\ mm^2)}{(32.5\ cm)(19.33\ cm)} = 68.9\ kg_f/cm^2\ (980\ psi)$$

Concrete compressive stress due to dead load 3.2 kg_f/cm^2 (46 psi)

Total compressive stress in concrete 72.1 kg_f/cm^2 (1025 psi)

Therefore, the higher vertical tendon stress in the model, when combined with the dead load stress, yields nearly the same compressive stress in the concrete as the prototype.

2.2 Construction

2.2.1 General Construction

Prior to construction of the PCCV model, during the initial development of the containment test site in 1993, the location of the PCCV model was selected, the surface soil was removed, and the existing subgrade was excavated to a depth of over 8 m (25') and replaced with a compacted engineered backfill. The allowable bearing capacity, based on limiting soil settlement to 25 mm (1") or less, is 3.11 kN/m^2 (6.5 ksf) [26].

The overall site plan was shown in Figure 1.3. A detail of the areas surrounding the PCCV model is shown in Figure 2.10. The model was oriented so the E/H opening was facing due south. (This was primarily for operational considerations rather than any test requirement.) An aerial view of the test site during construction is shown in Figure 2.11.

On-site construction of the model by Hensel Phelps Construction Co. commenced on January 3, 1997 with construction of a 19.8 m × 19.8 m × 30 centimeters thick (65' × 65' × 1') mudmat placed on the engineered back-fill (Figure 2.12). This mudmat was constructed of 'lean' concrete and reinforced with welded wire fabric to provide a level working surface on which to construct the model. Benchmark monuments were constructed of small concrete pads at each of the four cardinal azimuths (0 degrees, 90 degrees, 180 degrees, and 270 degrees) outside the perimeter of the construction zone. These control points were subsequently used for the model's layout.

After the mudmat concrete had cured, a steel frame to support the basemat rebar was erected (Figure 2.13) and the rebar for the first basemat lift (F1) was erected (Figure 2.14). After verifying the position of the rebar (Figure 2.15), the formwork was set (Figure 2.16) and the F1 concrete placed (Figure 2.17). While F1 concrete was placed directly on the mudmat, there was no positive connection between the two.

Most of the model reinforcing was prefabricated by Border Steel Co., El Paso, TX, although some field fabrication was required as the construction progressed. All concrete was batched by Lafarge Construction Materials (formerly doing business as Western Mobile NM), Albuquerque, NM, mixed in transit and placed by pumping. All sampling and quality control tests were conducted by AGRA Earth and Environmental, Inc., Albuquerque, NM. Slump (Figure 2.18) and air entrainment tests were conducted on each batch/truck of concrete delivered to the site and standard cylinders and beams

	Cylinder Hoop Tendon	Vertical Dome Tendon

The Actual PCCV

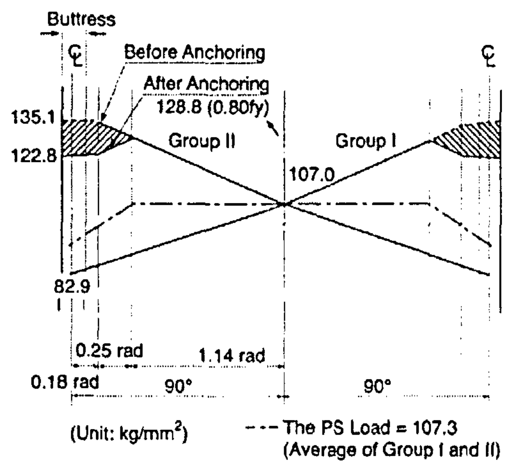

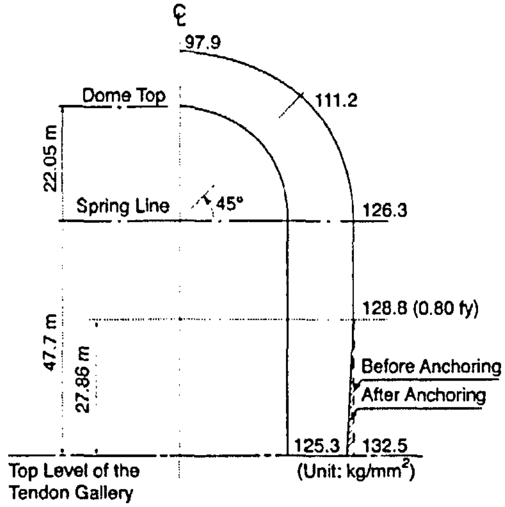

The Test Model

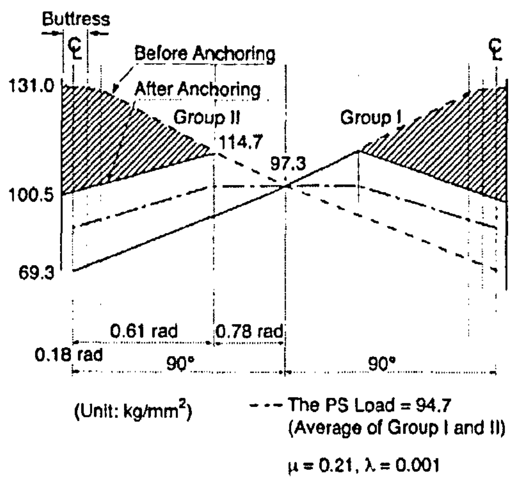

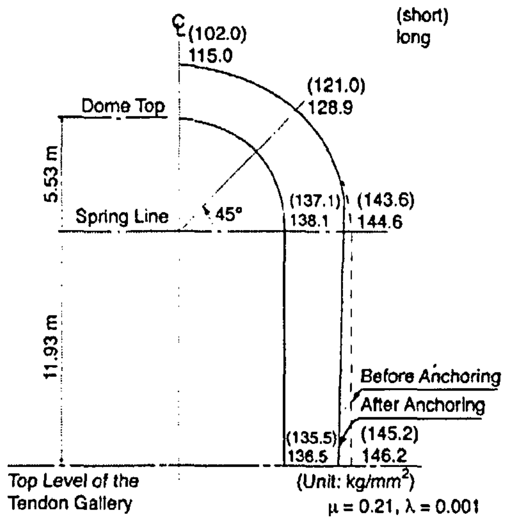

PS Load (unit: kg/mm²)

The Actual PCCV:

Portions		The PS Load	The Tendon Losses	The PS Load (after 40 years)	Tensioning Force (t) Before Anchor	Tensioning Force (t) After Anchor
Cylinder Hoop Tendon	Cylinder	107.3	22	85.3	733.5	666.7
Vertical Dome Tendons	Dome Top	97.9	19	78.9	719.3	680.3
	Spring Line	126.3	19	107.3		
	Cylinder Center	128.6	19	109.6		
	Anchored Portion	125.3	19	106.3		

The Test Model:

Portions		The PS Load	The Tendon Losses	The PS Load (after 40 years)	Tensioning Force (t) Before Anchor	Tensioning Force (t) After Anchor
Cylinder Hoop Tendon	Cylinder	94.7	9	85.7	44.4	3.1.1
Vertical Dome Tendons	Dome Top	(102.0) 115.0	9	(93.0) 106.0	(49.3) 49.6	(46.0) 46.3
	Spring Line	(137.1) 138.1	9	(128.1) 129.1		
	Cylinder Center	(136.3) 137.3	9	(127.3) 128.3		
	Anchored Portion	(135.5) 136.5	9	(126.5) 127.5		

Figure 2.9 PCCV Prototype and Model Tendon Design Stress Profiles

were cast (Figure 2.19) for testing at seven, 28, and 91 days and at the time of tensioning and pressure testing. Both standard-cure, SC, (two to four days in a water bath, then stored in a humidity controlled chamber until testing), and field-cured (FC) specimens (two to seven days in a water bath, then stored on-site until testing) were produced and tested.

Installation of rebar and concrete placement for F2, F3, and F4 followed a similar sequence (Figures 2.20-2.25). Strain gages and thermocouples (T/Cs) were mounted on some of the rebar prior to installation and the lead wires were routed through the forms prior to concrete placement. As noted previously, the concrete outside the tendon gallery was not placed, thus allowing access for insertion and tensioning of the vertical tendons. The bottom basemat rebar that extended beyond the initial basemat lifts was covered with a temporary plywood deck to protect it from damage during construction until the final basemat pours (F5 and F6) were made. Other rebar that extended beyond lifts F1 to F4 were terminated and equipped with mechanical splices.

Prior to construction of the cylinder wall, a mock-up of the wall, incorporating the E/H embossment, vertical buttress, tendon sheaths, and the liner, was constructed to develop and demonstrate the erection sequence and method for placing the cylinder wall concrete (Figure 2.26). Since the wall lifts were approximately 3 m (10') in height, form 'windows' were located at mid-height (Figure 2.27) to limit the drop height of the wet concrete. Due to the dense rebar pattern, the trunk of the concrete pump could not be inserted into the forms. After placing the concrete through the form window and using spud-type vibrators to consolidate the concrete and prevent voids, the windows were blocked and placement of concrete continued at the top of the mock-up. After the concrete had cured and the exterior form was removed, the mock-up was cored to inspect for voids in the concrete. None were discovered. While this sequence of construction was not completely identical to the sequence for the model wall (e.g. continuing vertical wall reinforcing would limit placement at the top of each lift), the mock-up demonstrated that the planned construction sequence would be successful.

Since New Mexico is subject to severe summer lightning storms and the PCCV model is in an exposed desert terrain, a lightning protection system, consisting of four 30 m (100') poles connected to a buried copper cable counterpoise, was installed around the model. The lightning protection system provides an alternate path to ground around the model, thereby preventing direct lightning strikes that might damage the instruments, wires, and data acquisition components. Until the dome was completed, only two of the poles at 0 degrees and 180 degrees could be installed to accommodate crane operations, thereby providing only partial protection. Nevertheless, the protection system appears to have functioned successfully, since no direct lightning strikes were ever recorded on the model, even though there was a strike on the chain-link fence surrounding the site that damaged unprotected telephone lines strung along the fence.

While the basemat and wall mock-up construction was being completed, the liner panels, which had been fabricated by MHI in Kobe, Japan, were shipped to the test site. The liner panels arrived at the site in June, 1997 (Figure 2.28). Prior to shipping the panels to the U.S., all the cylinder wall panels were temporarily erected in Kobe to ensure that they would fit. Typical liner panels with support jigs are shown in Figure 2.29.

At the same time the liner panels were being shipped, an internal structural steel frame was fabricated (in the U.S.) and also delivered to the test site. This structure, known as the instrumentation frame, provided the support structure from which to hang the liner panels, with jigs, prior to welding; provided internal support during concrete placement; and provided a work platform during liner welding and installation of the internal instrumentation. During testing, this internal frame also acted as the reference structure for measuring model displacements. Components and erection of the instrumentation frame are shown in Figures 2.30-2.33.

Beginning in September, 1997, the liner panels were erected and bolted to the frame (Figures 2.34-2.36). After all the panels were assembled, a crew of welders from MHI began welding the liner seams. First, the basemat liner plates were welded to the embedded anchors. The liner erection plan then called for the seam between the first liner ring and the basemat to be welded, followed by the horizontal seam between the first and second liner rings. After this, the vertical seams for the first ring were completed. The liner erection and welding specifications defined overall and local dimensional tolerances and nondestructive inspection criteria. All liner welds were radiographed and inspected for flaws (undercutting, inclusions, and porosity). Initial difficulties welding the 1.6 mm liner in the field resulted in most of first ring's liner welds is being rejected. These welds were then ground out and repair welds were made. While there was some improvement, some of the repair welds contained flaws that exceeded the welding specifications. After additional repairs, inspection, and laboratory tests of welded liner specimens, it was decided that the original welding specifications were overly conservative and the criteria on flaws were relaxed. (The original weld flaw acceptance criteria had been scaled from the prototype welding specifications.)

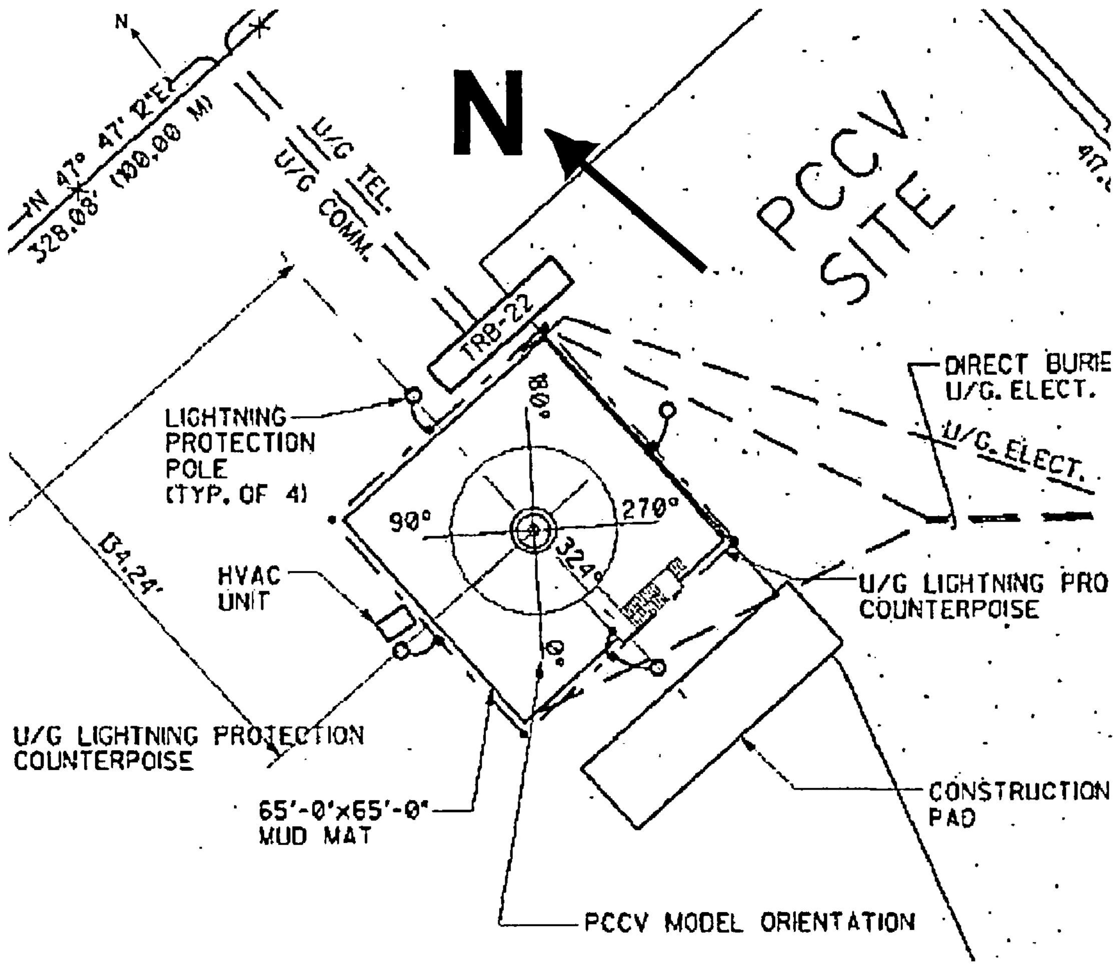

Figure 2.10 PCCV Model Layout

For the 6.4 mm (1/4") thick liner in the prototype, the liner seam welds could be made using double-sided full penetration welds. However, this method of welding could not be used for the 1.6 mm (1/16") thick model liner welds. The field welds in the model liner required back-up bars or, in some locations, back-up tape, and the full penetration welds were made from one side. Where welds were ground out and repaired, it was sometimes necessary to remove a section of the back-up bar and replace it with another segment. (Note that this created some local discontinuities in the model liner that became important during the pressure tests, but which were not representative of details in the prototype.) In areas where liner strains were expected to be high due to geometric discontinuities, the back-up bars were removed after the liner welds were completed to maintain the similarity with the prototype. In some locations, the weld bead was ground to reduce its profile, as well.

Both of these cosmetic post-weld treatments may have caused local thinning of the liner. Unfortunately, no measurements of the post-weld liner thickness were made. After the liner seam welds were completed, the penetration insert assemblies were welded to the liner and the stiffener, and liner anchor welds were completed.

To expedite the liner strain gage installation and the model's erection, a number of strain gages on the exterior surface of the liner, i.e. the concrete side of the liner, were installed prior to erection and welding of the liner panels. Since heat input from the welding operations could damage strain gages near the weld seams, only those gages over 10 cm (4") from the weld seams were installed prior to erection. This included gages on the liner anchors and stiffeners. Figure 2.36 shows two liner panels during installation of the strain gages. After the liner panels were erected and welded, the exterior

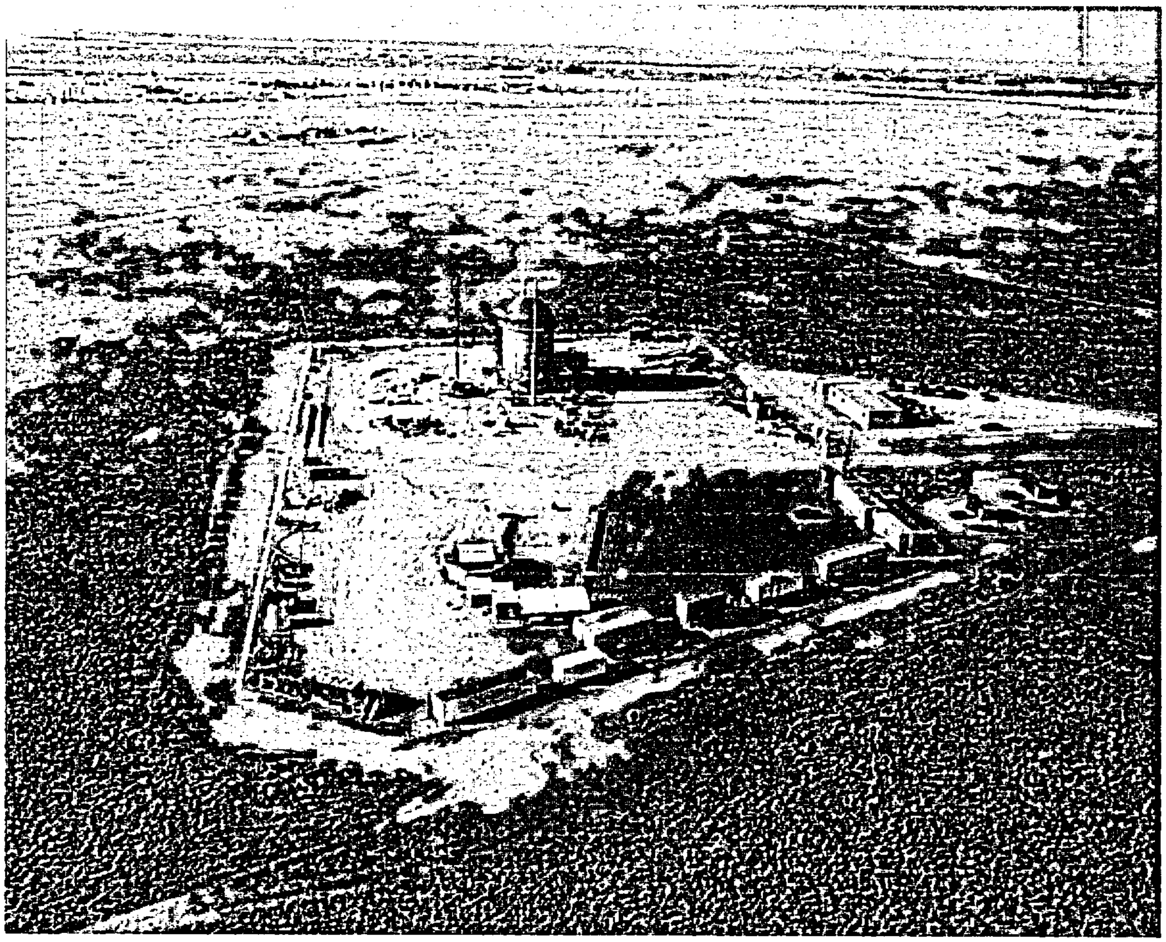

Figure 2.11 Aerial View of CTTF-West during PCCV Construction (March, 1999)

strain gages near the liner weld seams were installed. Figures 2.38 and 2.39 show typical strain gage installations near weld seams.

After all weld inspection criteria had been satisfied, construction of the model proceeded with the installation of inner horizontal and vertical rebar layers in the cylinder and dome (Figures 2.40-2.41). All instrumented rebar for these two layers was installed concurrently with the remainder of the reinforcing steel.

Next, the tendon sheath support frame, consisting of steel angles with support pins to correctly position the tendon sheaths, was installed (Figure 2.42). Except for the instrumented hoop tendons, which were preassembled with the sheath, all the tendon sheaths were all installed prior to outer reinforcing and shear reinforcing (Figures 2.43 and 2.44). The model construction then proceeded by lifts; C1 through C4 in the cylinder, and D1 to D3 in the dome. For each lift, the outer and radial rebar, including instrumented rebar and any instrumented hoop tendons, were installed first. Lead wires for the liner, rebar and tendon strain gages, embedded T/Cs, and fiber optic strain gages, were then routed through PVC ducts that had been placed in the previous lift. After checking that the gages and lead wires had not been damaged and were still functioning, the outer concrete forms were installed and concrete for each lift was placed. After the concrete had cured sufficiently, the outer forms were stripped and the cycle was repeated until the final dome pour was completed. The final dome pour, D3, was completed without the use of external forms. The plasticizer was not added for this lift, so a low slump was maintained and the final surface was hand finished, aided by a wooden template that defined the outer surface. This sequence of construction is illustrated in Figures 2.45 through 2.52.

After the D3 concrete achieved its specified strength, the liner jigs were cut loose from the liner, detached from the interior frame, and removed. This freed the containment wall from the interior frame, making both structures independent of each other. The instrumentation frame then functioned as a work platform and as the reference frame for measuring shell displacements.

After the liner jigs were removed, model construction was temporarily suspended while SNL assumed control of the model for installing of the interior instrumentation. Details of the instrumentation installation are provided in Chapter 3. Prior to installing the interior instrumentation, the interior of the liner surface was cleaned and painted white. Cardinal lines were surveyed and marked on the liner as reference for the installation of the interior instrumentation. The as-built radii at the intersections of the cardinal lines were also determined, and the results are tabulated in Appendix C.

Prior to beginning the interior instrumentation, interior lighting, power, and ventilation were installed. Structural steel stairs to the top of the basemat and E/H were erected, and a vestibule with locking doors for access control was installed over the E/H opening. Machined flange covers were installed over the M/S and F/W penetration sleeves. Six of these covers were drilled for the sealed instrumentation feedthroughs and the remaining two were equipped for the power feedthrough and the pressurization line.

While the interior instrumentation was completed, construction activities resumed after an approximately six-month hiatus with the insertion of prestressing tendons into the sheaths. After the interior instrumentation was completed and verified ready for operation, the DAS was started prior to tensioning the tendons. Details of the prestressing operations and results are described in Section 2.2.3. After prestressing was completed, model construction concluded with the placement of the final basemat concrete lifts, F5 and F6 (Figure 2.53). After the forms were stripped, Mitsubishi and Hensel Phelps demobilized and turned the model over to SNL on July 28, 2000. The completed PCCV model is shown in Figure 2.54.

2.2.2 Material Properties

Properties of all the PCCV model construction materials, except for the model concrete, were determined from tests prior to construction and summarized in Section 2.1. Model concrete properties were determined by testing standard specimens (cylinders and beams) cast during placement of each concrete lift.

All concrete testing was conducted according to ASTM standards[10] and the results are summarized in Appendix B. Quality control tests, consisting of standard 6-inch cylinder, unconfined compressive strength tests, were performed by AGRA Earth and Environmental, Inc. Specimens were cast from nearly every truck of concrete placed in the model. (Each truck contained approximately 7.6 m^3 (10 cubic yards.)) Standard Cured (SC) specimens were cured in a water bath for two to four days (depending on weekends) and stored in a humidity-controlled chamber until tested. FC specimens were also cured in a water bath for two to four days, then stored at the site, under blankets, until tested. Compression tests[11] of both SC and FC cylinders were conducted at seven, 28, and 91 days. 91-day strengths were compared to the specified design strengths.

The average 91-day FC strength results for the first two cylinder wall lifts, C1 = 389kg_f/cm^2 (5527 psi) and C2 = 436kg_f/cm^2 (6200 psi), failed to meet the minimum specified design strength of 450 kg_f/cm^2 (6400 psi). This may have resulted from cold weather conditions, which might have retarded the curing rate. Analysis of the test data suggested that the concrete would reach the specified minimum design strength by the time prestressing was scheduled to occur, so no action was deemed necessary. Nevertheless, the curing method of FC specimens for lifts C4 through D3 and F5 and F6 was modified to keep the cylinders in the water bath for seven days. This modified field curing method is designated FC' in the material data summary.

While the strength of the concrete in C1 and C2 was deemed adequate, there was a concern that the low strength might cause higher creep losses than anticipated in the prestressing design calculations. Creep tests[12] of two specimens each from C1 and C2 were conducted at the University of New Mexico and compared to the results of the trial mix creep tests

[10] *Annual Book of ASTM Standards*, American Society for Testing and Materials (ASTM), Philadelphia, PA.
[11] ASTM C39-94, "Standard Test Method for Compressive Strength of Cylindrical Concrete Specimens."
[12] ASTM C512-87, "Standard Test Method for Creep of Concrete in Compression" (modified).

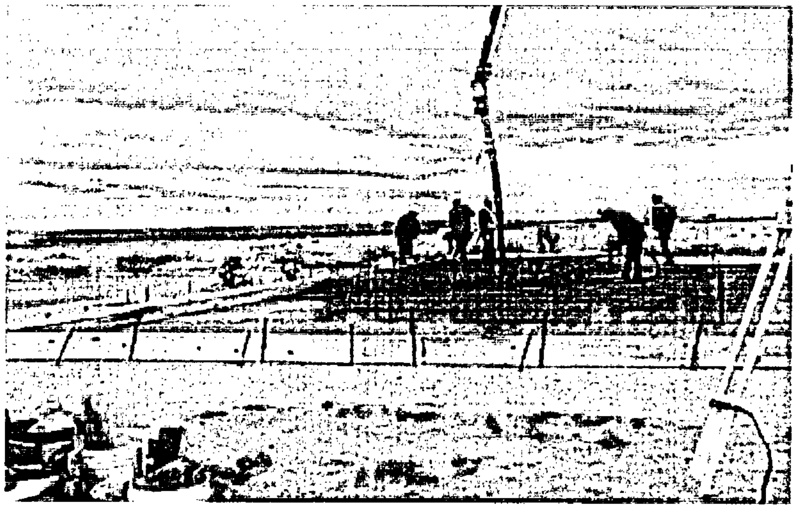

Figure 2.12 Placement of PCCV Mudmat

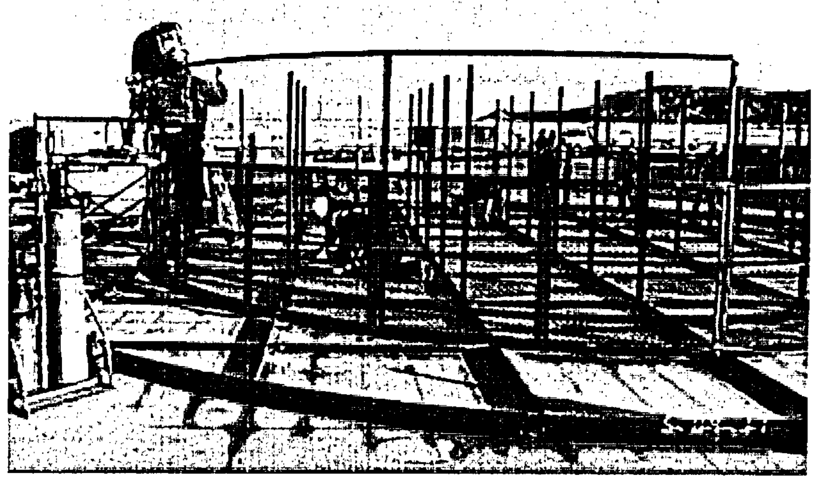

Figure 2.13 Basemat Rebar Support Frame

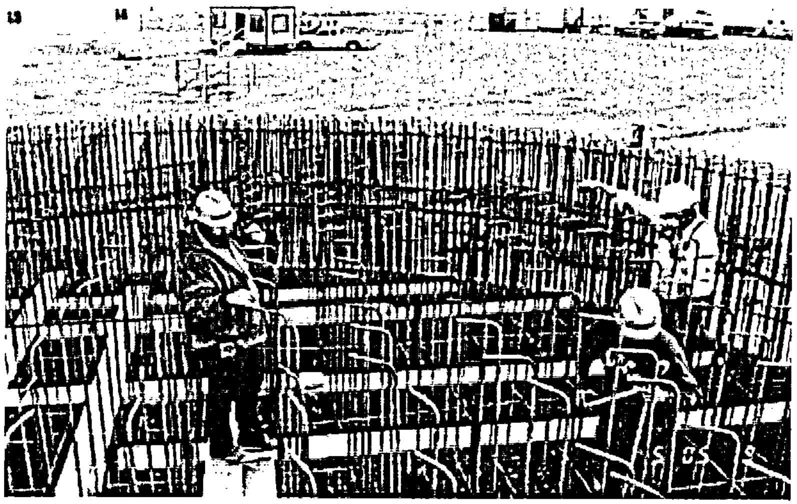

Figure 2.14 Basemat Bottom Bars and Vertical Ties

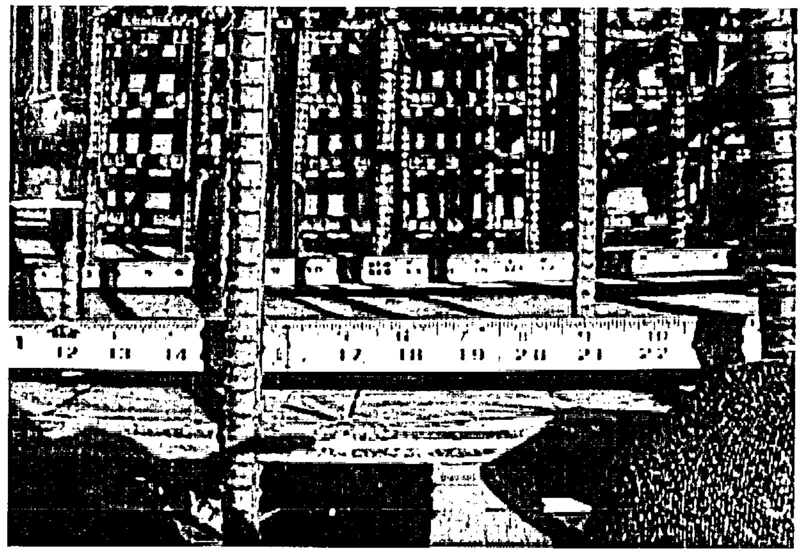

Figure 2.15 Measuring Rebar Location

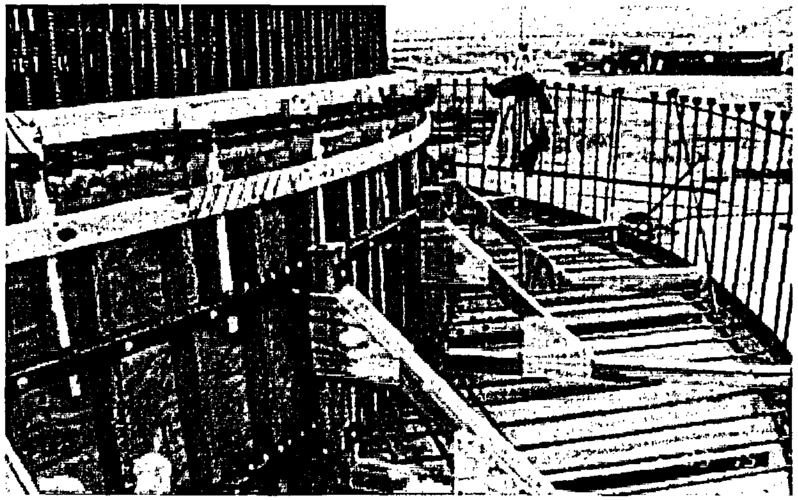

Figure 2.16 F1 Formwork

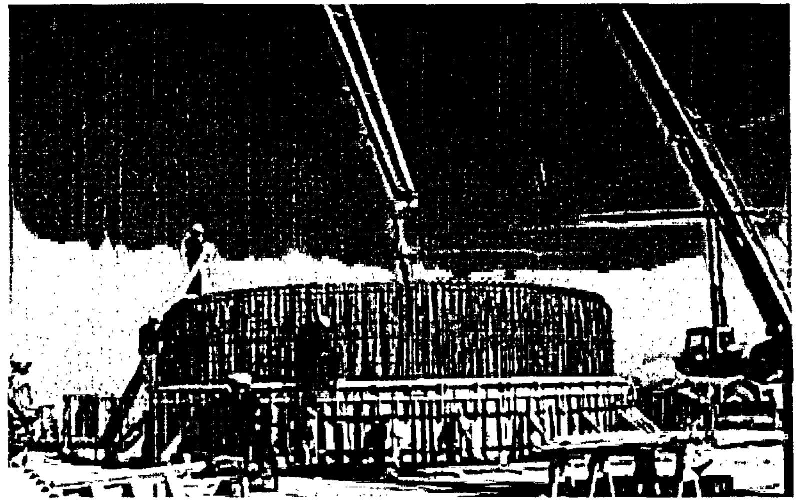

Figure 2.17 Placing F1 Concrete

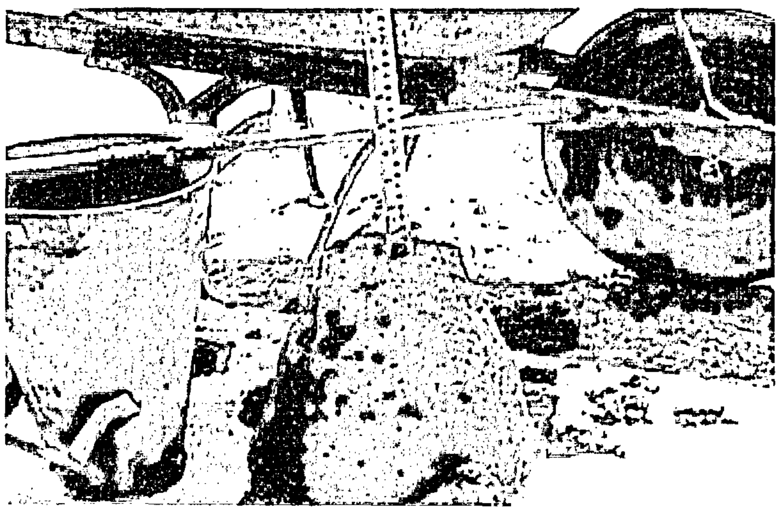

Figure 2.18 Measuring Concrete Slump

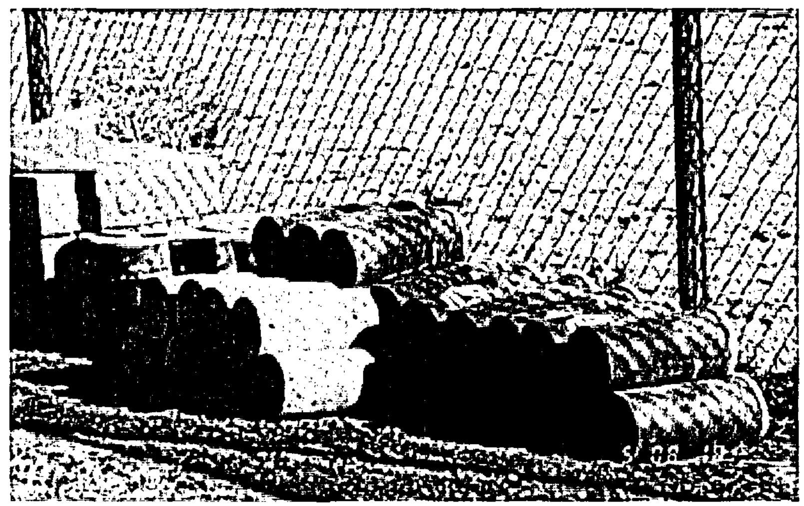

Figure 2.19 Concrete Test Cylinders and Beams

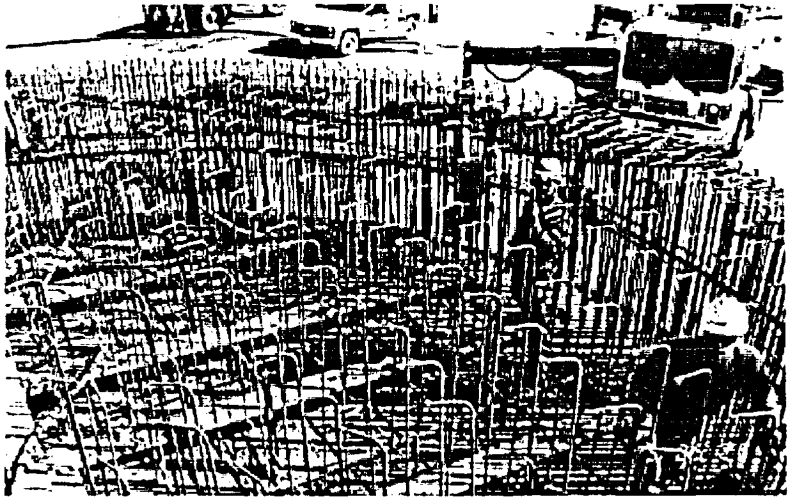

Figure 2.20 F2 Rebar Erection

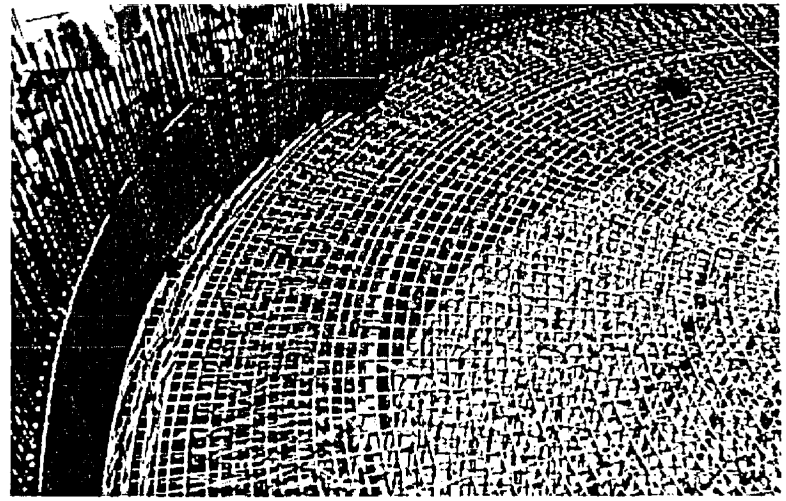

Figure 2.21 F3 Rebar

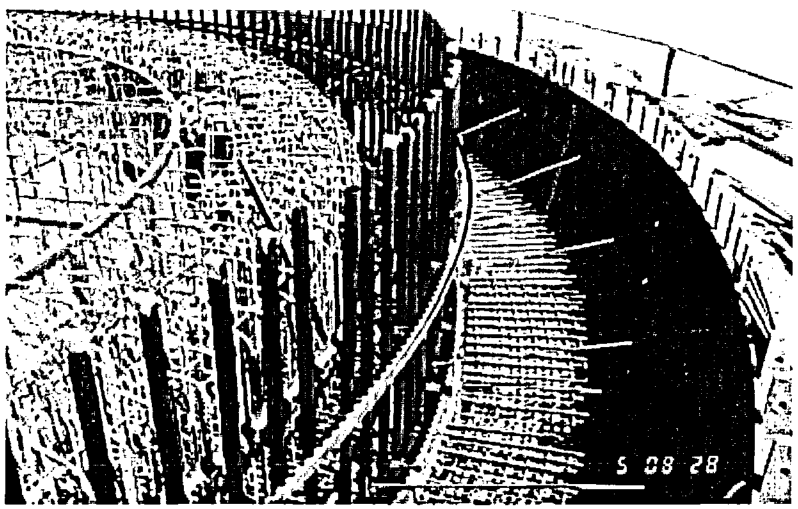

Figure 2.22 F3 Rebar and Formwork

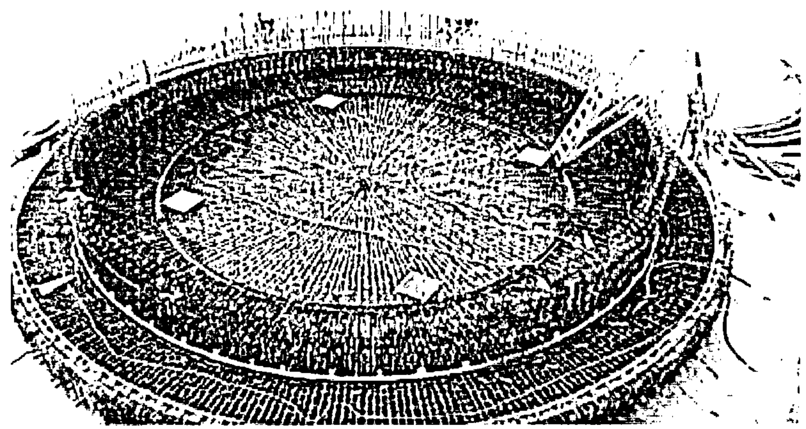

Figure 2.23 Basemat Top Rebar (F3) and Wall Dowels

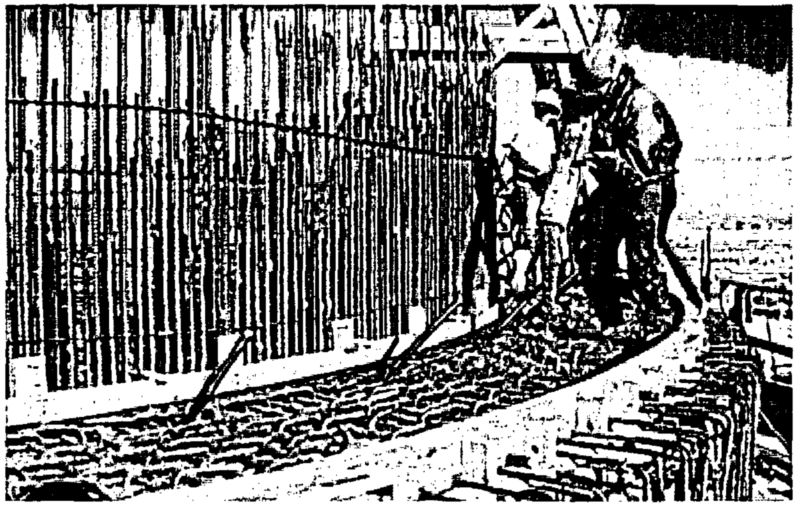
Figure 2.24 F3 Concrete Placement

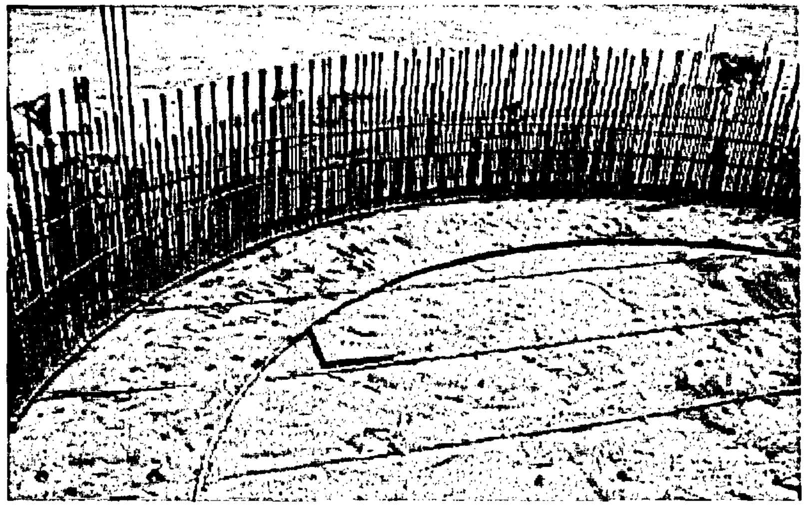
Figure 2.25 F4 Concrete


Figure 2.26 Wall Mock-Up Rebar

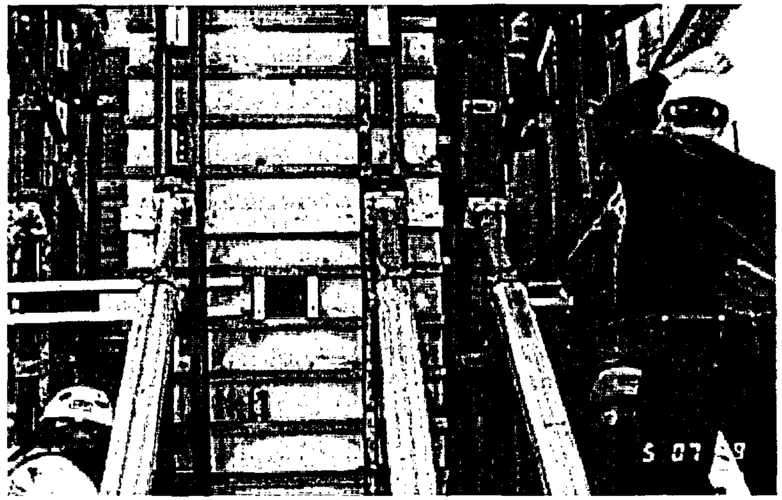
Figure 2.27 Wall Mock-up Form w/ Concrete 'Window'

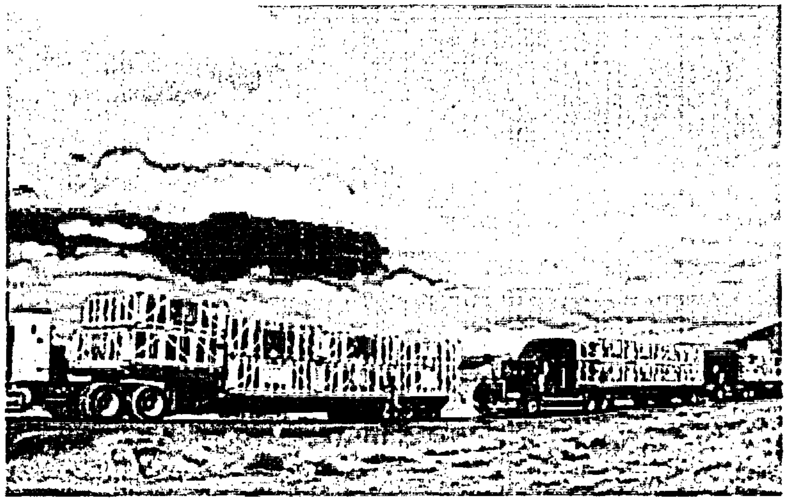

Figure 2.28 Delivery of Liner Panels

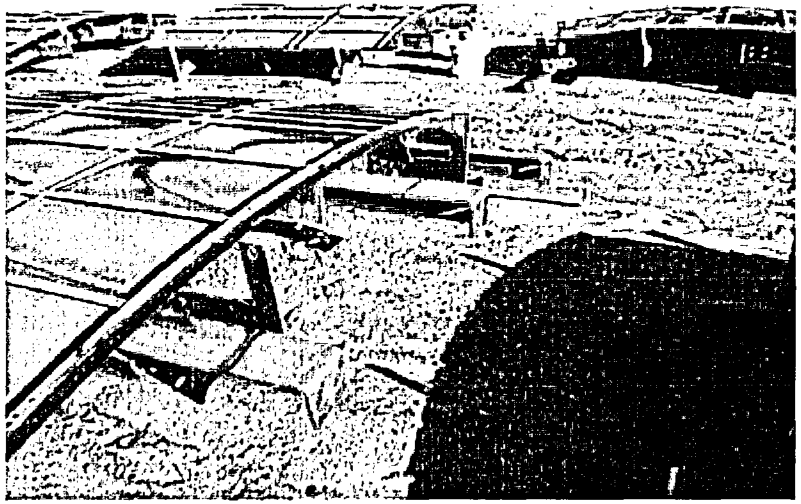

Figure 2.29 Liner Panels after 'Uncrating'

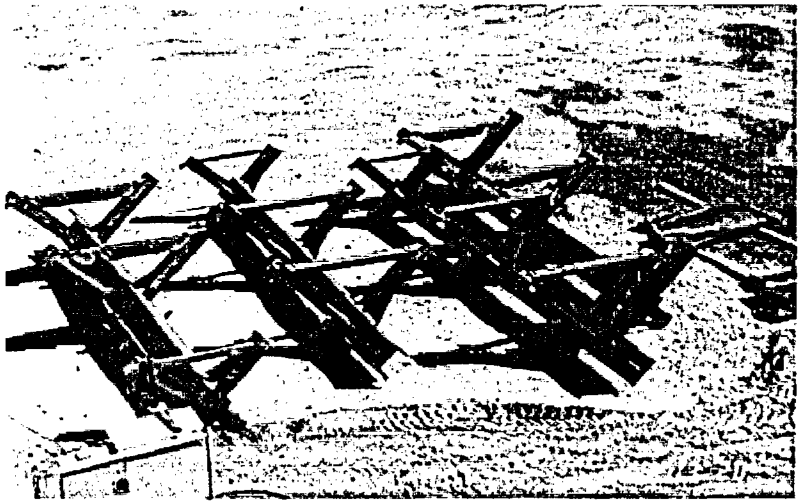

Figure 2.30 Instrumentation Frame Column 'Trees'

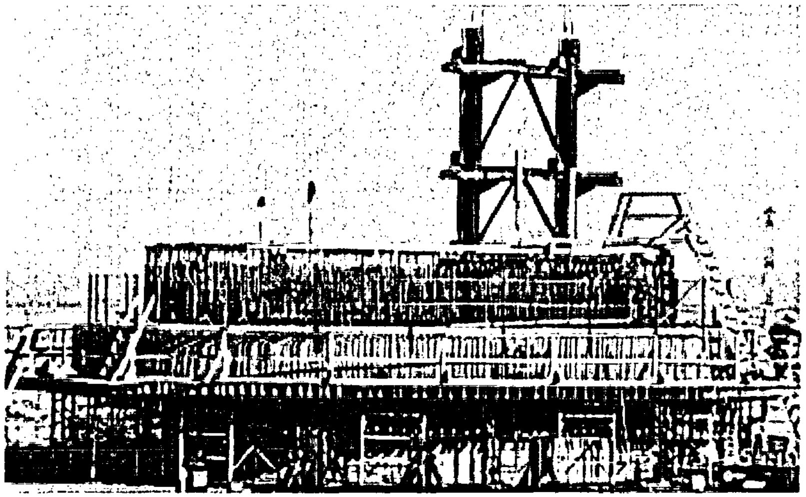

Figure 2.31 Instrumentation Frame Erection

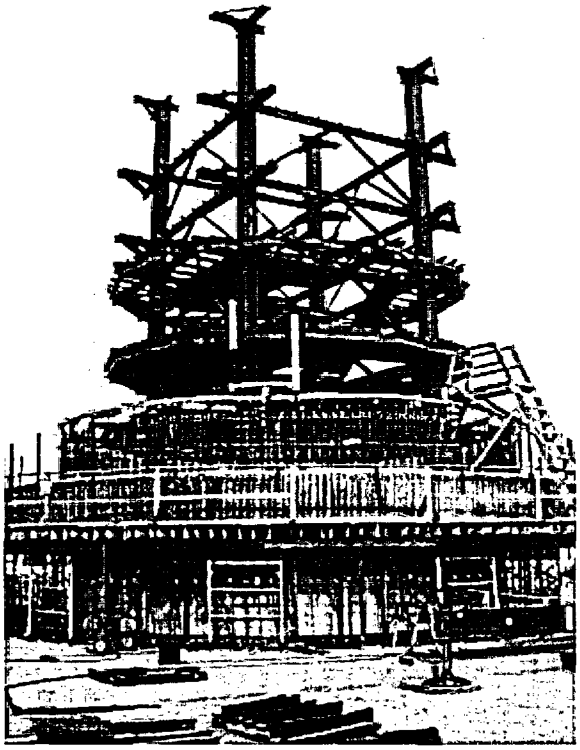

Figure 2.32 Instrument Frame Erection

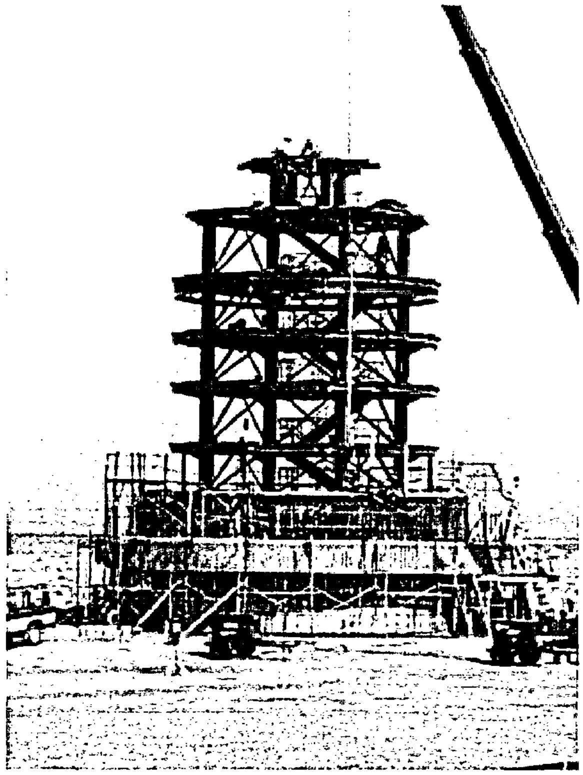

Figure 2.33 Completed Instrument Frame

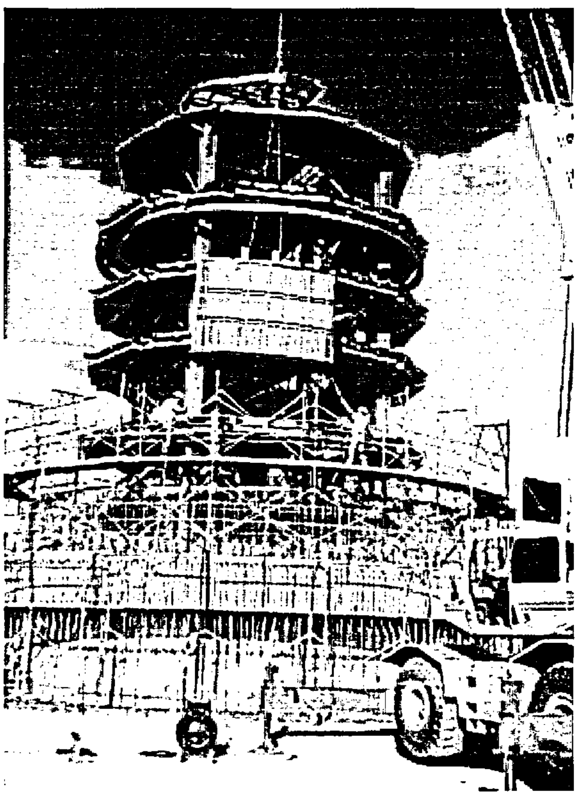

Figure 2.34 Liner Panel Erection

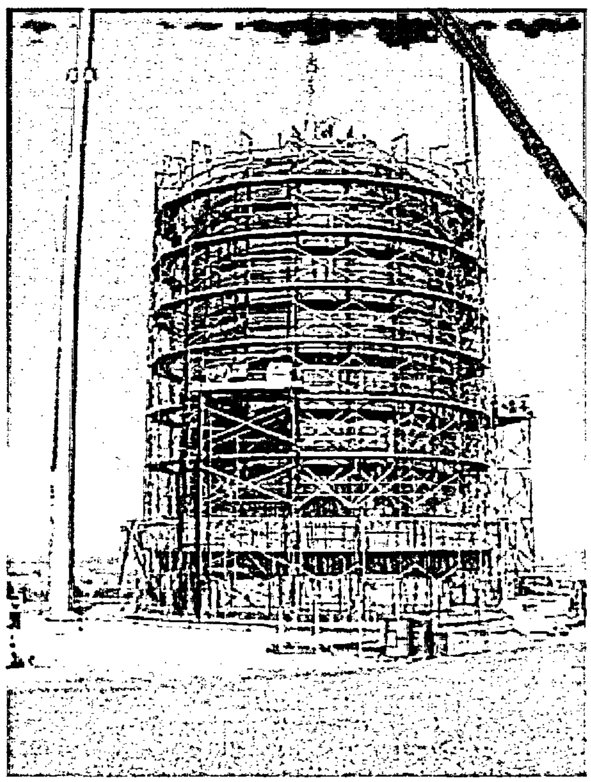

Figure 2.35 Dome Liner Erection

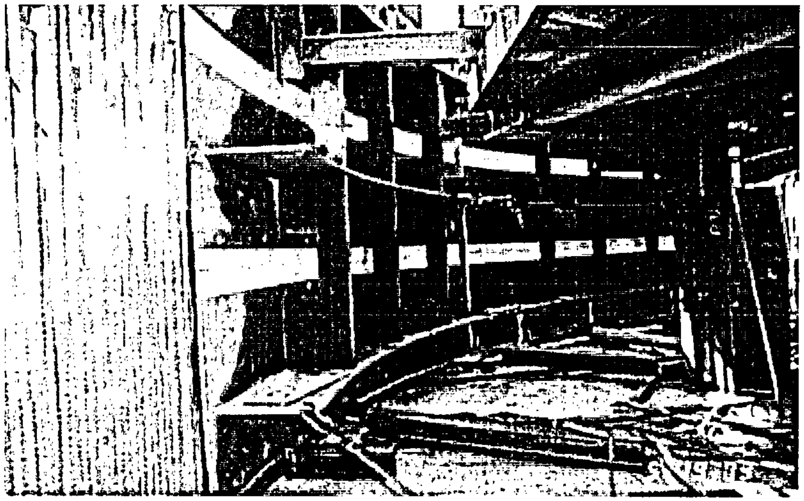

Figure 2.36 Liner Panels with Jigs

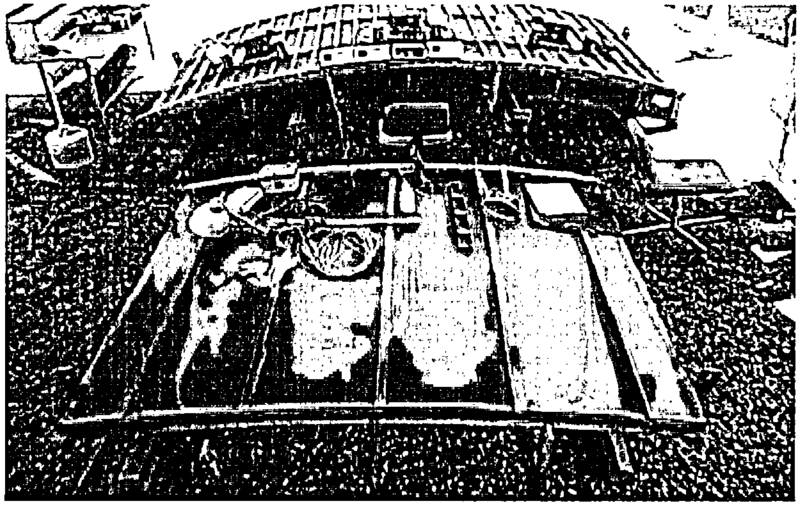

Figure 2.37 Liner Panel Instrumentation

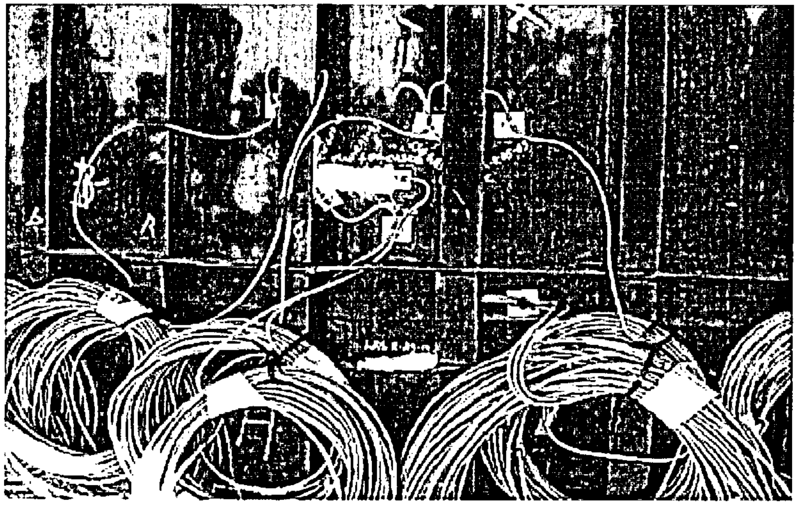

Figure 2.38 Liner Strain Gages after Welding

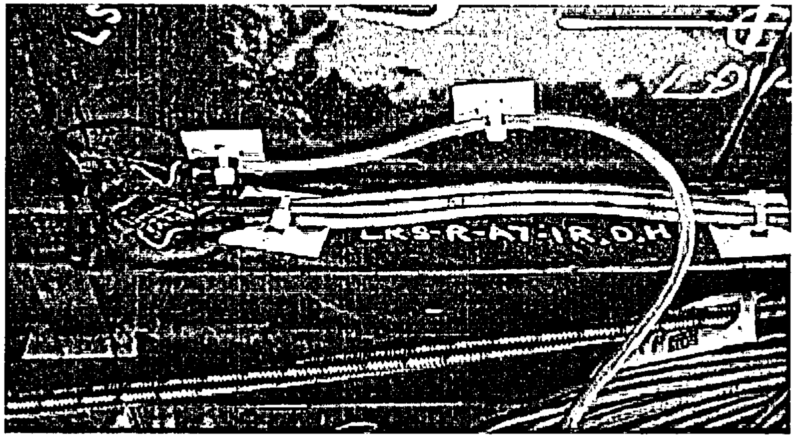

Figure 2.39 Close-Up of Liner Strain Gages near Weld

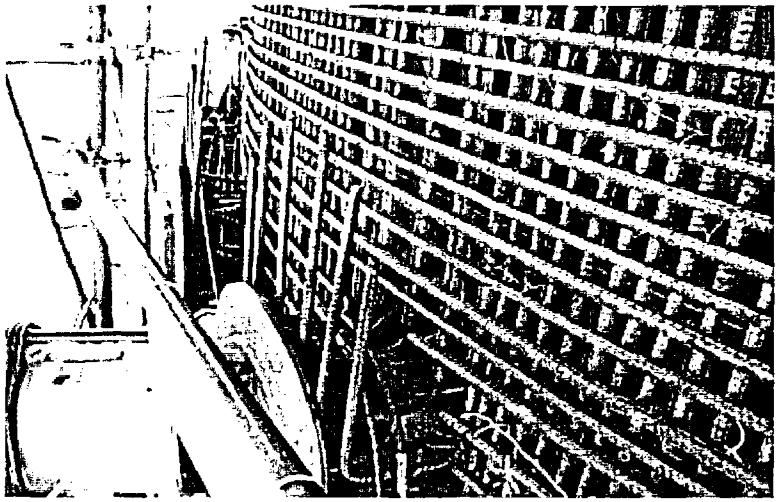

Figure 2.40 Inner Rebar at M/S Penetrations

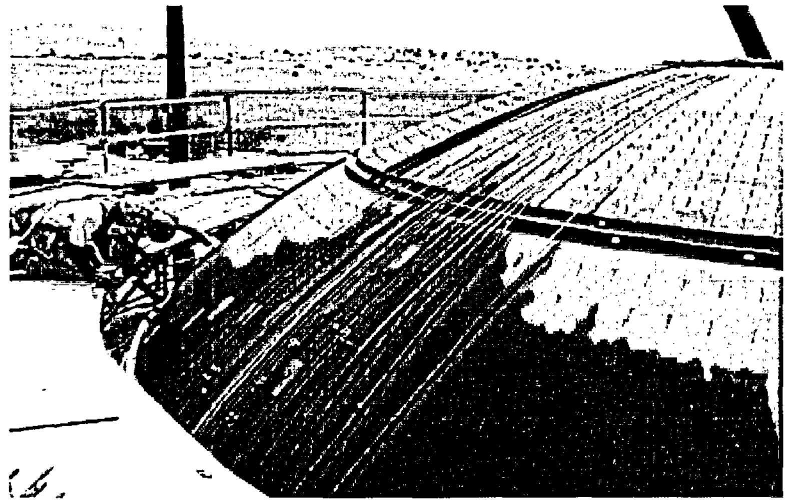

Figure 2.41 Installation of Inner Dome Rebar

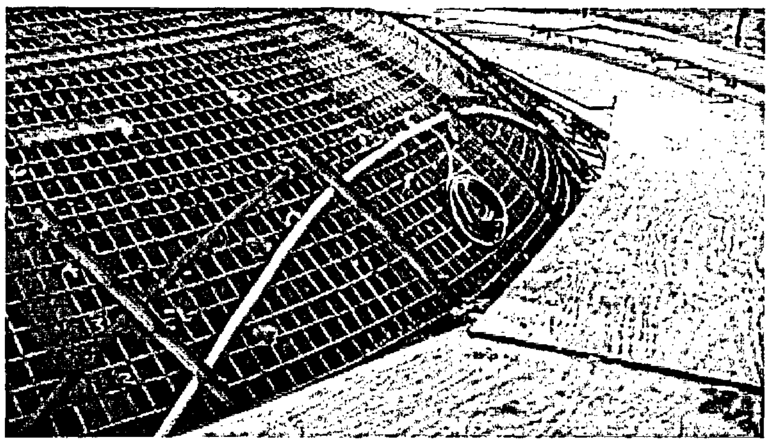

Figure 2.42 Tendon Sheath Support Frame

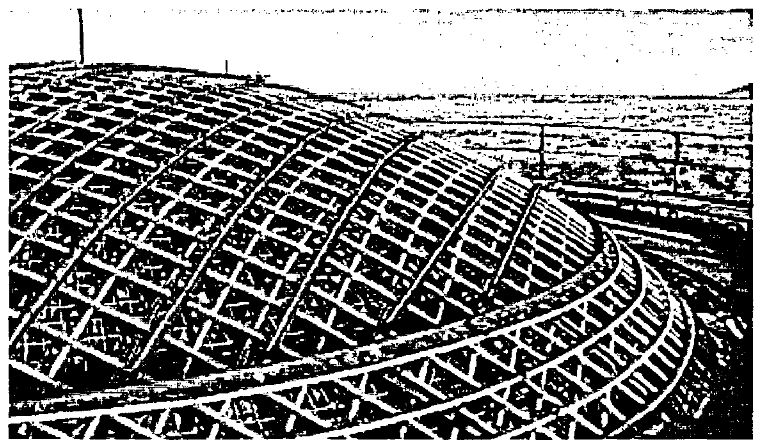

Figure 2.43 Dome Tendon Sheaths and Support Frame

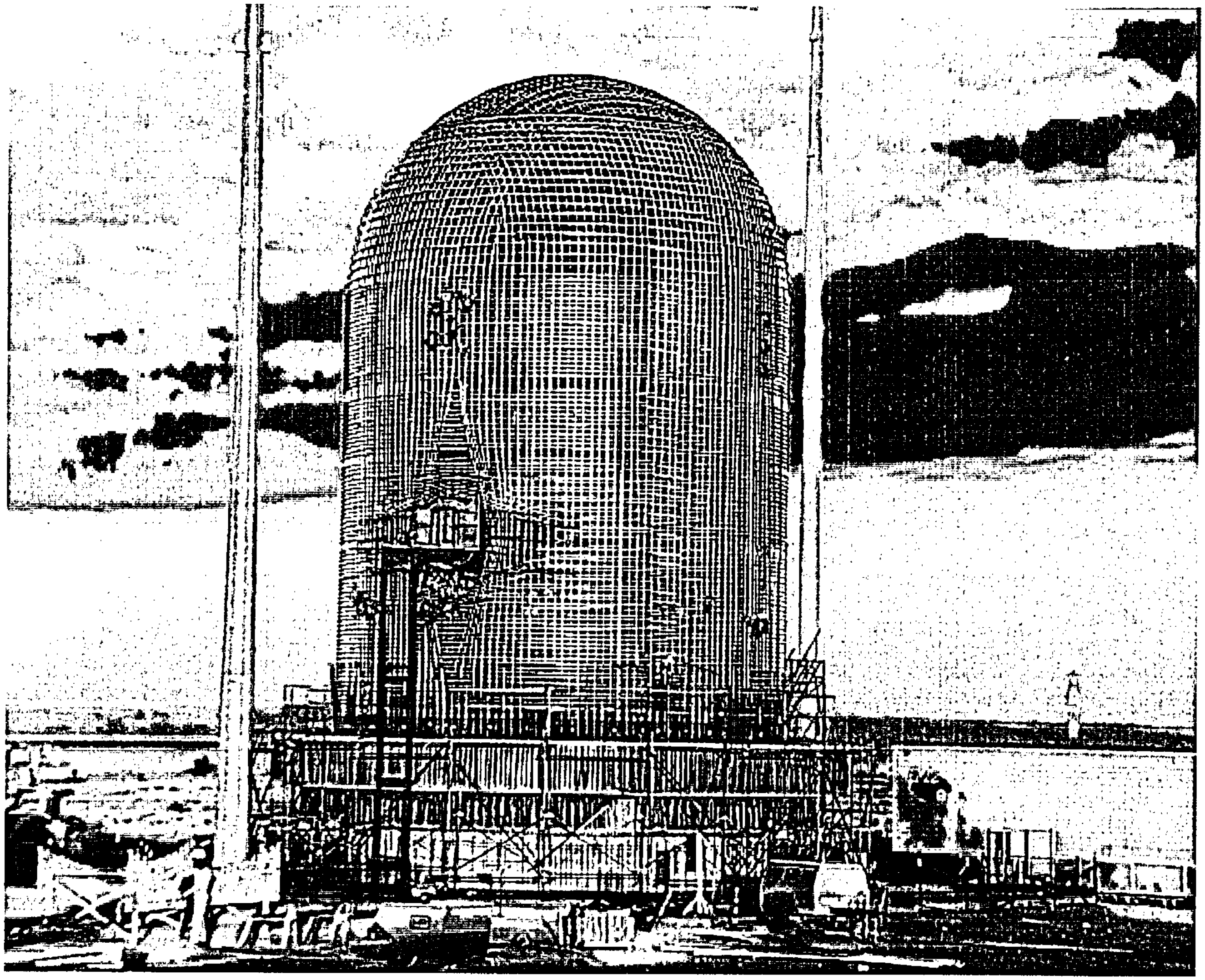

Figure 2.44 PCCV Model Tendon Sheaths

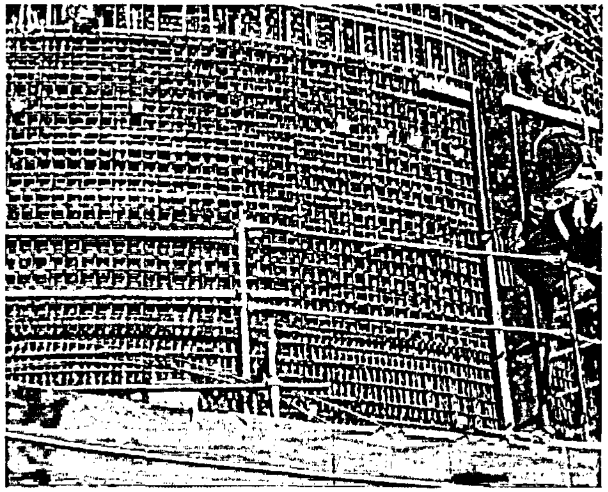

Figure 2.45 Outer Rebar for C1

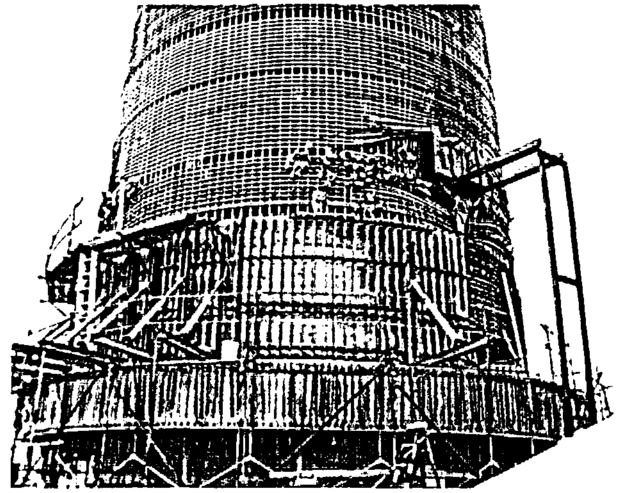

Figure 2.46 C1 Formwork Installation

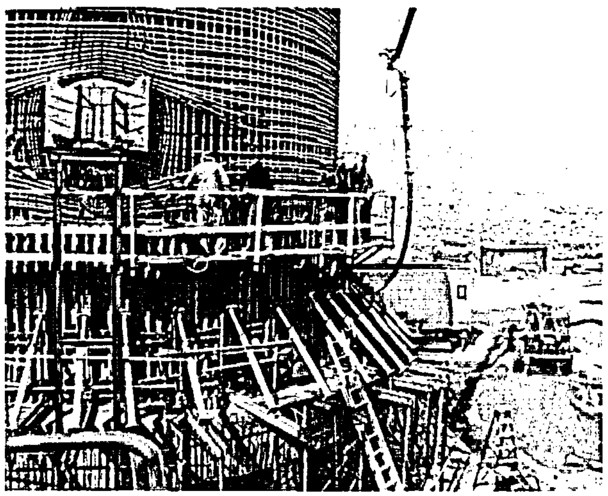

Figure 2.47 Placing C1 Concrete

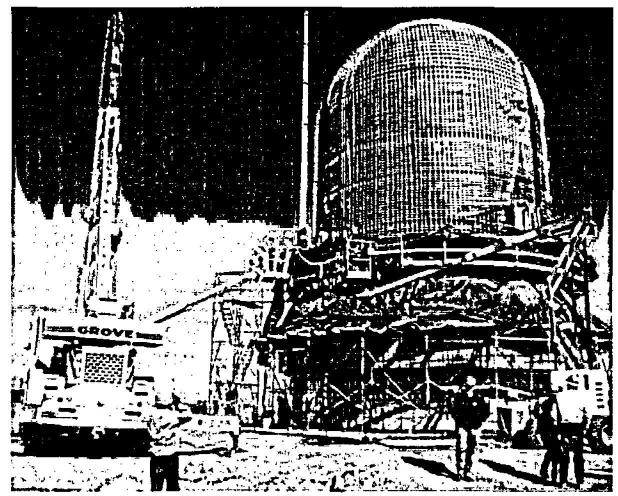

Figure 2.48 Installation of Instrumented Hoop Tendon.

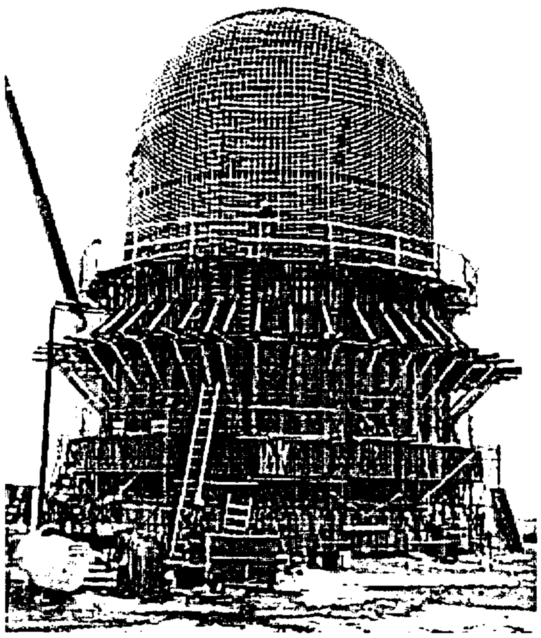

Figure 2.49 C2 Formwork

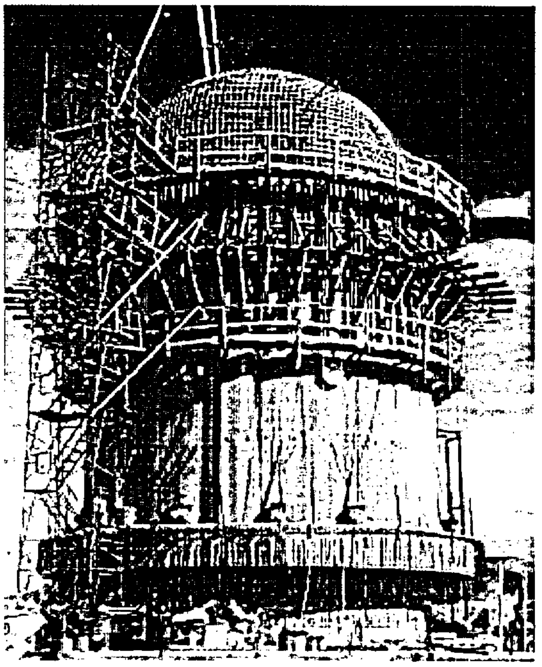

Figure 2.50 C4 Concrete Placement

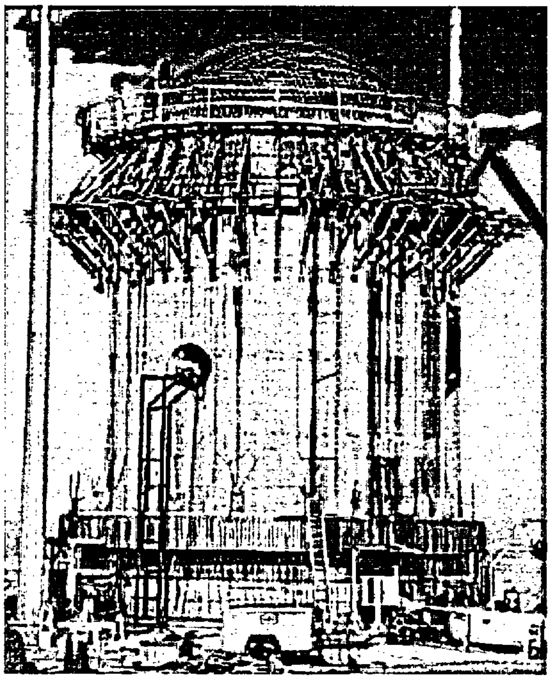

Figure 2.51 D1 Formwork Erection

Figure 2.52 D3 Concrete Placement

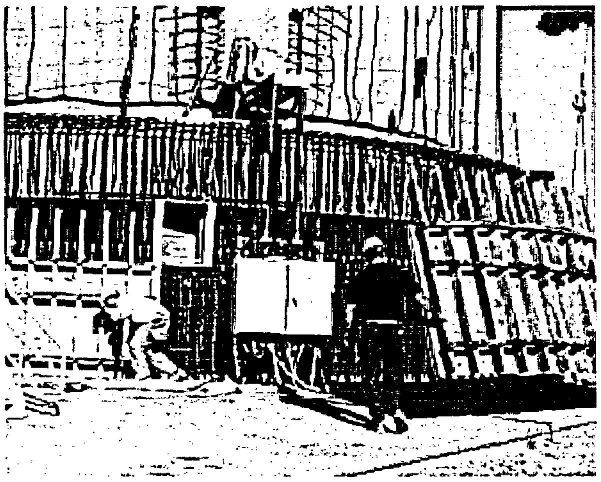

Figure 2.53 Final Basemat Concrete Lifts

[27]. These results, presented in Appendix B, showed higher amounts of creep and shrinkage than the trial mix data and indicated that creep losses in the prestressing might be higher than expected. This data was considered in specifying the tensioning forces for the tendons in Table 2.5.

More extensive material property tests for FC specimens were conducted around the time the model was being tensioned and just prior to the Limit State Test (LST). These tests provided more accurate material property data for concrete constitutive models used in the pre- and posttest analyses to predict and simulate the model response to pressure. These tests were also conducted at the University of New Mexico and included unconfined compression tests, compression tests to determine modulus of elasticity and Poisson's ratio[13], split cylinder tensile strength[14], and modulus of rupture[15]. The unit weight of the specimens was also determined and, since prediction of concrete cracking was one of the pretest analysis milestone objectives, a limited number of direct tension tests were conducted on specimens from the cylinder wall. The results of these tests and the direct tension test procedure are detailed in Reference [28] and summarized in Appendix B. A summary is also provided in Table 2.6.

A few other observations on the model concrete are worth noting:

1. The Coefficient of Variation (COV) in the compressive strength of the FC model concrete was 15.9% at 91-days and 13% at the time of prestressing. This COV is larger than typically observed for concrete from a central batch plant and indicates a significant degree of variation in the model concrete properties.

2. Compressive failure strains in the concrete specimens were typically in the range of 0.25 to 0.30%. While the tensile failure strain was not determined, the direct tension tests performed by the University yielded critical crack opening displacement data, which could be utilized in a fracture mechanics approach.

3. The modulus of elasticity in compression, determined from test data, is significantly lower than values usually computed from 'rules-of-thumb.' For example, ACI 318[16] recommends that $E_c = 57{,}000\sqrt{f_c'}$ in psi. Using 9300 psi as the average strength of the field cured cylinder/dome specimens yields an elastic modulus of 5.51×10^6 psi, compared to the measured value of 3.90×10^6 psi, a reduction of nearly 30%. If the modulus were based on the specified minimum strength of 6400 psi, the resulting value would be 4.56×10^6 psi, still higher than the measured value by 15%.

[13] ASTM C469-94, "Standard Test Method for Static Modulus of Elasticity and Poisson's Ratio of Concrete in Compression."

[14] ASTM 496-96, "Standard Test Method for Splitting Tensile Strength of Cylindrical Concrete Specimens."

[15] ASTM C78-94, "Standard Test Method for Flexural Strength of Concrete (Using Simple Beam with Third-Point Loading)."

[16] *Building Code Requirements for Structural Concrete,* ACI 318-02, American Concrete Institute, Farmington Hills, MI.

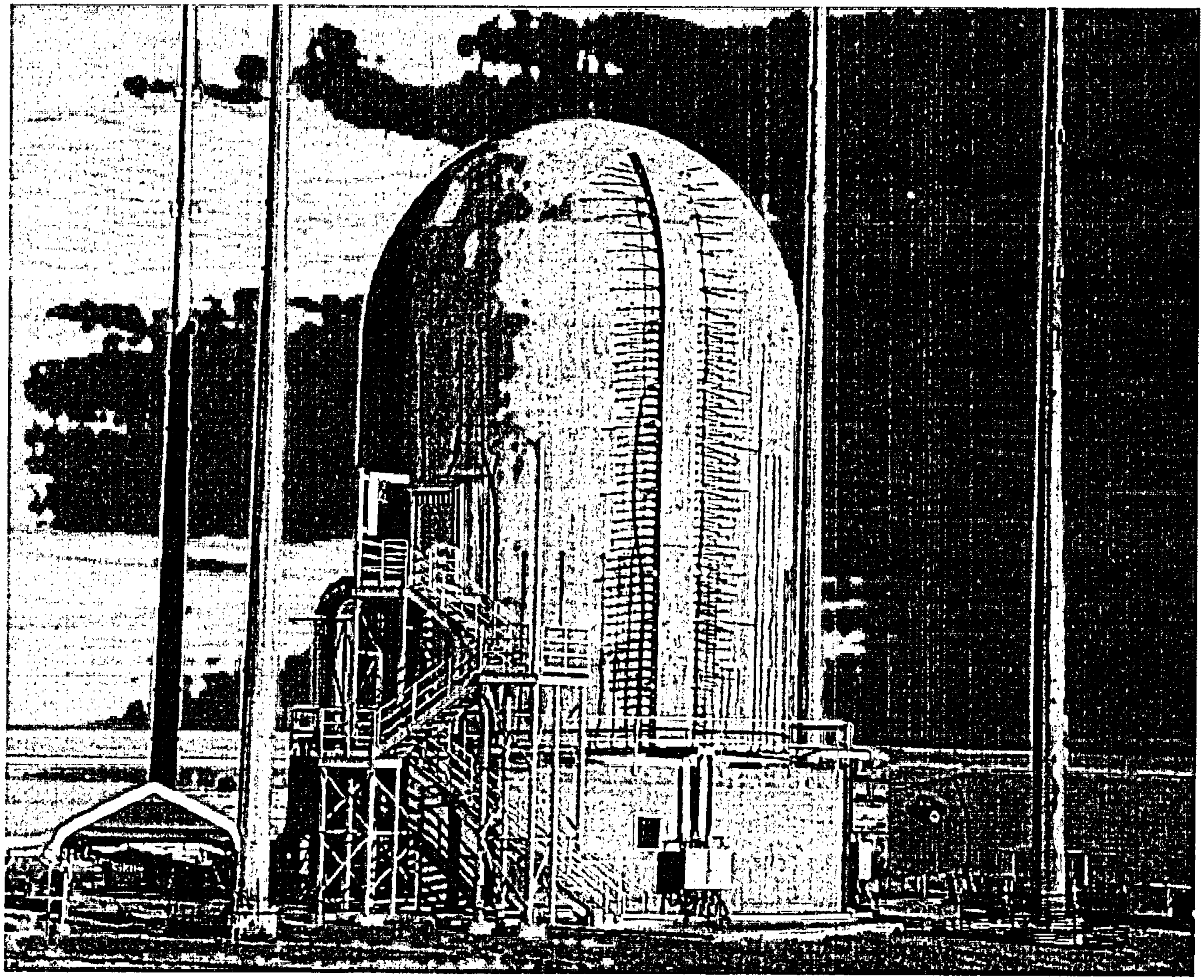

Figure 2.54 Completed PCCV Model

2.2.3 Prestressing Operations

With the majority of the model instrumentation suite installed, model construction resumed in February, 2000 with the insertion of noninstrumented tendon strands into the sheaths embedded in the model. Prior to insertion, the strands were coated with an anti-corrosive agent, but there was no other treatment. Insertion was achieved by feeding a 'puller cable' through the sheath equipped with a wire gripping sleeve that tightened on the strands as it was tensioned to pull them through the sheath (Figure 2.55). Except for a few minor obstacles, e.g. grout which had penetrated the sheath splices and had to be cleared, the sheaths were clear and insertion was accomplished without any difficulty.

Table 2.6 PCCV Model Average Concrete Properties

Design Compressive Strength		$300 kg_f/cm^2$	(4300 psi)	$450 kg_f/cm^2$	(6400 psi)
@ Prestressing					
Compressive Strength,	FC	570	(8102)	559	(7956)
	FC'	NA	NA	680	(9665)
Young's Modulus		25.7 GPa	(3.7×10^6 psi)	27.2 GPa	(4.0×10^6 psi)
@ Limit State Test					
Compressive Strength,	FC	562	(7998)	615	(8750)
	FC'	NA	NA	700	(9953)
Young's Modulus		27.2 GPa	(3.9×10^6 psi)	26.9 GPa	(3.9×10^6 psi)
Poisson's Ratio		0.21		0.22	
Split Tensile Strength		35	(497)	36	(519)
Direct Tensile Strength		NA	NA	23	(320)
Modulus of Rupture		NA	NA	42	(594)
Density		$2186 kg_f/m^3$	(136.4 pcf)	$2176 kg_f/m^3$	(135.8 pcf)

The suite of gages installed on the model prior to prestressing and installing the DAS cleared the final system checks, and the DAS was put into operation at 11:48 AM, March, 3, 2000. The initial data scan represented the initial or 'zero' reading for all the model transducers. All subsequent readings, through the LST until the DAS was shut down in October, are referenced to this initial scan. The model was scanned hourly for seven days to provide baseline information on the response to ambient temperature variations prior to tensioning the model and to verify the operational readiness of the DAS in attended and unattended modes.

Model prestressing began on March 10, 2000. The arrangement of the model tendons is shown in Appendix A. The nomenclature for identifying individual tendons consisted of an alpha designator 'H' for hoop tendons and 'V' for vertical tendons, followed by a numerical designator (1 through 98 for the hoop tendons and 1 through 90 for the vertical tendons). The hoop tendons were numbered consecutively from 1, the lowest tendon in the cylinder wall, to 98, at the midpoint of the dome. Even-numbered hoop tendons (H2, H4, H6,..., H98) were anchored at the 90 degree buttress and odd-numbered hoop tendons (H1, H3,..., H97) were anchored at the 270 degree buttress. Vertical tendons were numbered consecutively from V1 at 45 degrees, clockwise to V90 at 223 degrees. The vertical tendons were arranged in two orthogonal groups, with V1 through V45 spanning the dome in a plane (nearly) parallel to the 90 to 270 degree axis and V46 through V90 in an orthogonal plane approximately 0 to 180 degrees. This arrangement is illustrated more clearly in the design drawings and shown in Figure 2.44.

Figure 2.55 Pulling Hoop Tendons

Prestressing operations were defined by MHI in the project construction specifications[17]. The overall sequence of tensioning is illustrated in Figure 2.56. This sequence is identical to that used for the prototype and is intended to apply balanced prestressing forces to the model to prevent excessive local deformation or damage. The actual tensioning schedule is shown in Table 2.7. Prestressing operations were completed on May 3, 2000.

Thirty-four of the 188 tendons were instrumented with load cells at the anchors, and eight of these tendons, five hoop and three vertical, were also instrumented with strain gages at discrete locations along their length in an attempt to monitor and record the force distribution for comparison with the design calculations. The instrumented tendons are identified in Table 2.7 and their locations are illustrated in Figure 3.21. Details of the tendon instrumentation are given in Chapter 3.

Only one tendon was tensioned at a time (Figure 2.56). The procedure was to assemble the tensioning hardware at each end of the tendon. The tensioning hardware consisted of the tendon anchor and wedges, tensioning chair, hydraulic jack, and tensioning anchor. For the instrumented tendons, a pair of bearing plates, spherical washers, and the load cell was inserted between the tendon anchor and the bearing plate embedded in the model. This arrangement is shown in Figure 2.58. After the tensioning hardware was assembled, one end of the tendon, designated the 'B' end, was tensioned to 10% of the design load while the jack on the 'A' end was locked off. Then the B-end jack was locked off and the tensioning force was applied continuously by the jack at the A end until the jack pressure gage indicated that the force specified in Table 2.5 had been reached. (The jacks were calibrated prior to the start of prestressing and the conversion between hydraulic pressure and force was established for each jack.) In most cases, the tendon 'stretch' exceeded the maximum stroke of the jack and the strands had to be regripped to complete tensioning. When the A end was at the maximum load, the force at the B end was recorded and the friction coefficients for the tendon were computed and compared to the design values. (If the friction deviated from the design values by more than a specified range, the tendon was retensioned or, in some instances, the tendon was removed and new strands were inserted.) The B end was then tensioned to the specified force. When both ends were at the specified force, the anchors were seated.

---

[17] MH-K10-29, "Prestressing Work Procedure," Rev. 1, Mitsubishi Heavy Industries, May, 1999.

The seating loss, defined in terms of length, was measured as the difference between the length of the tendon extending beyond the anchor, before and after seating. This indicates the loss of elongation (and hence tension) in the tendon as the load is transferred from the jack grips to the tendon anchors. The measured seating loss was compared to the maximum design seating loss of 5 mm (0.2"), and, if it was excessive, the tendon was retensioned. After seating the tendon, each end was subjected to a 'lift-off' test in which the tendons were regripped and pulled until the tendon anchor lifted off the bearing plate enough to insert a feeler gage between them. The measured lift-off force was also compared to the value specified in Table 2.5.

The instrumented tendons, those with load cells only and those with strain gages, were closely monitored during tensioning but the load cell data was not reported to the tensioning contractor, VStructural, LLC., during prestressing. The tensioning procedure was modified for the eight instrumented tendons with strain gages. Since the lead wires for these gages would be damaged if the tendon was pulled in one direction first and then the other, causing the gages and the lead wires to travel back and forth in the sheath, these tendon were tensioned simultaneously at both the A and B ends. The tensioning forces were applied in small load increments and the tendon gages were monitored continuously during tensioning. The responses of the instrumented tendons are shown as force time histories in Figures 2.59 through 2.66.

These figures show the response of the load cells at each end of the tendons and the response of the surviving strain gages (converted to force by multiplying the strain by the nominal tendon area and elastic modulus of the strand). The strain gages on these tendons suffered a high mortality rate during prestressing, as shown in Table 2.8. Nevertheless, a high mortality rate was expected, and in most cases the surviving strain gages provided insight into the behavior of the tendons during prestressing and subsequent pressure testing.

The figures illustrate the range of strain in individual strand wires at a given measurement position, and also show when some of the strain gages failed. The data was not plotted after a gage had failed. It is interesting to note that the Tensmeg gages (TT) typically gave lower strain readings than the bonded foil gages (TF) mounted on individual wire strands. This is likely due to the Tensmeg end blocks slipping relative to the strand, resulting in an inaccurate measure of the strand strain. For most future discussions of the tendon response, only the data from the TF gages is considered as a reliable measure of the tendon strain and the TT data is ignored.

Figure 2.62 illustrates how the stages of the prestressing procedure are reflected in the test data. In the figure for H67, the surviving strain gages at each measurement position along the length of the tendon were averaged before converting them to a tendon force. This was done to simplify the plot, but this also recognizes that the force in individual wires in the tendon strands vary and the load cells (TL) forces and average forces from the strain gages (TF or TT) are plotted as a function of time. The force time history shows the load being applied incrementally at both ends of the tendon until the specified tensioning force was achieved and load was stable. Note that at a force of approximately 30T, the tendon was anchored and regripped when the stroke of the jacks was exceeded. After stabilizing at the maximum force, the tendons were seated, with the corresponding drop in load at and near the anchors. The slight increase in force at the anchors after seating reflects the lift-off test. (This shows that the force required to lift-off the anchor is slightly higher than the seated anchor force.)

Note also that the strain gages were most likely to fail near the tendon anchors and less likely to fail at the tendon mid-point. This occurs because the strands near the anchors travel the furthest during tensioning, increasing the likelihood that the gages or their lead wires were crushed against the sheath wall or another strand.

Considering Figure 2.62, it can be seen that the general force distribution along the length of the tendons is consistent with the design assumption, i.e., the highest tendon force is near the anchor and the lowest force is at the mid-point of the tendon. Figures 2.67 through 2.74 compare the measured force distribution in the tendons during and after tensioning with the design assumptions shown in Figure 2.9. The data for the horizontal tendons generally confirms the assumed design force distribution. The surviving gages do not provide enough data points to fully define the shape of the force distribution curve, notably where the effect of the anchor set loss disappears. Due to the discontinuities in the hoop tendon force distribution, only the data points are shown and no attempt was made to interpolate the hoop tendon force between measurement locations. In general, the data is consistent with the design assumptions and does not appear to contradict the predicted response.

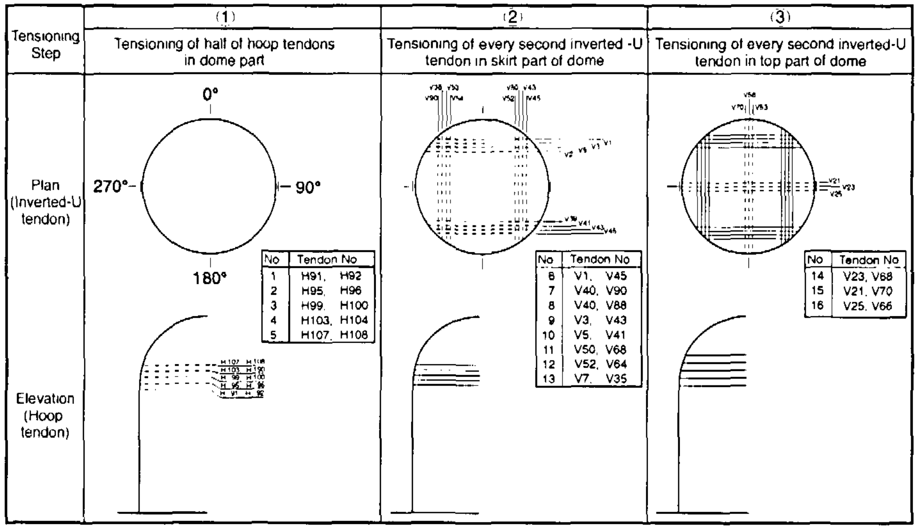

No	Tendon No
1	H91, H92
2	H95, H96
3	H99, H100
4	H103, H104
5	H107, H108

No	Tendon No
6	V1, V45
7	V40, V90
8	V40, V88
9	V3, V43
10	V5, V41
11	V50, V68
12	V52, V64
13	V7, V35

No	Tendon No
14	V23, V68
15	V21, V70
16	V25, V66

Tensioning Sequence (1/4)

Note: 1. Solid line shows tendon tensioned fully in the previous step.
2. Broken line shows tendon to be tensioned in this step.

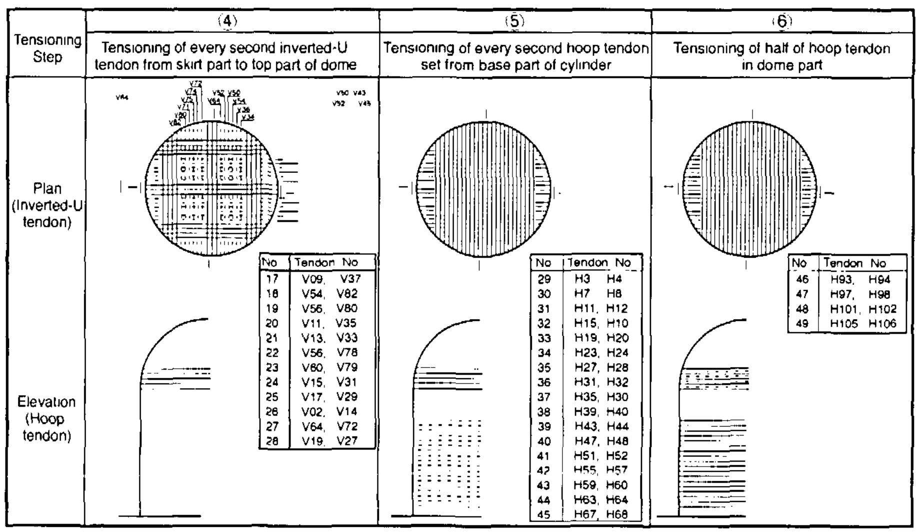

No	Tendon No
17	V09, V37
18	V54, V82
19	V56, V80
20	V11, V35
21	V13, V33
22	V56, V78
23	V60, V79
24	V15, V31
25	V17, V29
26	V02, V14
27	V64, V72
28	V19, V27

No	Tendon No
29	H3 H4
30	H7 H8
31	H11, H12
32	H15, H10
33	H19, H20
34	H23, H24
35	H27, H28
36	H31, H32
37	H35, H30
38	H39, H40
39	H43, H44
40	H47, H48
41	H51, H52
42	H55, H57
43	H59, H60
44	H63, H64
45	H67, H68

No	Tendon No
46	H93, H94
47	H97, H98
48	H101, H102
49	H105 H106

Tensioning Sequence (2/4)

Note: 1. Solid line shows tendon tensioned fully in the previous step.
2. Broken lines show tendon to be tensioned in this step.

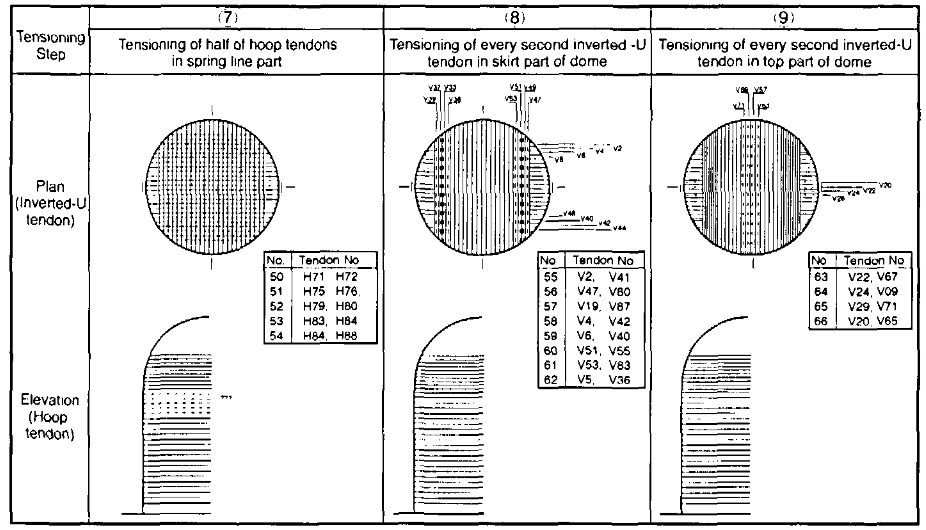

No.	Tendon No
50	H71 H72
51	H75 H76,
52	H79, H80
53	H83, H84
54	H84, H88

No	Tendon No
55	V2, V41
56	V47, V80
57	V19, V87
58	V4, V42
59	V6, V40
60	V51, V55
61	V53, V83
62	V5, V36

No	Tendon No
63	V22, V67
64	V24, V09
65	V29, V71
66	V20, V65

Tensioning Sequence (3/4)

Note: 1. Solid line shows tendon tensioned fully in the previous step.
2. Broken lines show tendon to be tensioned in this step.

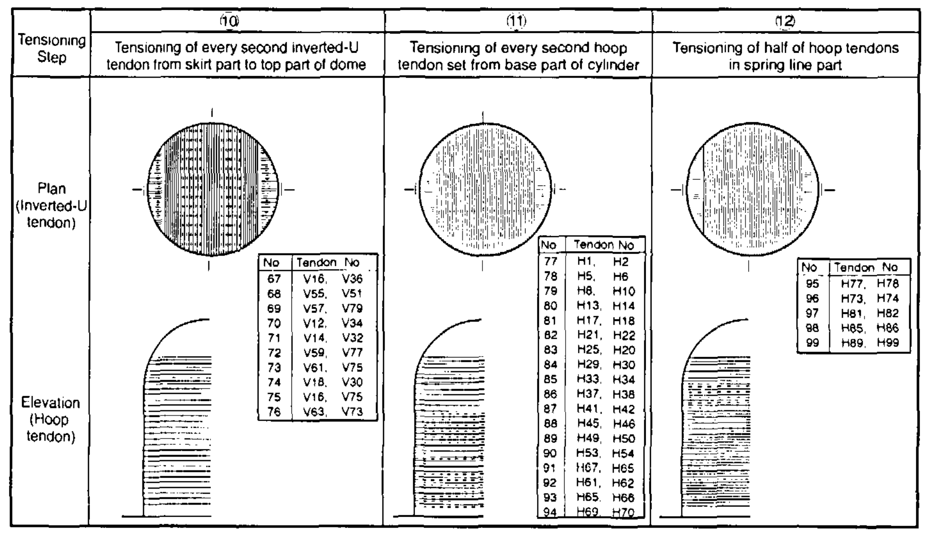

No	Tendon No
67	V16, V36
68	V55, V51
69	V57, V79
70	V12, V34
71	V14, V32
72	V59, V77
73	V61, V75
74	V18, V30
75	V16, V75
76	V63, V73

No	Tendon No
77	H1, H2
78	H5, H6
79	H8, H10
80	H13, H14
81	H17, H18
82	H21, H22
83	H25, H20
84	H29, H30
85	H33, H34
86	H37, H38
87	H41, H42
88	H45, H46
89	H49, H50
90	H53, H54
91	H67, H65
92	H61, H62
93	H65, H66
94	H69, H70

No	Tendon No
95	H77, H78
96	H73, H74
97	H81, H82
98	H85, H86
99	H89, H99

Tensioning Sequence (4/4)

Note: 1. Solid line shows tendon tensioned fully in the previous step.
2. Broken lines show tendon to be tensioned in this step.

Table 2.7 Model Prestressing Schedule

Sun	Mon	Tue	Wed	Thr	Fri	Sat
5-Mar	6-Mar	7-Mar	8-Mar	9-Mar	10-Mar	11-Mar
					H91	
					H92	
						V45

Sun	Mon	Tue	Wed	Thr	Fri	Sat
12-Mar	13-Mar	14-Mar	15-Mar	16-Mar	17-Mar	18-Mar
	H95	**H103***	**V1***	**V46**	V5	V86*(2)*
	H96	H104	V45*	V48	V41*(1)*	V52
	H99	H107*	V90	V88	V50	V84
	H100	H108*		V3		**V7**
	H103	**V1**		**V43**		
		*retensioning required				
						V54

Sun	Mon	Tue	Wed	Thr	Fri	Sat
19-Mar	20-Mar	21-Mar	22-Mar	23-Mar	24-Mar	25-Mar
	V39	V66*	**V37**	V11	V76*	V62
	V23	**V25 (3)**	***NUPEC***	***PRP***	V15	V74
	V68	V9	***AUDIT***	***SITE***	**V31**	V64
	V21		***INSP.***	***VISIT***	V17	V72
	V70		V54	V35*	V29	**V19**
	V25*(3)*		V82	**V13**		V27
	V66		V56*	V33		
			V80	V58		
				V78		
				V60		**H11**

Sun	Mon	Tue	Wed	Thr	Fri	Sat
26-Mar	27-Mar	28-Mar	29-Mar	30-Mar	31-Mar	1-Apr
	H3	**H11**	H16	H32	PS Op's suspended due to high winds.	
	H4	H16 *(4)*	H19	H36		
	H7*	H15	H20	**H35***(5)*		
	H8		H23	**H40**		
			H24			
	H12		H27			
			H28			
			H31			**H63**

Sun	Mon	Tue	Wed	Thr	Fri	Sat
2-Apr	3-Apr	4-Apr	5-Apr	6-Apr	7-Apr	8-Apr
	H39*	H56	**H63**	H93	H105	
	H44	H55	**H67**	H94	H106	
	H43	H60	**H68**	H97		
	H48	H59		H98		
	H47	H64		H102		
	H52	H63*		H101		
	H51					**V49**

Sequence

1	H91	58	**H4**
2	H92	59	H7**
3	H95	60	H8**
4	**H96**	61	**H11**
5	H99	62	H12
6	H100	63	H15
7	**H103**	64	H16
8	H104	65	H19
9	H107	66	H20
10	H108	67	H23
11	**V1**	68	H24
12	V45	69	H27
13	**V46**	70	H28
14	V90	71	H31
15	V48	72	H32
16	V88	73	**H35**
17	V3	74	H36
18	**V43**	75	H39
19	V5	76	**H40**
20	V41	77	H43
21	V50	78	H44
22	V86**	79	H47
23	V52	80	H48
24	V84	81	H51
25	**V7**	82	H52
26	V39	83	H55
27	V23	84	H56
28	V68	85	H59
29	V21	86	H60
30	V70	87	**H63**
31	**V25**	88	H64
32	V66	89	**H67**
33	V9	90	**H68**
34	**V37**	91	H93
35	V54	92	H94
36	V82	93	H97
37	V56	94	H98
38	V80	95	H101
39	V11	96	H102
40	V35	97	H105
41	**V13**	98	H106
42	V33	99	H71
43	V58	100	H72
44	V78	101	**H75**
45	V60	102	H76
46	V76	103	H79
47	V15	104	H80
48	**V31**	105	H83
49	V17	106	H84
50	V29	107	H87
51	V62	108	H88
52	V74	109	V2
53	V64	110	V44
54	V72	111	V47
55	**V19**	112	V89
56	V27	113	**V49**
57	H3		

Load Cell | *Schedule Impact*

Instrumented | **Tendon to be replaced

Completed | **Weekend Milestone**

C01

Table 2.7 Model Prestressing Schedule (continued)

Sun	Mon	Tue	Wed	Thr	Fri	Sat
9-Apr	10-Apr	11-Apr	12-Apr	13-Apr	14-Apr	15-Apr
	Jack Re-calibration	PS Op's suspended due to high winds.	H71	H87	V87	
			H72	H88	V4	
			H75	V2	V42	
			H76	V44	V6*(1)*	
			H79	V47*	V40*(2)*	
			H80	V89	V51	
			H83	**V49**		
			H84			V12
Sun	**Mon**	**Tue**	**Wed**	**Thr**	**Fri**	**Sat**
16-Apr	17-Apr	18-Apr	19-Apr	20-Apr	21-Apr	22-Apr
	<u>**V85**</u>		<u>**V85**</u>	V8*	V26*	V36(6)
	Op Error		V53	V38	V71	**V55**
	damaged		V83	V22	V20	V81
	19/31	Op's		**V67***	V65	V57
	gages.	suspended		V24	V10	
	Op's			V69	V36	
	suspended					
						H22
Sun	**Mon**	**Tue**	**Wed**	**Thr**	**Fri**	**Sat**
23-Apr	24-Apr	25-Apr	26-Apr	27-Apr	28-Apr	29-Apr
	V79*	V77	H1	H17	H41	
	V12	**V61***	H2	H18	H42	
	V34	V75	H5	H21	H45	
	V14	V16	H6	H22	**H46**	
	V32*(6)*	V30	H9	**H25**	H49	
	V59	V18	H10	H26	H50	
		V28	H13	H29		
		V63	H14	**H30**		
		V73		H33		
				H34		
				H37		
				H38		H73
Sun	**Mon**	**Tue**	**Wed**	**Thr**	**Fri**	**Sat**
30-Apr	1-May	2-May	3-May	4-May	5-May	6-May
	H54	**H58**	H85			
	<u>**H53**</u>	H61	H86			
	H57	H62	**H89**			
		H65	H90			
		H66				
		H69				
		H70				
		H73				
		H74				
		H77				
		H78				
		H81				
		H82				
			H90			

<u>Sequence</u>

114	V87	157	H9**
115	V4	158	H10
116	V42	159	H13
117	V6*(1)*	160	H14
118	V40*(2)*	161	H17
119	V51	162	**H18**
120	<u>**V85**</u>	163	H21
121	V53	164	H22
122	V83	165	**H25**
123	V8	166	H26
124	V38	167	H29
125	V22	168	**H30**
126	**V67**	169	H33
127	V24	170	H34
128	V69	171	H37
129	V26	172	H38
130	V71	173	H41
131	V20	174	H42
132	V65	175	H45
133	V10	176	**H46**
134	V36	177	H49
135	**V55**	178	H50
136	V81	179	<u>**H53**</u>
137	V57	180	H54
138	**V79**	181	H57
139	V12	182	**H58**
140	V34	183	H61
141	V14	184	H62
142	V32	185	H65
143	V59	186	H66
144	V77	187	H69
145	**V61**	188	H70
146	V75	189	H73
147	V16	190	H74
148	V30	191	H77
149	V18	192	H78
150	V28	193	H81
151	V63	194	**H82**
152	**V73**	195	H85
153	H1	196	H86
154	H2	197	**H89**
155	H5	198	H90
156	H6		

<u>Notes:</u>

(1) V41 removed and replaced with V6. V41 set-loss, friction and loft-off were high.
(2) V86 (mock-up tendon) removed and replaced with V40 tendon.

(3) Remove V25, friciton loss too high (>0.25), detension, remove LC's, remove and replace strand, reinstall LC's tomorrow (3/21) AM.
(4) Remove and replace tendon due to lift-off force too high.
(5) Tensioning of H35 delayed due to water in LC connectors, connectors removed and hardwired
(6) V36 removed and replaced, friction not within specifications.

C02

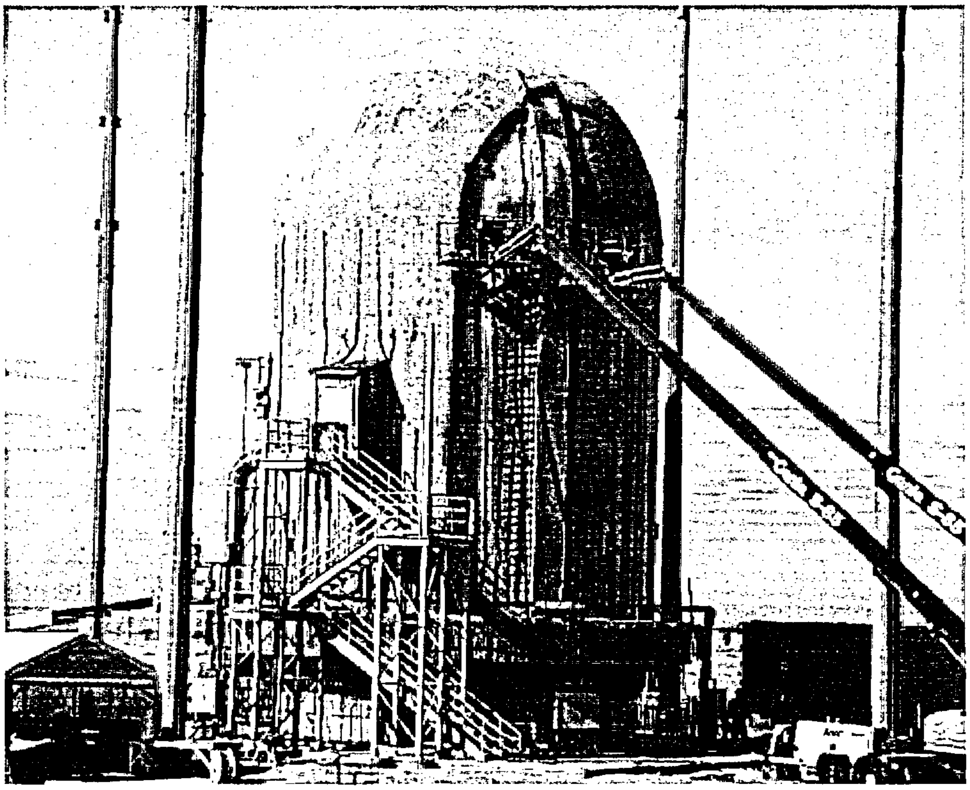

Figure 2.57 Tensioning Hoop Tendons

Figure 2.58 Tensioning Hardware Assembly and Load Cell

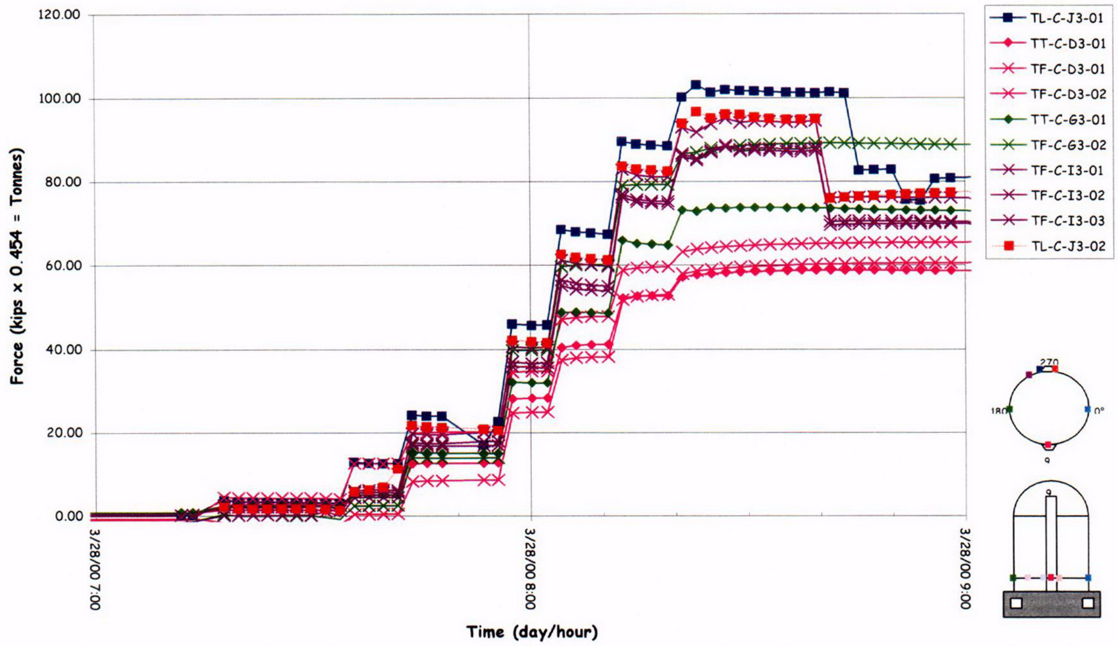

Figure 2.59 Tendon H11 Tensioning Force Time History

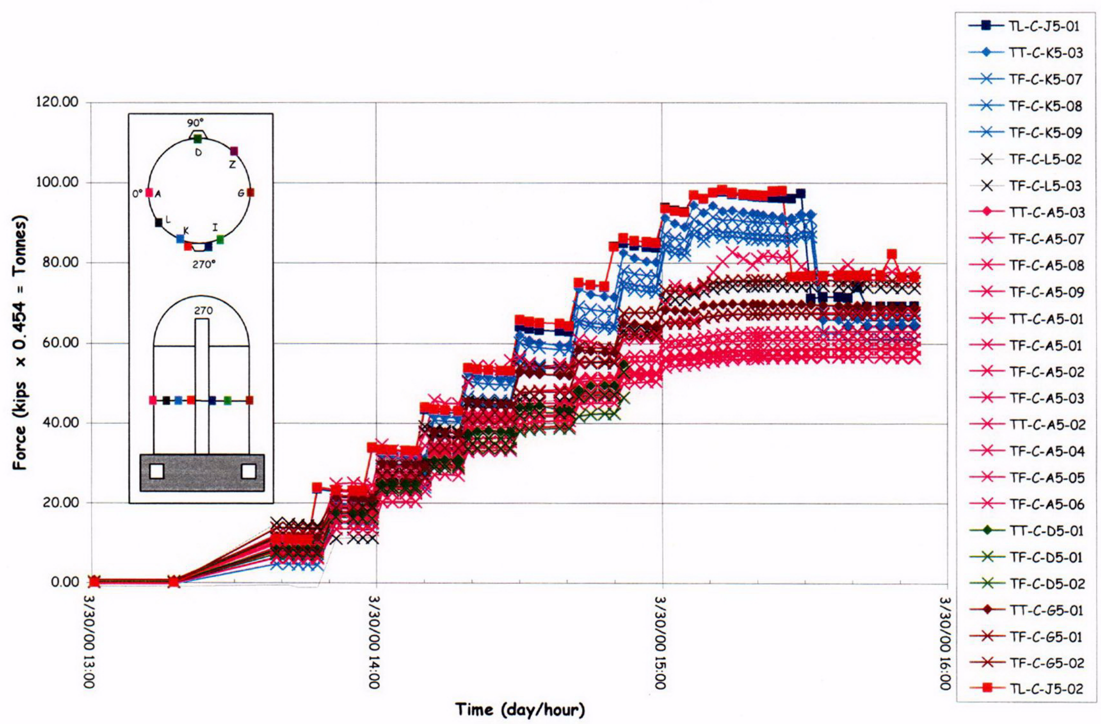

Figure 2.60 Tendon H35 Tensioning Force Time History

C03

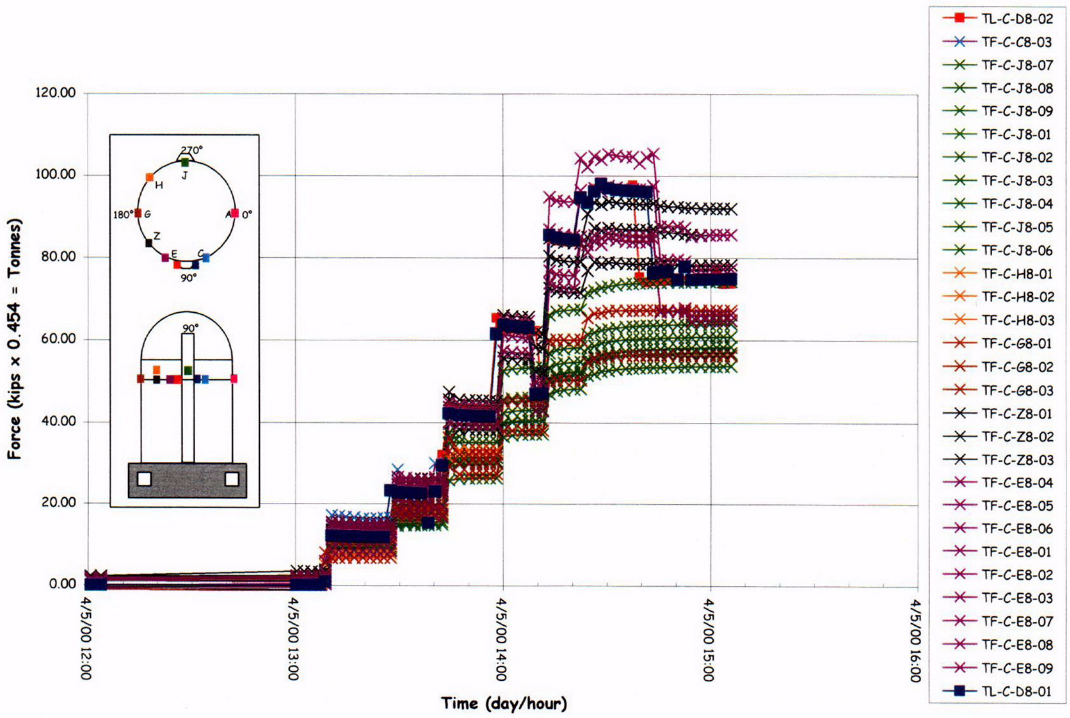

Figure 2.61 Tendon H53 Tensioning Force Time History

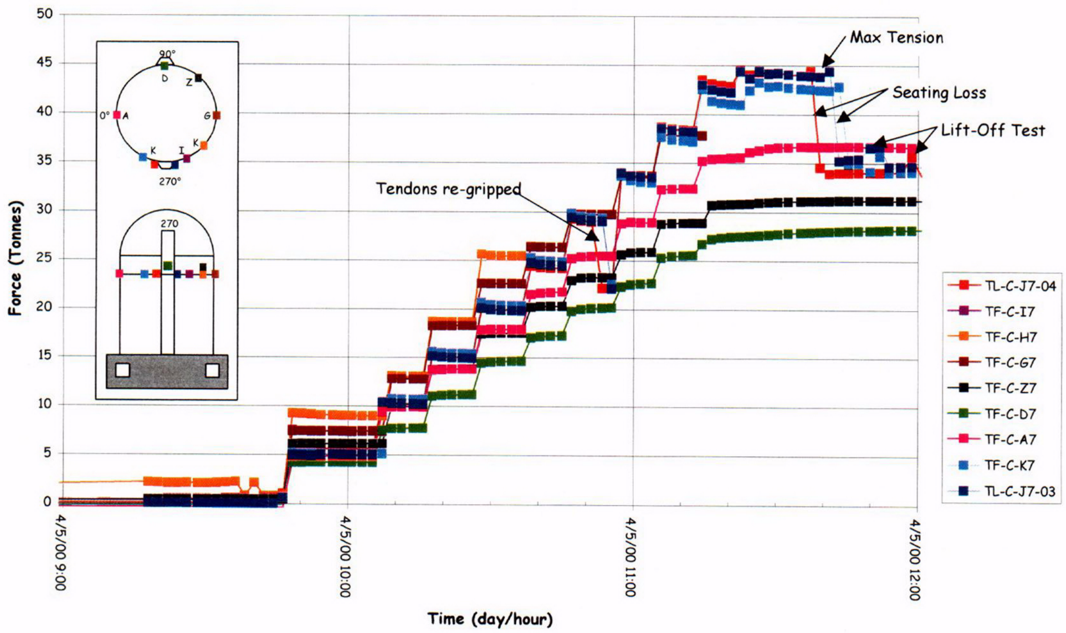

Figure 2.62 Tendon H67 Tensioning Force Time History

C04

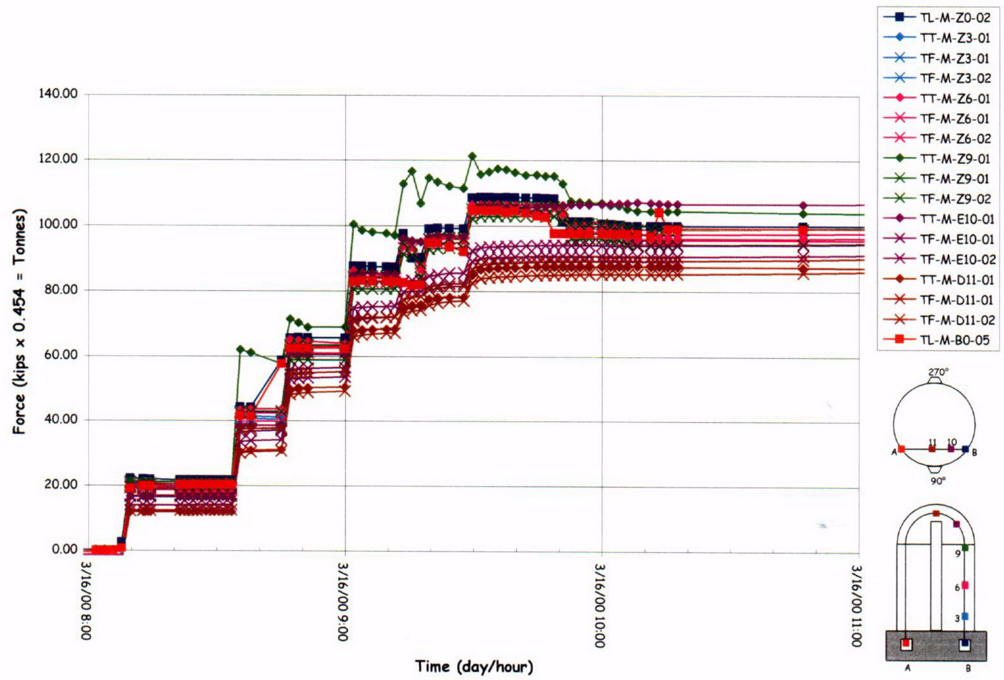

Figure 2.63 Tendon H68 Tensioning Force Time History

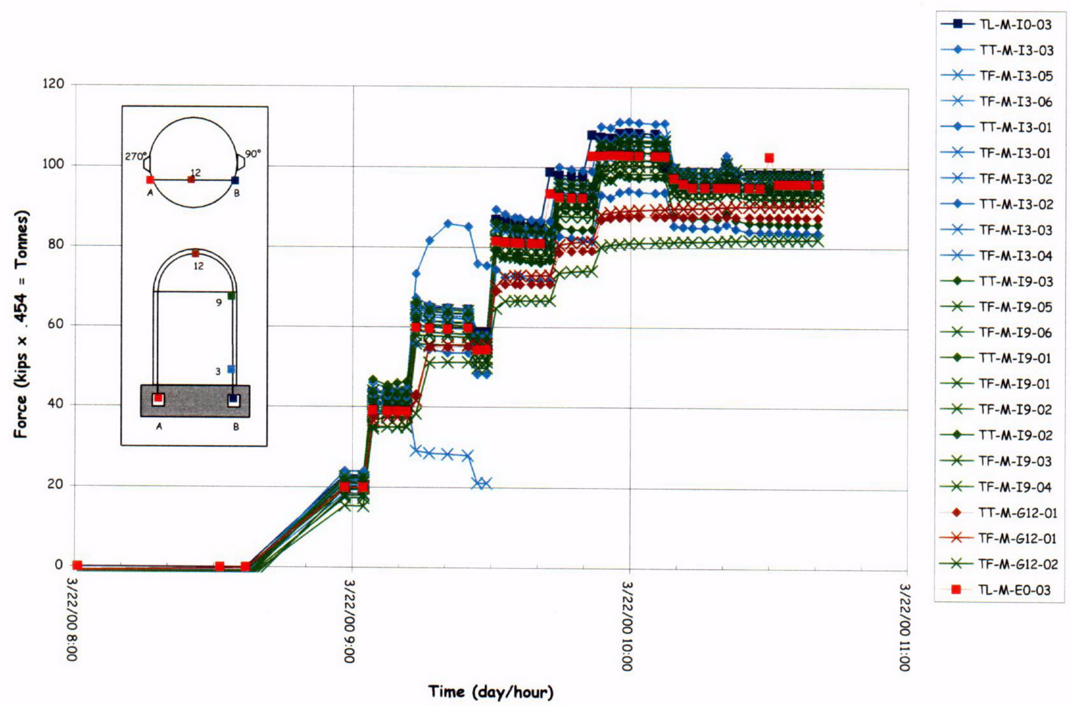

Figure 2.64 Tendon V37 Tensioning Force Time History

C05

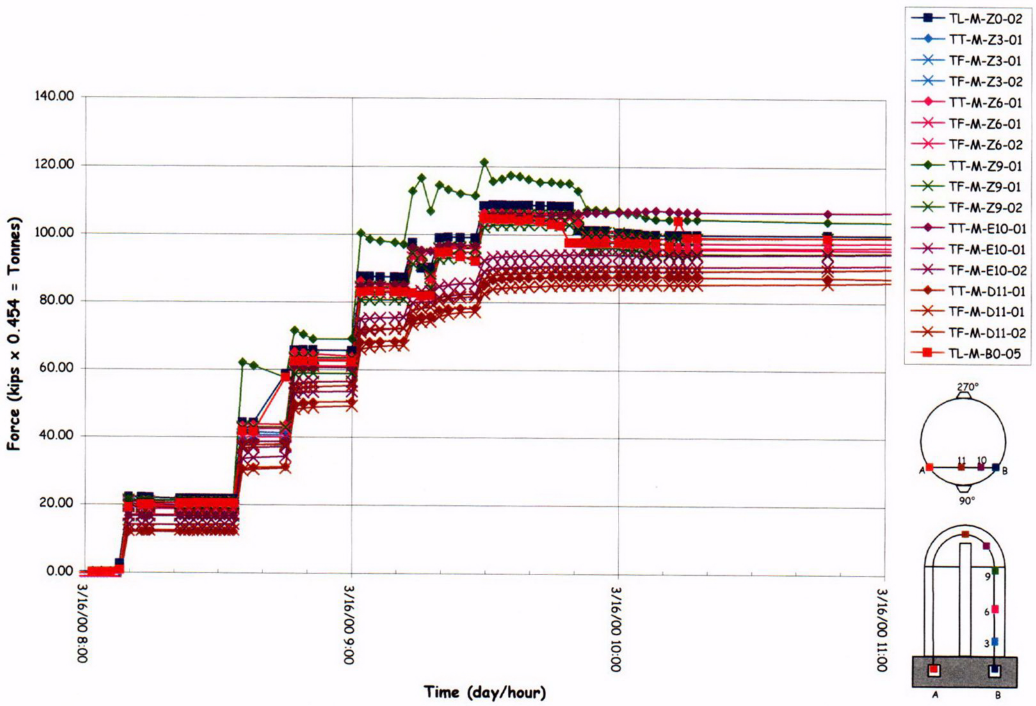

Figure 2.65 Tendon V46 Tensioning Force Time History

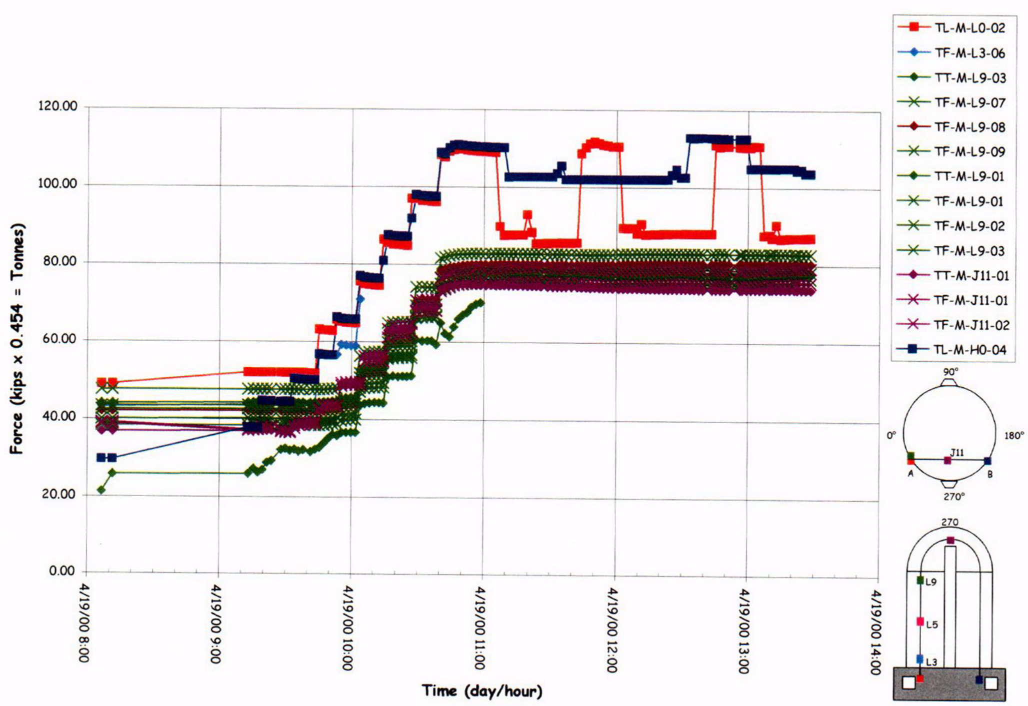

Figure 2.66 Tendon V85 Tensioning Force Time History

C06

Table 2.8 Instrumented Tendon Gage Performance during Prestressing

H11:	4/12 strain gages failed	33% mortality
H35:	23/39 strain gages failed	59% mortality
H53:	14/22 strain gages failed	59% mortality
H67:	11/21 strain gages failed	52% mortality
H68:	18/33 strain gages failed	54% mortality
V46:	3/15 strain gages failed	20 % mortality
V85:	20/30 strain gages failed	67% mortality (operator error)
Overall*:	96/193 strain gages failed	50% mortality
*Six additional gages failed prior to pressure testing: (102/193, 53%)		

The vertical tendon data, however, appears to suggest that the wobble friction in the straight portion of the cylinder wall may be underestimated, while the angular friction in the dome may be overestimated. Since the majority of the strain gages on V37 and V46 survived and the force distribution is more nearly a continuous function, a curve was fitted through the test data to facilitate interpreting and comparing the design assumptions. Unfortunately, due to operator error prior to the start of prestressing operations, most of the gages on V85 (which is deflected around the E/H), were damaged. While the force distribution around the penetration was not obtained, it is apparent that deflecting the tendon around the penetration results in additional losses, as expected.

Finally, the prestressing contractor's data and the load cell data was summarized for comparison with the design specification in Table 2.9.

Table 2.9 Prestressing Data Summary

	Hoop Tendons		Vertical Tendons	
Average Tension Force:				
Design:	44.41 T	97.9 kips	49.57 T	109.3 kips
Jack:	43.53 T	95.97 kips	49.02 T	108.07 kips
Jack (w/ Load Cells only):	43.61 T	96.14 kips	49.09 T	108.23 kips
Load Cells:	43.21 T	95.27 kips	48.20 T	106.27 kips
Average Lift-off Force:				
Design:	34.11 T	75.2 kips	46.31 T	102.1 kips
Jacks:	34.02 T	75.01 kips	44.22 T	97.49 kips
Average Friction Coefficient:	0.18		0.22	
Average Seating Loss:	3.95 mm	0.16"	4.9 mm	0.19"
Jack:	9.51 T	20.96 kips	4.80 T	10.58 kips
Load Cell:	9.86 T	21.75 kips	4.64 T	10.23 kips
Average Final Load Cell Force:	33.34 T	73.52 kips	43.56 T	96.04 kips
Average Elastic Loss:	0.27 T	0.59 kips	0.58 T	1.29 kips

One Tonne = 1000 kg_f = 9.807 kN = 2.205 kips

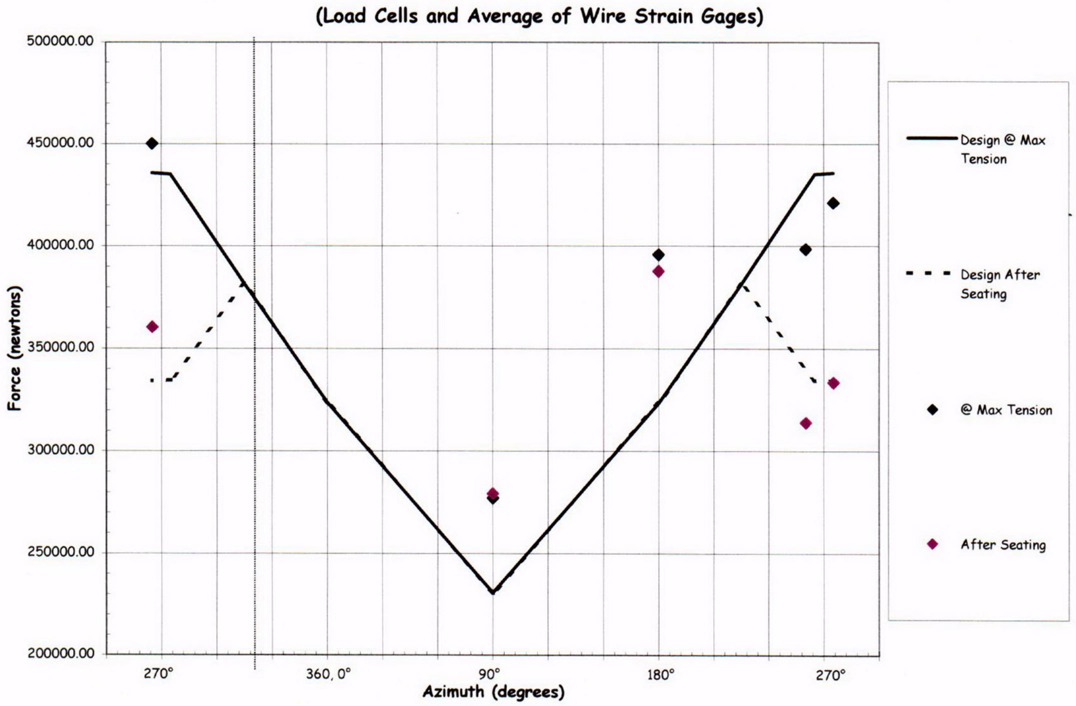

Figure 2.67 H11 Tendon Force Distribution, Elev. 1854

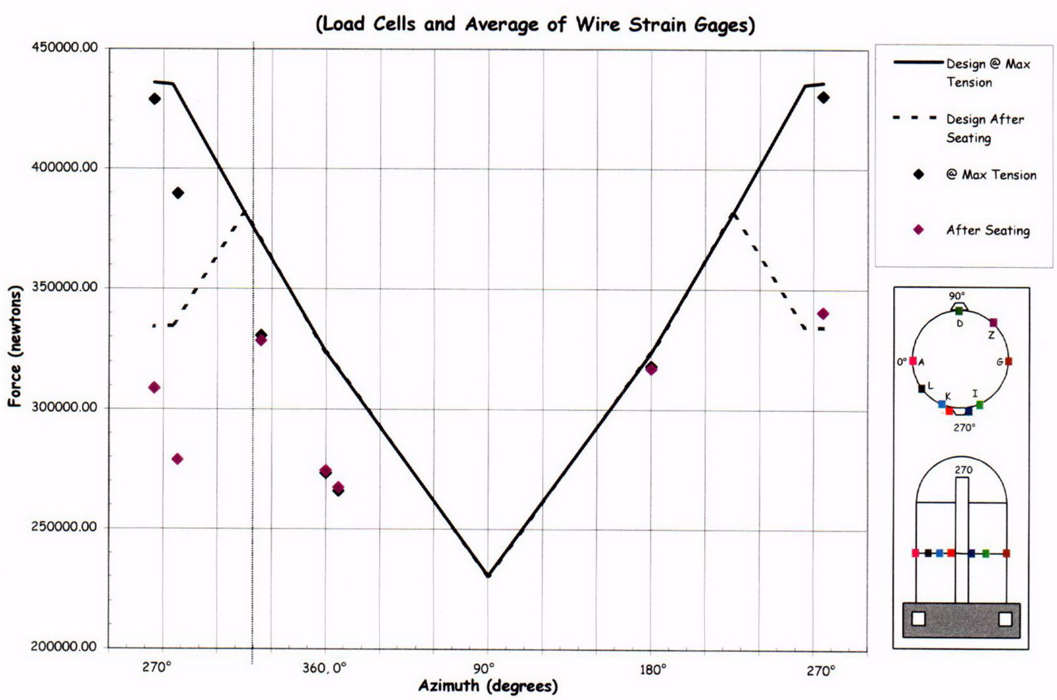

Figure 2.68 H35 Tendon Force Distribution, Elev. 4572

C07

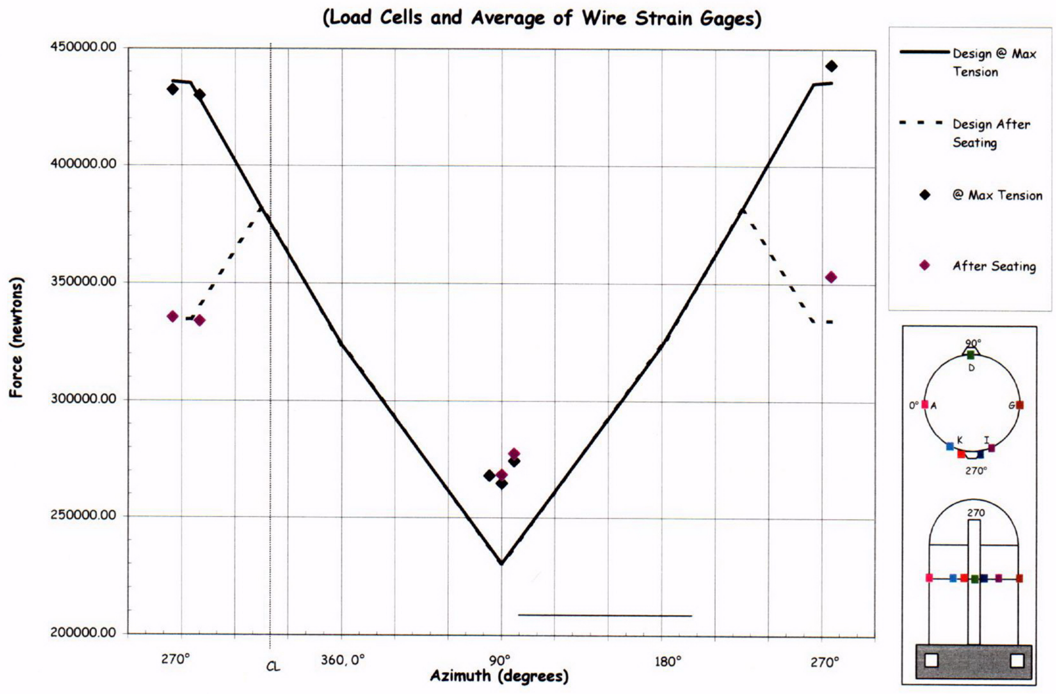

Figure 2.69 H53 Tendon Force Distribution, Elev. 6579

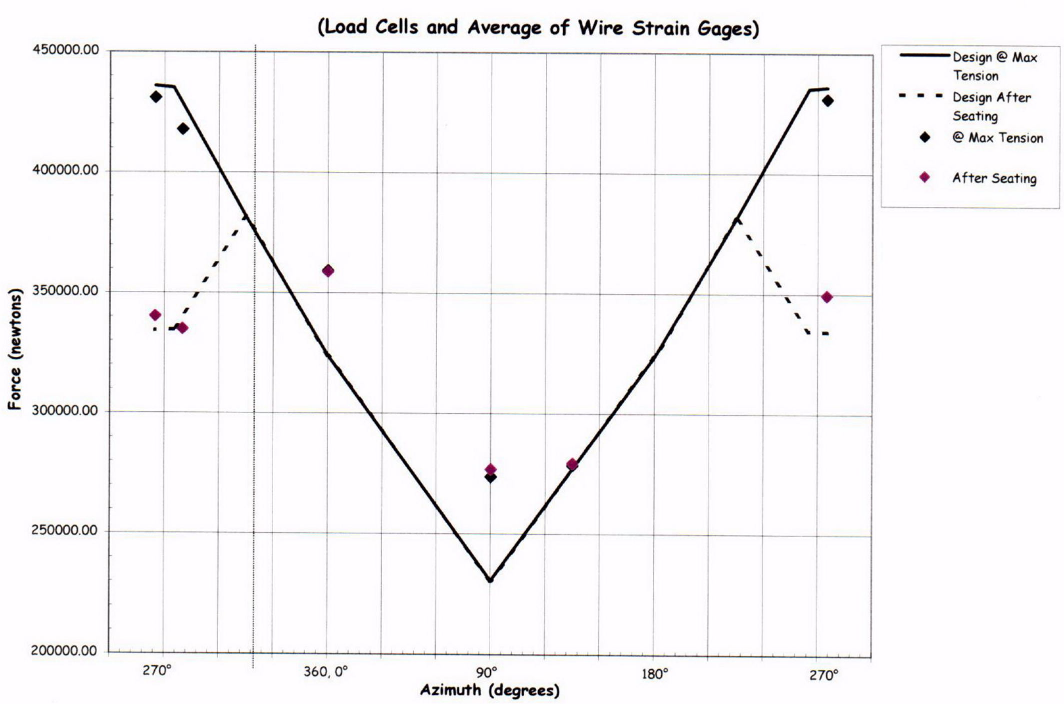

Figure 2.70 H67 Tendon Force Distribution, Elev. 8153

C08

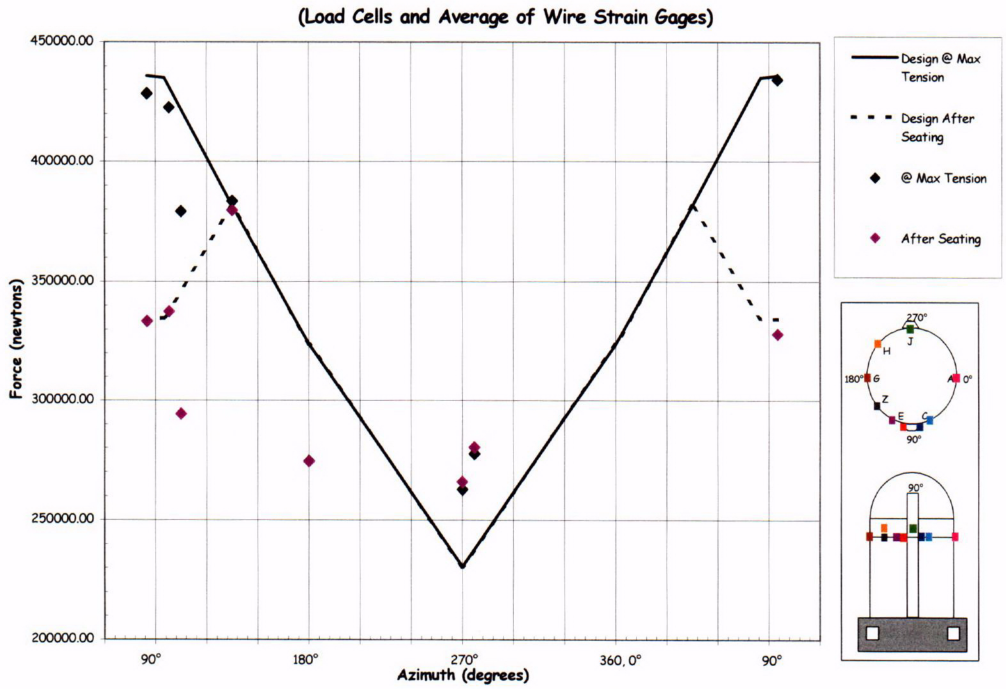

Figure 2.71 H68 Tendon Force Distribution, Elev. 8280

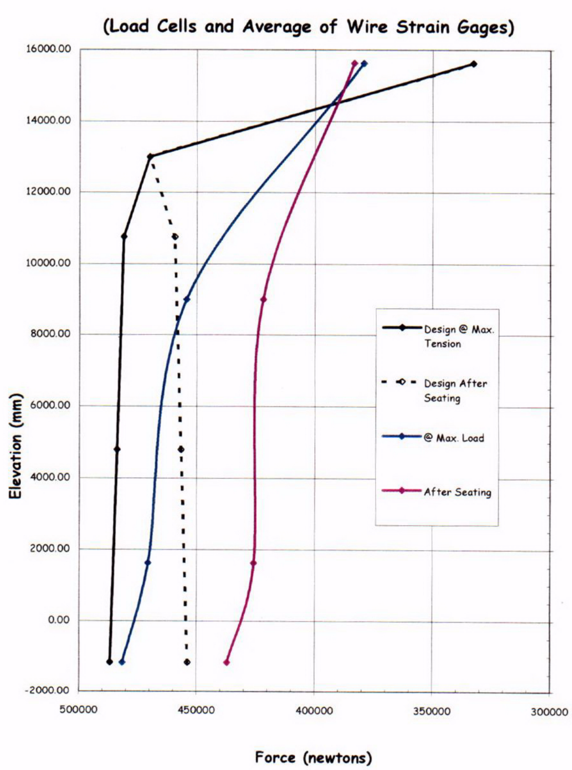

Figure 2.72 V37 Tendon Force Distribution, Azimuth 240 Degrees

C09

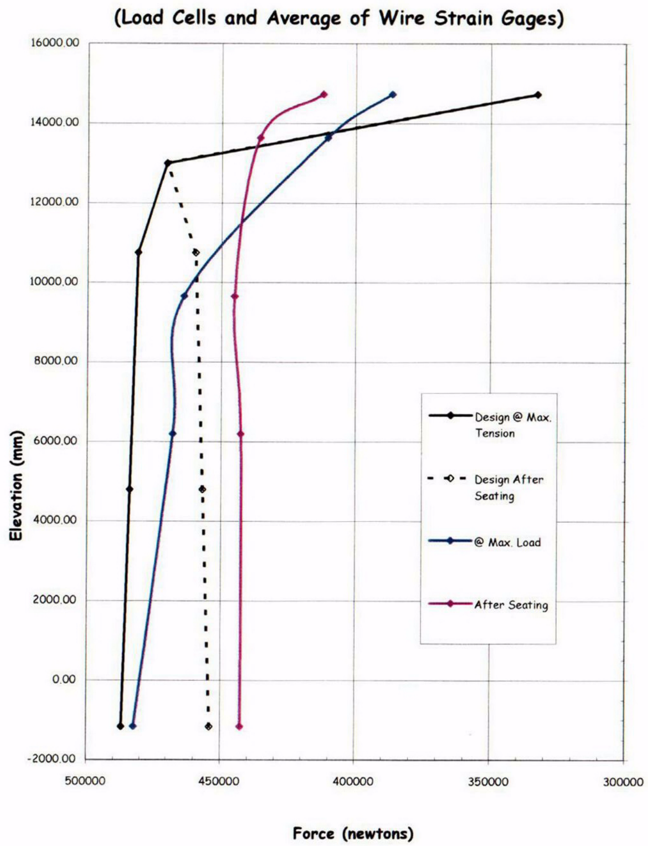

Figure 2.73 V46 Tendon Force Distribution, Azimuth 135 Degrees

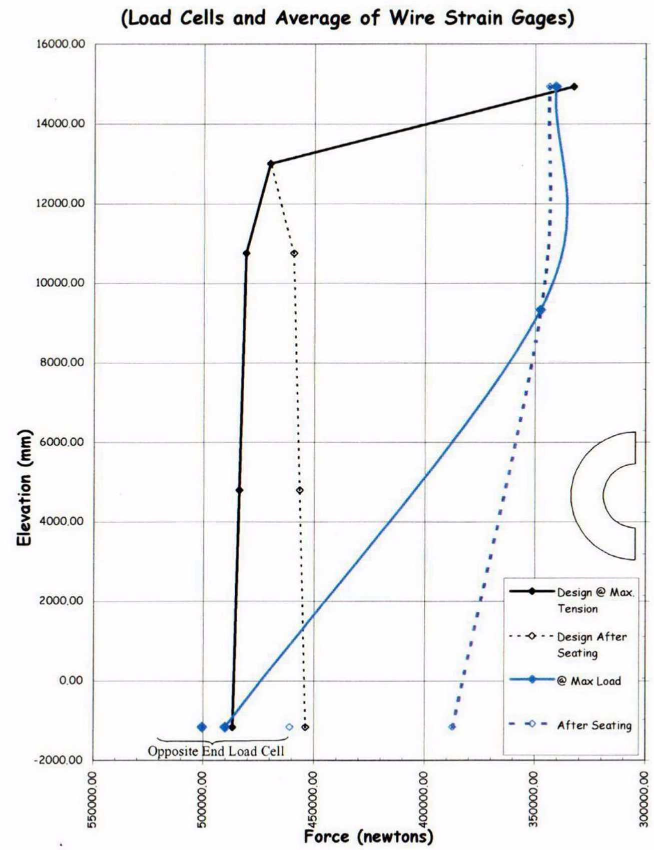

Figure 2.74 V85 Tendon Force Distribution, Azimuth 325 Degrees

C10

3. INSTRUMENTATION

3.1 Background

The instrumentation suite installed on the PCCV model was designed to support the test program objectives, i.e., to provide data on the response of model to internal pressure loading well into the inelastic regime, for comparison with analytical models; and to provide insight and information into response and failure mechanisms that may be representative of actual nuclear power plant containment structures.

Since most types of instrumentation are only capable of measuring a single response parameter at a discrete location, the task of designing the instrumentation suite consisted of identifying critical response parameters and locations from which the overall and local response of the model could be inferred, selecting transducers with the requisite accuracy and range, meeting other operating constraints (pressure, temperature, size, etc.) and integrating them with the other transducers and the data acquisition system. The design of the instrumentation suite also required the specification of quality control procedures to ensure the transducers would perform as designed and that the output could be reliably interpreted in terms of the response parameters of interest.

This chapter describes the considerations given in the design of the instrumentation, gives specifications for the transducers selected, and provides a list of all the transducers installed on the model, along with details of the location, installation, and quality control procedures.

3.1.1 Design Considerations

The basic instrumentation plan was outlined by NUPEC in early 1992 during the initial planning for the PCCV model test [29]. After extensive discussions between NUPEC, its subcontractors, the NRC, and SNL, the details of the instrumentation were agreed upon and documented [30, 31]. Preliminary analyses of the PCCV model guided the selection and location of the final suite of measurements [32]. The detailed PCCV Instrumentation Plan provides a complete description of the instrumentation system and was updated throughout the model design and construction, finally reflecting the 'as-built' configuration employed during the pressure tests.

Considering the basic design philosophy, described in Section 2.1, the basic instrumentation plan identified the following measurements to be taken during the PCCV pressure tests:

1. load (internal pressure),
2. displacement,
3. rebar strain,
4. concrete strain,
5. concrete crack width,
6. liner and liner anchor strain,
7. tendon force, and
8. temperature.

These parameters would be measured at a number of locations to characterize both the global and local response of the model. The basic plan also called for the instrumentation to provide information regarding the potential failure modes identified in Section 2.1. Table 3.1 shows the relationship between instrument location, instrument type, measurement type, and measurement objective. The measurement objectives are either to capture global or local response at specified locations in the PCCV or to measure the behavior of potential failure modes, as shown above. The measurement types and the various instrument types to be specified are discussed in Section 3.2. Installation and locations of the instruments are discussed in Section 3.3.

The basic instrumentation plan also specified a grid of azimuths and elevations which would form the basis for the instrumentation layout and provide a scheme for incorporating the nominal gage locations in the individual gage IDs. This basic grid of cardinal lines is shown in Figure 3.1.

Thirteen cardinal elevations were established, from 1 at the top of the basemat (elev. 0.00) to 13 at the dome apex. Twelve cardinal azimuths, spaced roughly 30 degrees apart, were established with A at 0 degrees (or 360 degrees) to L at 324 degrees. A thirteenth cardinal azimuth was established at 135 degrees and designated Z. This azimuth was selected to represent the global axisymmetric response of the containment based on preliminary analysis results. While the PCCV model is not axisymmetric in terms of geometry and stiffness, Azimuth Z is reasonably distant from any major structural discontinuities and the net hoop prestressing force is close to the average.

The cardinal lines of the model were selected because they correspond to the measurement locations for the prototype Structural Integrity Test (SIT). The SITs were carried out on the containments of the Ohi Nuclear Power Station (Units 3 and 4) in 1991 and 1992. Comparison of the SIT results from the prototype with the model SIT results might be useful for investigating the similarity between the structures. The SIT for both the Ohi containment and the model were performed at 1.125 times design pressure.

Table 3.1 Instrumentation Objectives

Location	Material	Measurement Type	Instrument Type	Measurement Objective
Free-Field Cylinder and	Liner	Strain	Strain gage	Response and Liner failure
Dome	Liner anchor	Strain	Strain gage	Response
	Rebar	Strain	Strain gage	Response
	Tendon	Strain	Tensmeg & Strain gage	Response and Tendon failure
		Force	Load cells	Response
	Concrete	Strain	Strain gage	Response
		Cracking	Video	Response
	All	Displacement	CPOT and TLDT	Response
Wall-Basemat	Liner	Strain	Strain gage	Liner failure
Juncture	Liner anchor	Strain	Strain gage	Liner failure
	Rebar	Strain	Strain gage	Shear failure
	Concrete	Strain	Gage bars	Shear failure
		Cracking	Video	Shear failure
On E/H or A/L	Steel hatch	Strain	Strain Gage	E/H or A/L failure
		Displacement	LVDT	Response
Around E/H or	Plate and Liner	Strain	Strain gage	Liner failure
A/L	Liner anchor	Strain	Strain gage	Liner failure
	Concrete	Cracking	Video	Response
Other	Steel Plate	Strain	Strain gage	Penetration failure
Penetrations	Liner	Strain	Strain gage	Liner failure
	Liner anchor	Strain	Strain gage	Liner failure
Basemat/ Tendon	Tendons	Force	Load cell	Response and Tendon failure
Gallery	Rebar	Strain	Strain gage	Shear failure
	Concrete	Uplift Displacement	LVDT	Response
Buttress	Liner	Strain	Strain gage	Response and Liner failure
	Rebar	Strain	Strain gage	Response
	Tendon	Force	Load cell	Response and Tendon failure

CPOT - Cable Potentiometer
LVDT - Linear Variable Differential Transformer
TLDT – Temposonics Linear Displacement Transducer

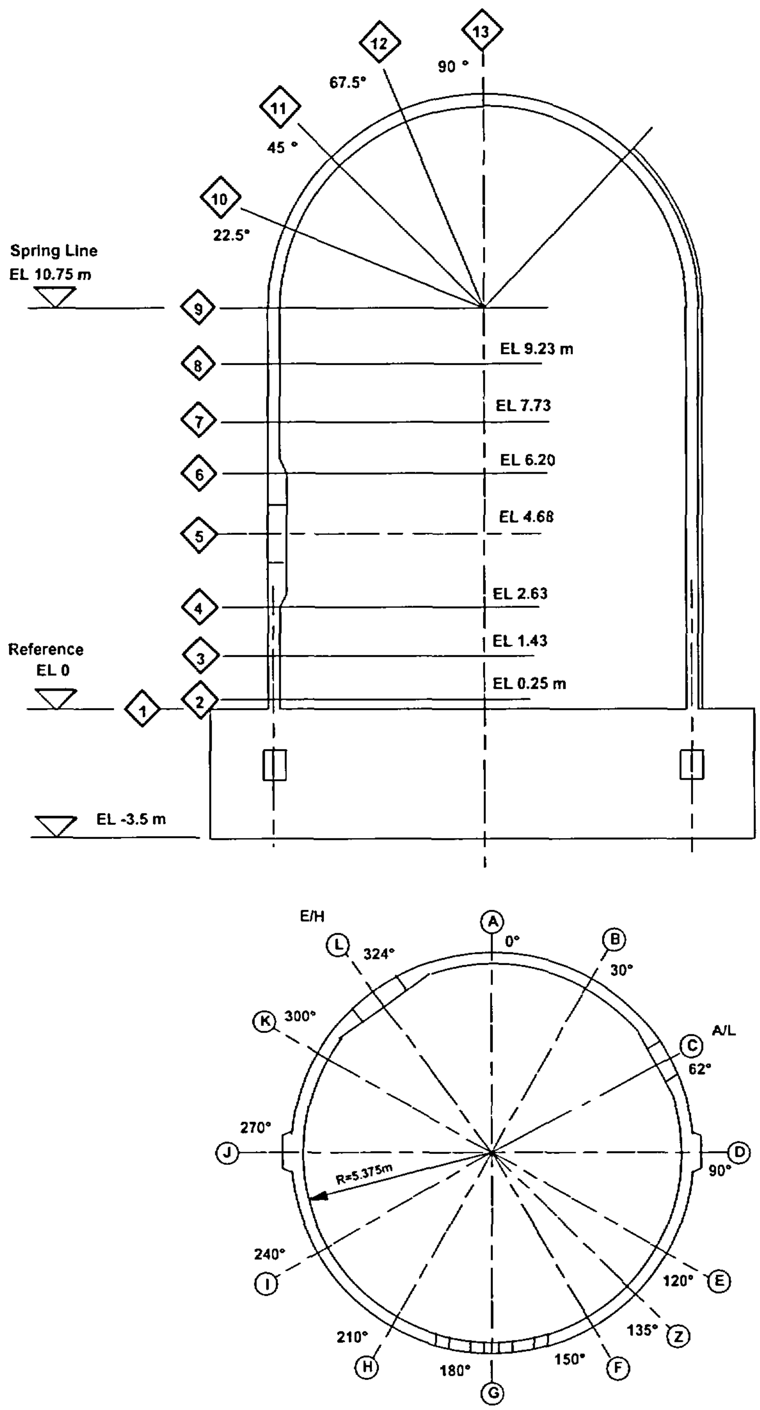

Figure 3.1 Cardinal Instrumentation Layout Lines

3.2 Types of Measurements

This section summarizes the types of measurements required to meet the PCCV test objectives. Details of what and why measurements were taken are included. These measurement types correspond to those shown previously in Table 3.1.

3.2.1 Pressure

Accurate measurement of the internal gas pressure in the PCCV during pressure tests was necessary for several reasons. First, the pressurization of the vessel for the test needed to be carefully controlled and accurately recorded to allow comparison of model response with pre- and posttest analytical results as a function of pressure. Next, accurate calculation of the integrated gross leak rate of the vessel during low pressure testing and detection of leaks and leak rate estimation during high pressure testing dictated the need for accurate pressure and temperature data. These data, along with knowledge of the gas properties in the vessel, allow calculation of leak rates during the tests.

The specifications for the pressure sensors are presented in Table 3.2. The accuracy requirements dictate voltage output devices (rather than millivolt output) with integrated signal conditioning electronics included.

Table 3.2 Pressure Transducer Specifications

Specification Item	Data
Type of measurement required	Gage pressure inside PCCV model
Anticipated exposure conditions	Non-purified nitrogen gas at pressures from ambient to approx. 2.1 Mpa-g (300 psig) for durations no more than 20 days (500 hours)
Operational range	1% of full scale < P_{op} < 2.4 Mpa-g (350 psig) (125% of anticipated rupture pressure)
Desired output	Amplified voltage
Total desired accuracy (i.e., linearity, repeatability, hysteresis, sensitivity)	Less than or equal to 0.1% of span
Temperature effect	< 0.05% full scale per °F over temperature compensated range
Logistics (electrical connection, cabling requirements, etc.)	Pressure taps from vessel will be installed so the transducer housing will represent part of the pressure boundary, typical four wire connection with independent power supply required (i.e., not provided by VXI mainframes), specifications for power supply dependent on type of pressure transducer (i.e., input voltage needs)

Two high-accuracy pressure transducers, Mensor Model 4040 high-accuracy digital units[18], were installed in the vessel to provide redundancy in the measurements. Although the predicted failure pressure of the model was not known with certainty, preliminary calculations indicated it would be in the range of 1.6MPa-g (230 psig). The pressurization system and all equipment was designed for an upper-bound capacity estimate of 2.1Mpa-g (300 psig). Applying an overpressure margin of 15%, the specified range for the pressure transducers was 2.4 MPa-g (350 psig).

---

[18] Mensor Corporation, 201 Barnes Drive, San Marcos, Texas, 78666. (http://www.mensor.com/Digital_Pressure_Transducer_4000.htm)

(An independent pressure transducer was supplied with the pressurization system to control test operations. This transducer was independently calibrated; however, all test results are reported against the 'official' pressure transducers.)

3.2.2 Temperature

Both model material and internal gas temperatures were measured. Material temperature measurements were made to provide data for thermal compensation of all strain gages within the PCCV model and to provide data to correlate the response of the model to changes in ambient thermal conditions and the effects of direct radiant heating. Two types of T/Cs were used: Omega Model SA1-T T/Cs were placed on the inside surface of the PCCV liner, while Omega Model TQSS-116 were embedded within the concrete[19]. Due to the low sensitivity of the strain gages to temperatures around 23°C and the anticipated low temperature gradients along the inside surface of the model, low cost thermocouples were installed so that one T/C compensated several gages. Therefore, only a relatively small number of T/Cs were required to fulfill the temperature compensation requirements for the entire suite of strain gages. These were uniformly distributed, along with additional liner T/Cs near the E/H and A/L.

Internal gas temperature measurements were required to evaluate the integrated leak rate from the vessel prior to and during the pressure tests. High accuracy transducers were required for this purpose due to the small magnitude of the overall leak rate compared to the large volume of the vessel. Resistance temperature detectors (RTDs), Omega Model RD 805 precision gas temperature monitoring units[19], were used for this purpose. The RTDs were distributed fairly uniformly throughout the model so that the tributary volumes associated with each sensor were approximately equal. These temperature measurements, in conjunction with the pressure measurements, provided data to detect leaks and estimate leak rates. Fans were available to circulate the gas inside the model in order to minimize thermal stratification during testing. A single RTD was also located outside the model (on the north side, i.e., in the shade) to provide ambient air temperature data.

The requirements for each of the two temperature monitoring instruments are provided in Tables 3.3 and 3.4 For the PCCV tests, three wire, lead-resistance-compensation-type sensors with low self-heating errors were used.

Table 3.3 Thermocouple Specifications

Specification Item	Data
Type of measurement required	Temperature measurements of inside surface of PCCV model
Anticipated exposure conditions	Nitrogen, from ambient to 2.1 MPa-g (300 psig), expected maximum temp. range from -5 to 50°C
Operational range	-10 to 100 °C
Desired accuracy	< 2% of total input range
Temporal response times	Unspecified, not critical
Junction characteristics	Ungrounded, sheathed
Logistics (electrical connection, cabling requirements, etc.)	Two-wire twisted, insulated leads of same material as thermoelement junction pair, junctions at pin-type pressure feedthroughs (requires pins of same materials as conductors)

[19] Omega Engineering, Inc., One Omega Drive, Stamford, Conn. 06907-0047. (http://www.omega.com/temperature/tsc.html)

Table 3.4 RTD Specifications

Specification Item	Data
Type of measurement required	PCCV internal gas temperature measurements
Anticipated exposure conditions	Nitrogen, ambient to 2.1 MPa-g (300 psig)
Operational range	-10 to 100°C
Desired accuracy	< 2% of total input range
Desired sensitivity	N/A
Logistics (electrical connection, cabling requirements, etc.)	Four-wire twisted, insulated leads. Requires constant current source (typically 1ma).

3.2.3 Displacement

Displacements were measured at discrete locations to compare with analysis and allow construction of the global response of the model. The types of displacement measured included:

1. radial displacements of the cylinder wall at regular azimuths and elevations relative to a reference point on the instrumentation frame,
2. vertical displacements at the springline at regular azimuths relative to the top of the basemat liner,
3. horizontal and vertical displacements in the dome at regular azimuths and elevations relative to the instrumentation frame,
4. vertical displacements at the apex of the dome relative to the instrumentation frame,
5. changes in internal diameter (i.e. ovalization) of the E/H and A/L barrels,
6. vertical displacement or uplift of the basemat relative to the mudmat.

The range of displacements to be measured included small, elastic deformations during prestressing and subsequent changes due to ambient temperature variation, creep, etc., through large inelastic deformations during pressure testing.

For the PCCV model test, three types of displacement transducers allowed a wide range of expected displacement to be measured. Overall global deformations at the cardinal points were typically measured using CPOT Celesco Model PT 101[20] (Figure 3.2). Where deformations were expected to be small, such as at the wall-junction or where higher precision was desirable, such as measuring local deformations at penetrations, Schaevitz HCD series[21] LVDTs with ranges on the order of 4" or less were used (Figure 3.3). In some locations where both high accuracy and long range were required, Temposonics® magnetostrictive high-accuracy TLDTs[22] were used (Figure 3.4). The specifications for each of these displacement transducers are provided in Tables 3.5, 3.6, and 3.7.

Note that all displacement data represents the relative motion between the point of interest and a reference point. Ideally, the reference point is fixed and not influenced by the loads applied to the test structure; however, in most cases, this is impractical. For the case of the PCCV model, most displacements were measured internally and referenced to the instrumentation frame or the top of the basemat. Since the basemat was judged to be, essentially, a rigid mass, the only consideration required for the instrumentation frame was its response to variations in internal temperature. A set of transducers were mounted on the instrumentation frame to measure changes in height and plan dimensions and determine if there was any effect on the cylinder or dome displacements. These frame displacement transducers consisted of

[20] Celesco Transducer Products, Inc., 20630 Plummer St., Chatsworth, CA, 91311. (http://www.celesco.com/cet/index.html)

[21] Measurement Specialties, Inc., Sensor Products Division, 950 Forge Ave. Bldg B, Norristown, PA 19403. (http://www.msiusa.com/schaevitz/products/LVDT/index.html)

[22] MTS Systems Corp., Sensors Group, 3001 Sheldon Drive, Cary, NC 27513. (http://www.mtssensors.com/)

CPOTs and two Spectron Model SSY0140 dual-axis inclinometers[23] to monitor tilt of the frame due to possible basemat curvature.

In addition, the internal displacement transducers were attached to the liner surface, assuming that the liner was 'perfectly' bonded to the concrete. This assumption, while valid in most cases, was incorrect in a number of cases (which will be discussed in Chapter 5) and it is worth remembering that all internal displacement data represents the position or motion of the liner, not necessarily the concrete wall.

Similarly, uplift of the basemat was measured relative to the mudmat (Figure 3.5) and, as was previously identified, any motion of the mudmat would affect the uplift data.

Table 3.5 Displacement Transducer Specifications (CPOT)

Specification Item	Data
Type of measurement required	Radial or vertical displacement of internal surface of the PCCV model
Anticipated exposure conditions	Nitrogen, from ambient to 2.1 MPa-g (300 psig)
Operational range	5 cm, 12.5 cm, 25 cm, and 38 cm (2", 5", 10" and 15")
Desired accuracy (linearity and repeatability)	0.15 to 0.25% full scale
Logistics (electrical connection, cabling requirements, etc.)	Power supply required (not included on VXI card), multi-pin cable connector needed

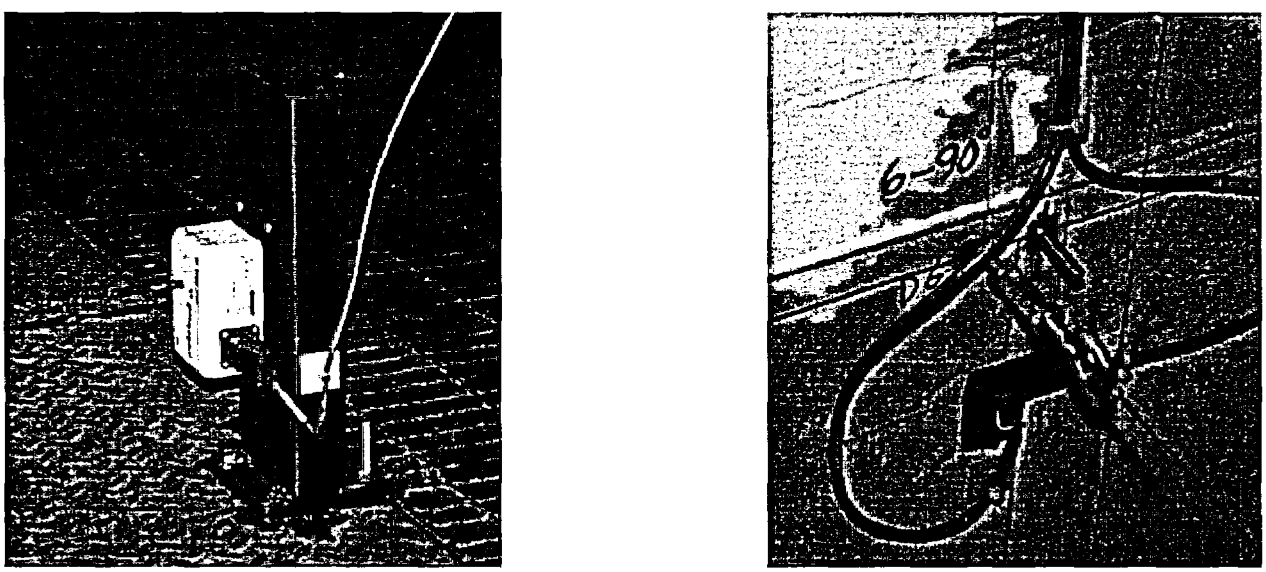

Figure 3.2 CPOT Mounted on Instrumentation Frame and Attachment to PCCV Liner

[23] Spectron Systems Technology, Inc., 595 Old Willets Path, Hauppage, NY 11788. (http://www.spectronsensors.com/inclinomter.htm)

Table 3.6 LVDT Specifications

Specification Item	Data
Type of measurement required	Radial or vertical displacement of internal surface of the PCCV model Ovalization of equipment hatch and personnel airlock, basemat uplift
Anticipated exposure conditions	Nitrogen, from ambient to approx. 2.1 MPa-g (300 psig)
Operational range	2.5 and 10 cm (1" and 4")
Desired sensitivity	< 1% total input range
Deviation from linearity	0.25% full scale
Logistics (electrical connection, cabling requirements, etc.)	Same as CPOT requirements

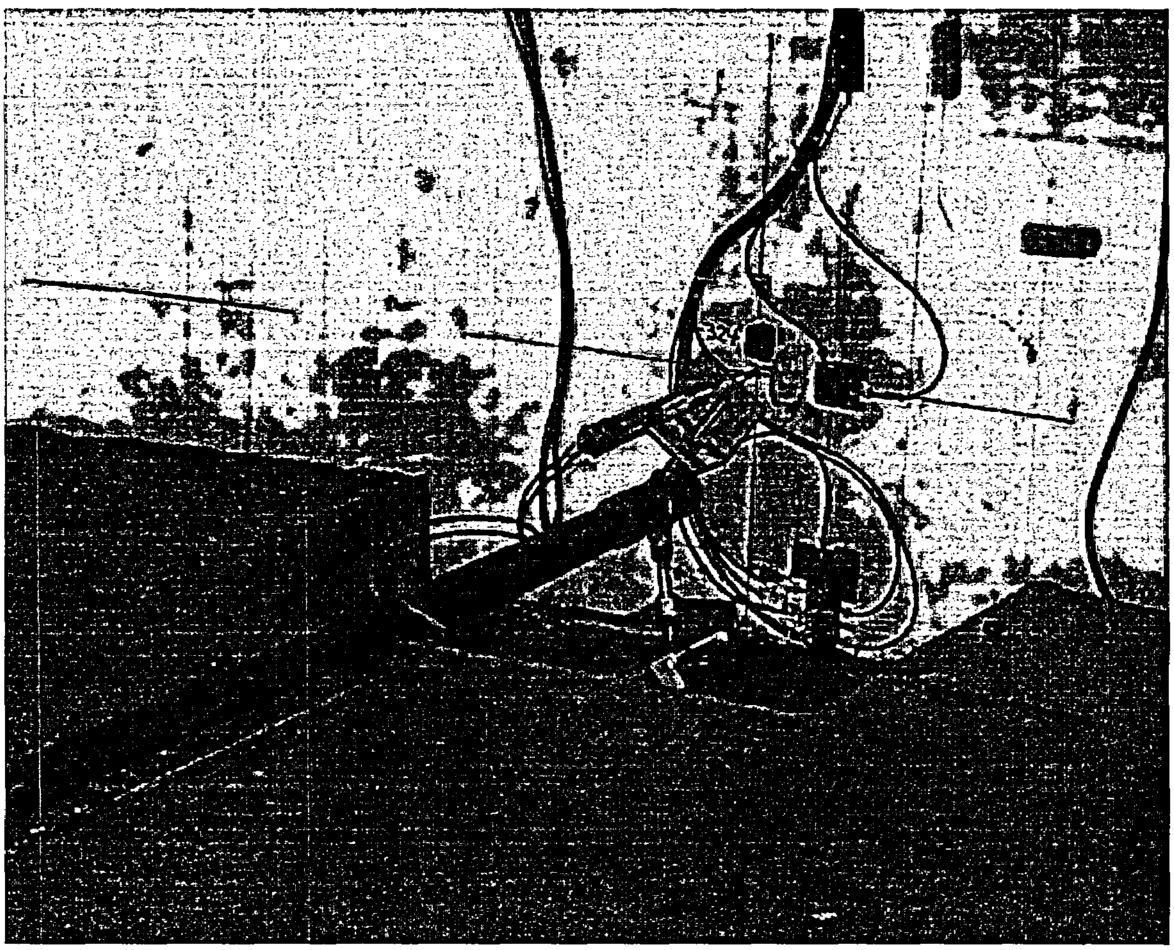

Figure 3.3 LVDTs at Wall-Base Junction (Azimuth 324 degrees, Elev. 0.0 and 250.0)

Table 3.7 Temposonics Linear Displacement Transducer Specifications (TLDT)

Specification Item	Data
Type of measurement required	Accurate and high range measurements of linear displacement of internal surface of PCCV model
Anticipated exposure conditions	Nitrogen, from ambient to approx. 2.1 MPa-g (300 psig)
Operational range	38 cm (15")
Desired sensitivity	< 1% total input range
Deviation from linearity	0.02% full scale (min 13 mm)
Logistics (electrical connection, cabling requirements, etc.)	Same as CPOT requirements

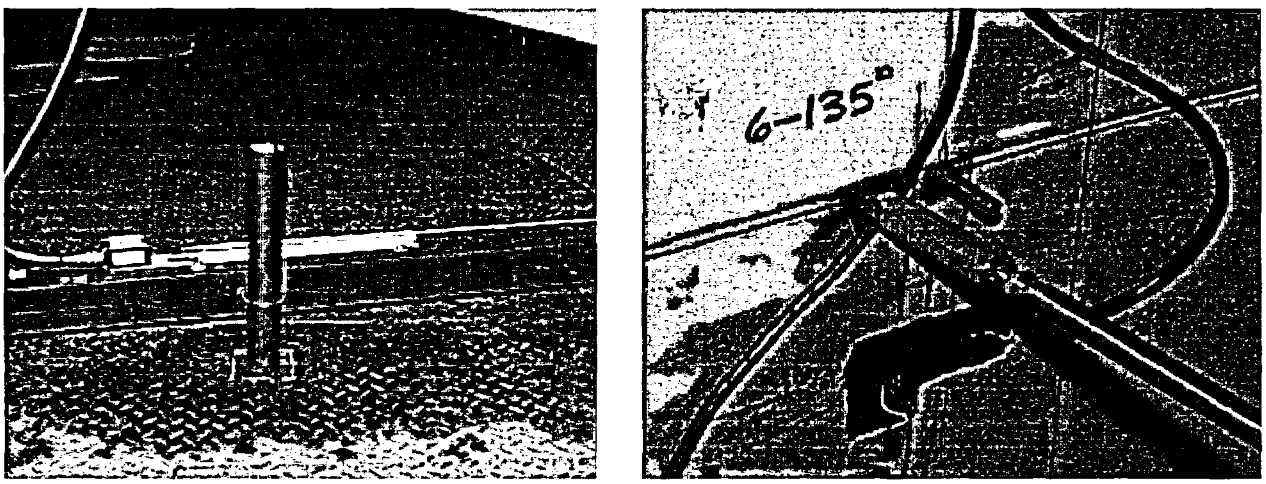

Figure 3.4 TLDT Mounted on Instrumentation Frame and Attachment to PCCV Liner

3.2.4 Concrete Cracking

The basic instrumentation plan identified the relationship between concrete cracking and load or pressure as one of the response mechanisms to observe during the PCCV test. In order to thoroughly model and understand concrete cracking mechanisms, several parameters to measure were identified:

1. the strain in the concrete,
2. when and where a crack first occurs,
3. crack propagation, and
4. crack width.

Measurement of discrete concrete crack width is, however, difficult to perform in practice. A discrete crack must be identified prior to placing a gage at the crack location. However, since most cracks of interest will not form until the test pressure exceeds the design pressure (and the prestressing load), safety constraints prohibit the installation of gages during testing. Several schemes for measuring concrete crack width were considered, including pre-cracking the model, placing crack width gages at a number of shrinkage cracks, or using high resolution video monitoring. However, none of these schemes was considered to be practical or cost-effective. The decision was made to abandon requirements to measure concrete crack width and focus on crack detection and crack propagation.

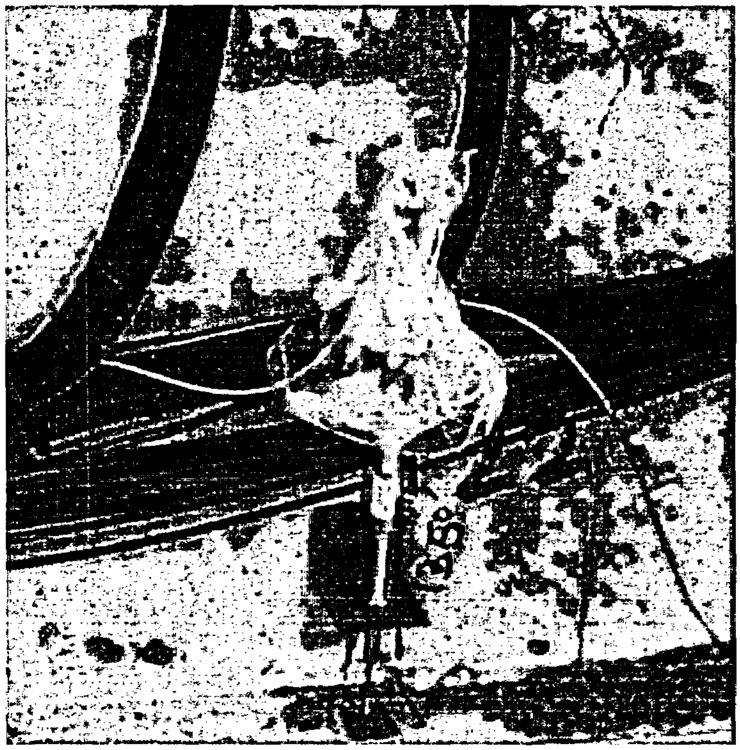

Figure 3.5 External LVDT Measuring Displacement between Basemat and Mudmat

Crack initiation and propagation were monitored by performing detailed visual inspection to construct crack maps in areas of interest following critical load steps. These crack maps are supported by photographic records of all the areas inspected. Detection of crack initiation during pressure testing was also attempted via acoustic monitoring, described in Section 3.2.8.

Concrete strain measurements are discussed in Section 3.2.5.2.

3.2.5 Strain Measurements

Strain gages applied to individual structural elements provide information on the discrete strain in the element being interrogated and are also capable, when used in groups, of providing insight into local and global strain fields in the structure. Extensive experience through the previous history of containment testing at SNL and elsewhere formed the basis for the specification of strain gage requirements for the PCCV experiment. Standard electrical-resistance type, bonded strain gages were chosen for their simplicity and accuracy, as well as low relative cost. All foil-type strain gages used on the PCCV model were high-elongation-type EP Micro-Measurements gages constructed of annealed constantan on a polyimide backing.[24] These gages were used to measure strains in the rebar, concrete, liner, liner anchor, hatches and penetrations, and tendons. In some cases, noted below, special types of strain gages were used in addition to the bonded foil gages to provide additional response information.

Care must be exercised, however, when interpreting strain gage output, since very small gage length strain gages are highly susceptible to the influence of local structural discontinuities or as-built conditions and positioning of the gage in areas with high strain gradients can significantly affect the results. These factors should be considered when comparing strain data with analysis results at discrete points in a structure. Furthermore, the application of the strain gage to the structural element may perturb the strain fields in the vicinity of the gage and these effects should, if present, also be considered.

---

[24] Micro-Measurements Division, Vishay Measurements Group, Inc., Raleigh, NC 27611. (http://www.vishay.com/brands/measurements_group/strain_gages/mm.htm)

3.2.5.1 Reinforcing Bar Strain

Strain gages, mounted to meridional, hoop, and transverse reinforcing steel, were used to measure the global 'free-field' or local membrane, bending and shearing strains in the model as a function of pressure. Reinforcing strain measurements were generally not made in areas where the reinforcing was highly congested, such as around penetrations, or to determine local strain concentrations. Exceptions to the latter case included the wall-basemat intersection and around the tendon gallery. In areas of highly congested reinforcing, rebar strains were measured at the perimeter of the reinforcing grid to confirm boundary conditions for comparison with pretest analyses. Typical reinforcing strain measurements included:

1. Free-field strain measurements of meridional and hoop reinforcing steel at regular azimuths and elevations in the cylinder wall and dome for comparison with pretest axisymmetric and global 3D analyses and to determine the global strains at which local failures were expected to occur. Typically, both inner and outer reinforcing strains were measured to resolve membrane and bending behavior.
2. Near-field strain measurements of meridional and hoop reinforcing steel at the boundaries of local reinforcing areas, e.g. E/H, A/L, etc., were acquired for confirm boundary conditions for local submodels in pretest and posttest analyses.
3. Near-field strain measurements of radial ties in the vicinity of structural discontinuities where large shears or large bending moments were predicted to occur, and to measure triaxial state of strain (stress) for evaluating failure models. In addition, inclined gage bars were used, based on the predicted orientation of principal tensile stresses.

The specifications for the rebar (and tendon wire) strain gages are summarized in Table 3.8. Figures 3.6 and 3.7 show a typical rebar strain gage after mounting on the bar and in place in the model, with protective epoxy cover.

Understanding the method of mounting the strain gages on the rebar is important to interpreting the rebar strain data. One of the first considerations is that the surface of the rebar to which the gage is to be bonded must be ground smooth. This typically removes a portion of the bar's cross-section, which can result in a local strain concentration in the bar. This phenomenon is described in more detail in Section 5.3.2.1.5. Second, requirements to protect the strain gages during erection and concrete placement locally debond the rebar from the concrete, so that local strains between the rebar and concrete may not be compatible. Finally, strain gages on rebar are located away from the ends of bars or mechanical splices to ensure the bars are fully developed and to avoid end effects. However, in some cases, end effects may be a factor and the location of the gage relative to the bar end should be known.

Table 3.8 Strain Gage Specifications (Rebar & Tendon wire)

Specification Item	Data
Type of measurement required	Point strain (approx.) in the "hoop," "meridional," and "radial" directions attached to the reinforcing steel and the prestressing tendon strand wires.
Anticipated exposure conditions	Concrete placement, curing, long term exposure, temperatures from -5 to 50°C
Operational range	Wire gages: 4 - 6% Rebar gages: 5 - 10%
Desired strain sensitivity (gage factor, k)	$1 < k < 2$ (all gages)
Transverse sensitivity, k_t	$k_t < 2\%$ (all gages)
Mounting configuration	Strain gages will be adhesively bonded to the reinforcing steel and tendon wire strands
Logistics (installation, electrical connection, cabling requirements, etc.)	Three wire twisted, insulated cables

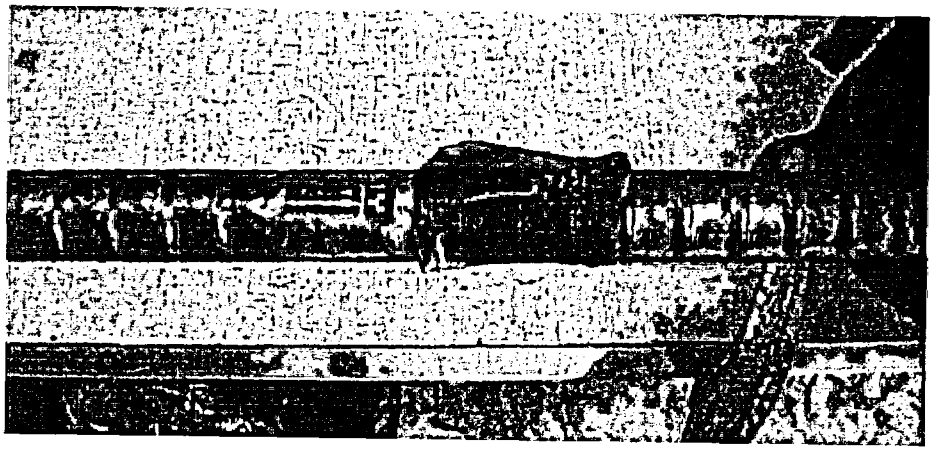

Figure 3.6 Rebar Strain Gage

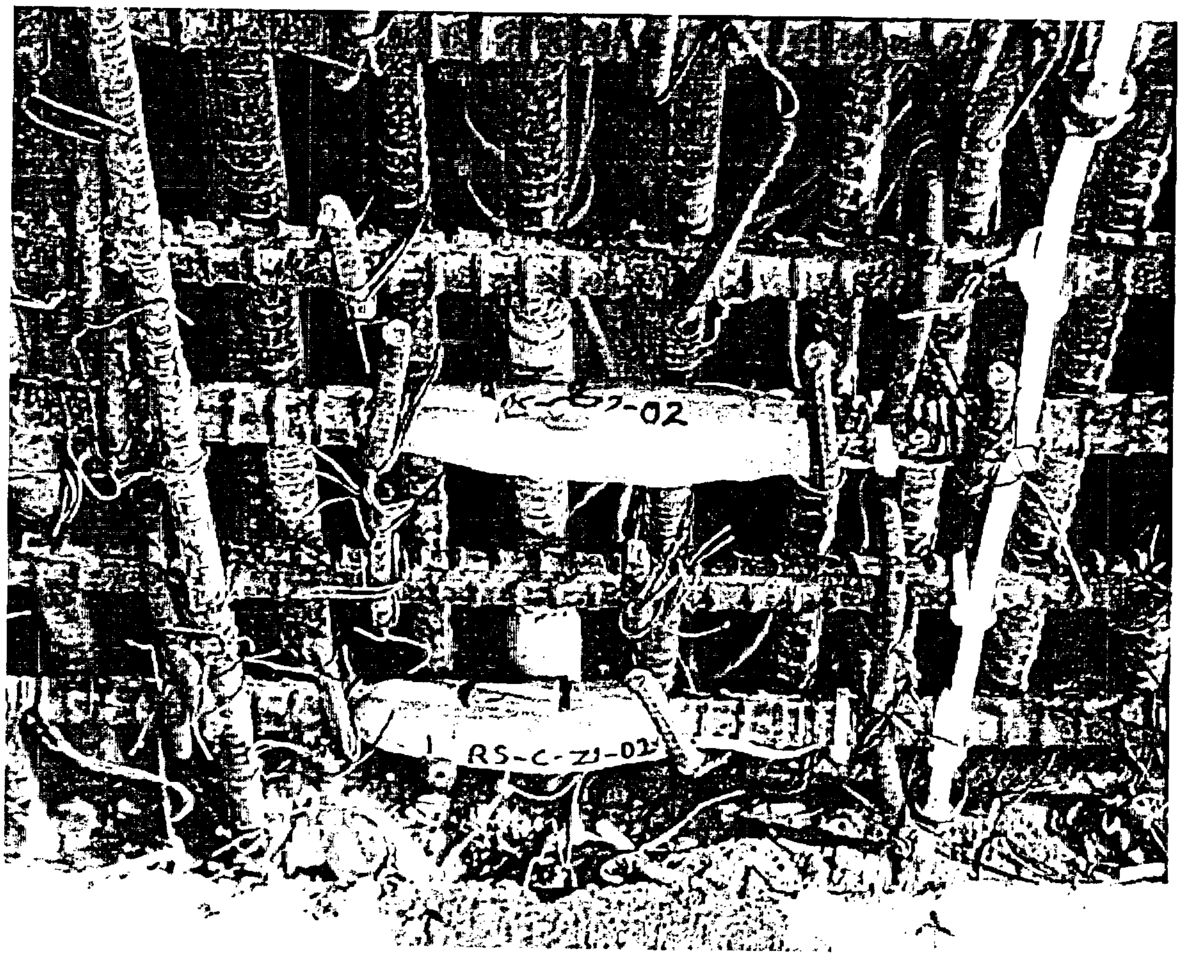

Figure 3.7 Rebar Strain Gages Installed in PCCV Model
(Note SOFO Fiber Optic Concrete Strain Gage at right)

3.2.5.2 Concrete Strain

As noted above, since rebar gages are susceptible to local strain concentration and may be debonded from the concrete, rebar strains may not provide an accurate indication of the concrete strain. Measurement of concrete strains, therefore, may require the use of independent gages designed specifically for this purpose. Based on experience during previous model tests, commercially-available concrete strain gages were not judged reliable or cost-effective. Measurement of global concrete strain can be most accurately and reliably be determined from displacement data using the kinematic relationship $\varepsilon = \Delta r/R$. Specially fabricated bars, or gage bars, which are not part of the normal reinforcing, along with long-gage length fiber-optic gages, were installed to help measure local concrete strains, such as where significant bending occurs (e.g. at the wall base junction, adjacent to the buttresses and near penetrations) and for comparison with rebar strain measurements.

Specifications for the gage bar strain gages are summarized in Tables 3.9. The configuration of the gage bars is illustrated in Figure 3.8. Sample rebar and gage bar strain gages are compared in Figure 3.9.

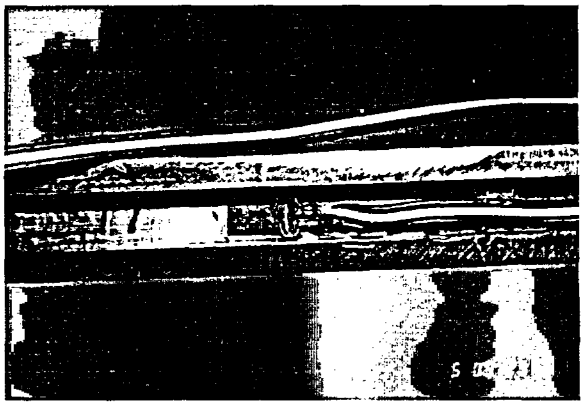

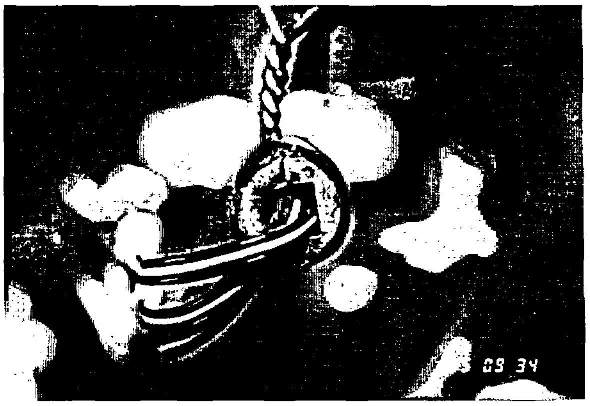

Figure 3.8 Concrete Strain Gage Bars

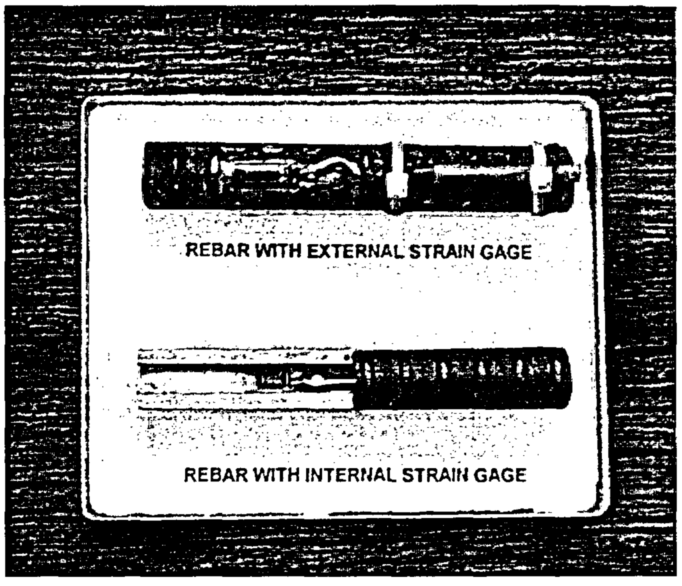

Figure 3.9 Sample Rebar and Gage Bar Strain Gages

Table 3.9 Strain Gage Specifications (Concrete Gage Bars)

Specification Item	Data
Type of measurement required	Point strain (approx.) in the "hoop" and "meridional" directions, embedded in the concrete.
Anticipated exposure conditions	Concrete placement, curing, long term exposure, temperatures from -5 to 50°C
Operational range	5 – 10%
Desired strain sensitivity (gage factor, k)	$1 < k < 2$ (all gages)
Transverse sensitivity, k_t	$k_t < 2\%$ (all gages)
Mounting configuration	Attached to the reinforcing steel prior to concrete placement
Logistics (installation, electrical connection, cabling requirements, etc.)	Three wire twisted, insulated cables

Specifications for the fiber optic gages SOFO Model 500[25] are summarized in Table 3.10. The SOFO gage, prior to installation, is shown in Figure 3.10. The active gage length is between the two 'anchors,' shown at the bottom, and the remainder is the fiber optic transmission cable. The installed SOFO gage was shown in Figure 3.7.

Table 3.10 Strain Gage Specifications (Fiber Optic Gages)

Specification Item	Data
Type of measurement required	Global or 'near-field' strain in the "hoop" and "meridional" directions in the concrete
Anticipated exposure conditions	Concrete placement, curing, long term exposure, temperatures from -5 to 50°C
Operational range	50 cm (20") gage length, 1 – 2%
Desired strain sensitivity (gage factor, k)	NA
Transverse sensitivity, k_t	NA
Mounting configuration	Place between reinforcing steel prior to concrete placement
Logistics (installation, electrical connection, cabling requirements, etc.)	Fiber optic leads running to 10 channel SOFO DAS reader

3.2.5.3 Liner and Liner Anchor Strain

Both the membrane and bending strains in the liner, as well as strains in the liner anchors, were measured. Strain gages were used to measure both free-field and local strains near liner discontinuities where strain concentrations might occur. Liner anchor strain measurements were included to investigate shear transfer across anchor, pullout force on anchor, and reinforcement contribution in the axial direction of the liner anchor. The specifications for the liner and liner anchor strain gages are summarized in Table 3.11.

At particular details and locations, arrays of gages were applied to allow characterization of the local strain fields and provide insight into the mechanism that tears the liner. Note that gages located adjacent to tears often exhibit much lower strains than expected since the tear acts as a strain relief mechanism on the surrounding structure. In areas where bending strains were likely to occur, strain gages were applied to both sides of the liner to allow them to be resolved into bending and membrane components. In areas where bending was unlikely, strain gages were only applied to the inside surface of the liner. Typical interior and exterior liner and liner anchor gages are shown in Figure 3.11.

---

[25]SMARTEC SA, Via Pobbiette 11, 6928 Manno, Switzerland. (http://www.smartec.ch/Home.htm)

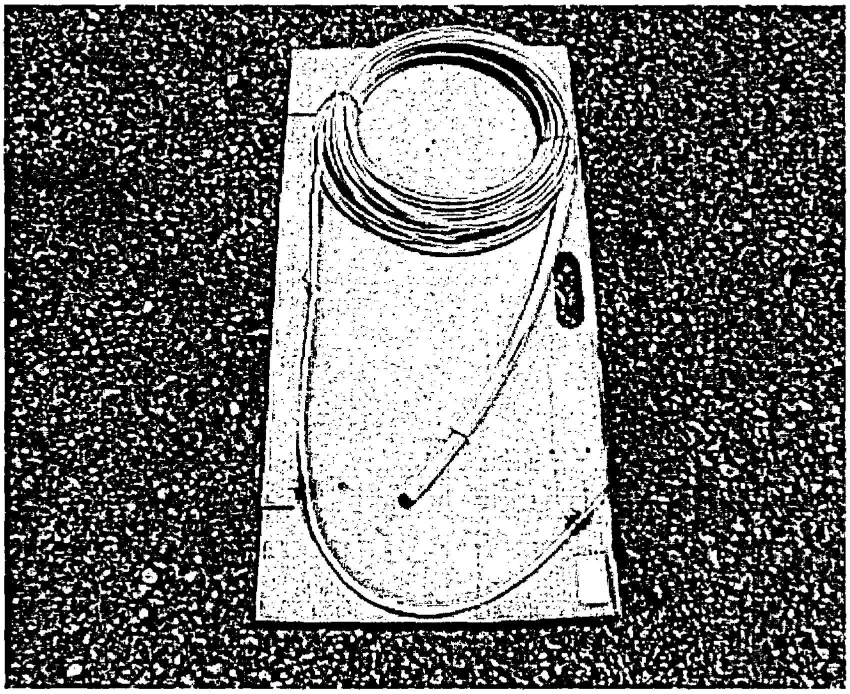

Figure 3.10 SOFO Fiber Optic Strain Gage

Table 3.11 Strain Gage Specifications (Liner & Liner Anchor)

Specification Item	Data
Type of measurement required	Point strain (approx.) in the "hoop," "meridional," and "radial" directions, both internal and external on the liner, liner anchors, and stiffeners embedded in the concrete.
Anticipated exposure conditions	**Internal:** non-purified nitrogen gas at pressures from ambient to approx. 2.1 MPa-g (300 psig), duration of elevated pressures not more than 20 days (500 hours), temperatures from -5 to 50°C. **External:** concrete placement, curing, and long term exposure
Operational range	Strip gages (2-10 elements): 20% 0-45-90 rosettes (3 elements): 20% single gages: 10 - 20%
Desired strain sensitivity (gage factor, k)	$1 < k < 2$ (all gages)
Transverse sensitivity, k_t	$k_t < 2\%$ (all gages)
Mounting configuration	Carrier matrix material bonded to surface of liner (both internal and external), model liner material is carbon steel, painted internally
Logistics (installation, electrical connection, cabling requirements, etc.)	Three wire twisted, insulated cable, junctions to pin-type pressure feedthroughs

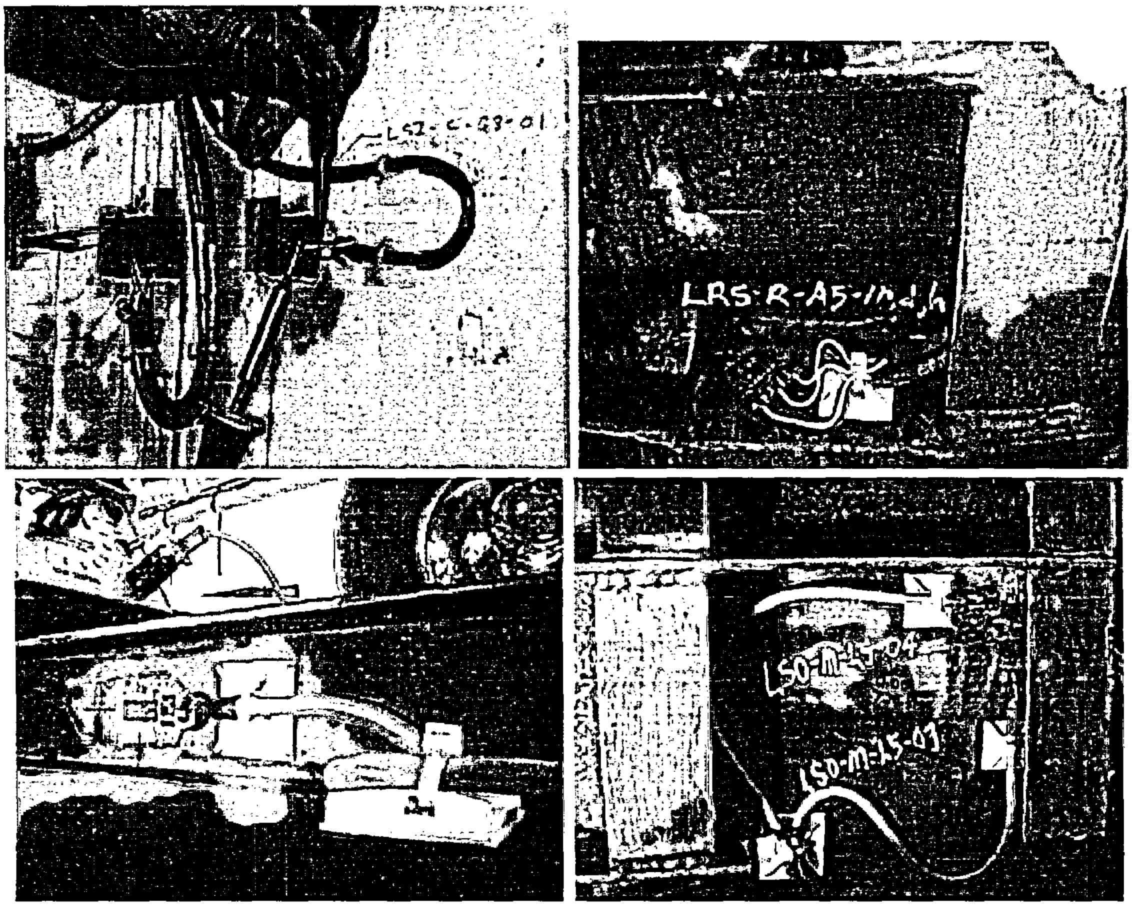

Figure 3.11 Liner and Liner Anchor Strain Gages

3.2.5.4 Residual Liner Strain

Considering pretest analysis results that predicted high liner strain concentrations around the E/H insert plate and ranked them most likely to tear the liner, an attempt was made to measure the residual strain fields in the liner at this location after high pressure testing. This was performed by placing a grid on the interior liner surface and, using a digital position mapping tool, recording the position of the grid points before and after testing. Based on the change in position, coupled with strain data from liner strain gages located within the grid, it was hoped that a more accurate map of the strain field could be obtained. The grid placed around the E/H is shown in Figure 3.12

3.2.6 Tendon Measurements

Tendon strain and force measurements were discussed Section 2.2.3 in the context of prestressing operations. The basic instrumentation plan called only for tendon anchor forces to be measured during the tests. It was, however, desirable to measure the force at points along the tendon length to confirm the design force distribution described in Section 2.1.3, both initially, after prestressing, and during pressure testing as the PCCV model deformed.

3.2.6.1 Tendon Anchor Force (At Ends)

Load cells were installed at both ends of selected hoop tendons and meridional hairpin tendons to measure the anchor forces during and after prestressing and during pressure testing. Due to the relatively high cost of the load cells, only approximately one-sixth of the model tendons were monitored with load cells. The load cells were inserted between the tendon anchor and the bearing plate embedded in the concrete to measure the compressive force.

GRID LAYOUT

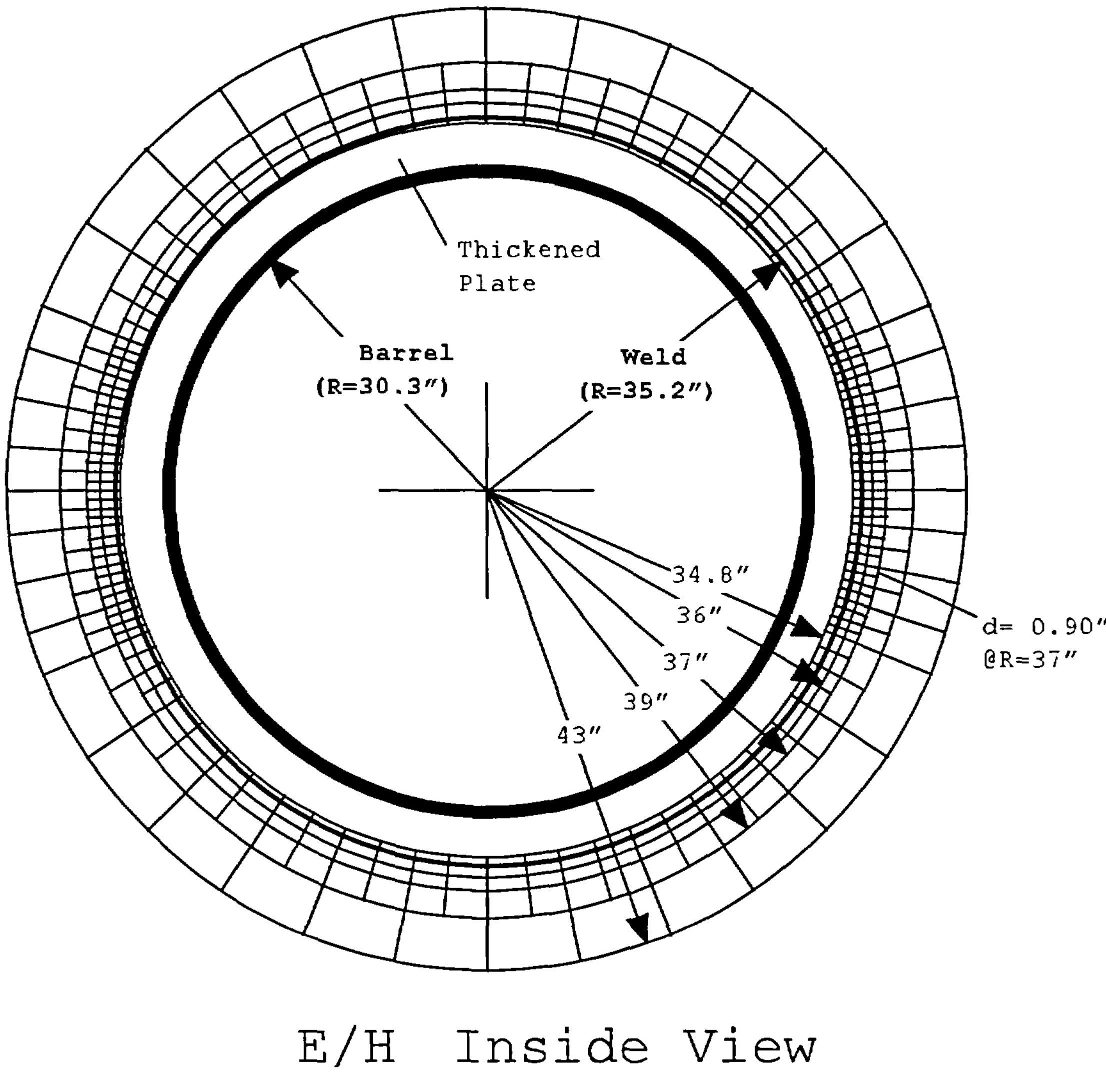

5 radial Circles
120 radial Lines
480 points
Smallest grid ~ 1" x 1"

Figure 3.12 Grid Layout around Inside of E/H

From this data, tensile stresses at each end of the tendons were computed. All loads cells were installed just prior to the prestressing operations and measurements were taken throughout the prestressing operations. The requirements for the load cells are provided in Table 3.12.

Table 3.12 Load Cell Specifications

Specification Item	Data
Type of measurement required	Tendon load at both ends
Anticipated exposure conditions	Ambient outdoor temperatures and humidity
Operational range	0 to 890 kN (200 kips)
Desired accuracy	1% of total input range
Temporal response times	Unspecified, not critical
Logistics (electrical connection, cabling requirements, etc.)	Six wire, twisted insulated pairs

Due to limited availability and to reduce cost, two different load cells were used in the model. Higher accuracy (and higher cost) HBM Model C6-100t load cells[26] were used for the instrumented tendons, while somewhat lower accuracy (and less expensive) Geokon Model GK-3000-200-2.0[27] load cells were used for the remaining tendons. The HBM load cell with spherical washers (provided to balance the force applied to the load cell) and bearing plates are shown in Figure 3.13. Both the installation jig used for positioning the load cells for the hoop tendons and the arrangement for the vertical tendons is shown. The Geokon load cell with the bearing plates is shown in Figure 3.14. Although the Geokon load cells came equipped with spherical washers provided by the manufacturer, laboratory calibration tests showed the output was more accurate if very thick bearing plates were used in place of the spherical washers. (Also, the spherical washers exhibited an unfortunate tendency to shatter at loads below the load cell capacity, ejecting fragments in a highly energetic manner.) Both the installation jig used for positioning the load cells for the hoop tendons and the arrangement for the vertical tendons is shown.

3.2.6.2 Tendon Force Distribution (Along Length)

The tendon force distribution was determined by measuring the strain at discrete points of individual wires and strands comprising the tendon. Extensive research was conducted to investigate the efficacy of commercially-available transducers to provide the desired data. Laboratory and mock-up testing of tendon strands were conducted to investigate the performance of the gages and led to a scheme utilizing two types of gages. These tests were also used to develop calibration relationships between wire or strand strain and tendon force, and demonstrate methods to protect the gages from damage during construction and tensioning.

In addition to standard strain gages placed directly on the wires (specified in Table 3.8), strain gages specially designed to measure the axial strain in seven-wire strands, Tensmeg®[28] gages, were used. Tensmeg gages are a single wire gage attached with rubber end-blocks around a tendon strand to measure uniaxial strain in the tendon. The specifications for the Tensmeg gages are summarized in Table 3.13.

Based on the laboratory and mock-up tests that demonstrated the variability of strain from wire to wire within a given strand and from strand to strand, along with the likelihood of a high mortality rate for the strain gages, each measurement location used combinations of wire and strand strain gages, along with special hardware, to protect the gages and lead wires. Special handling and tensioning procedures were also employed to minimize damage to the tendon strain gages.

---

[26] HBM, Inc., 19 Bartlett Street, Marlborough, MA 01752. (http://www.hbm.com)

[27] Geokon, Inc., 48 Spencer Street, Lebanon, NH 03766. (http://www.geokon.com/)

[28] Roctest Ltd., 665 Pine Avenue, Saint-Lambert, Quebec, Canada J4P 2P4. (http://www.roctest.com/roctelemac/product/product/tensmeg.htm)

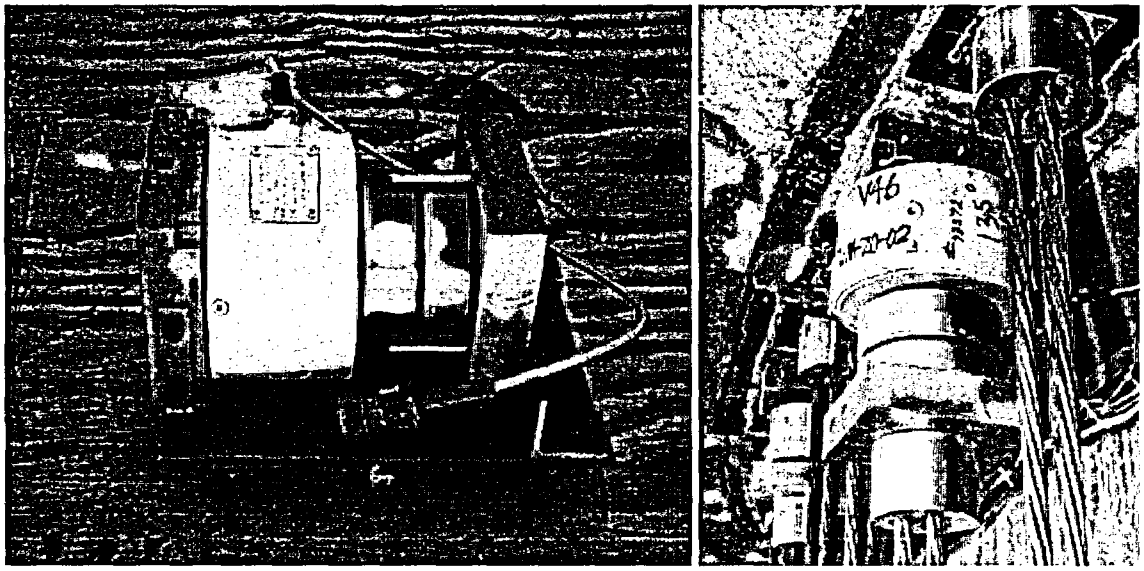

Figure 3.13 HBM Load Cell (a) Installation Jig, (b) In-Place

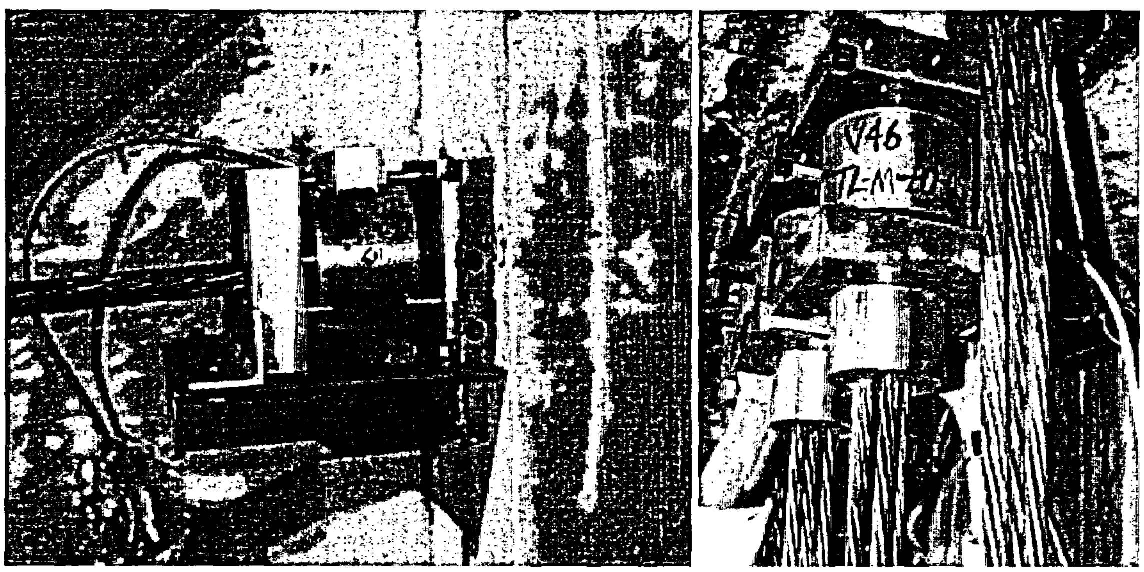

Figure 3.14 Geokon Load Cell (a) Installation Jig, (b) In-Place

Table 3.13 Tensmeg Gage Specifications

Specification Item	Data
Type of measurement required	Point strain (approx.) in the "hoop" and "meridional" directions, inside the tendon ducts, embedded in the concrete
Anticipated exposure conditions	Concrete placement, curing, and long term exposure
Operational range	4 – 6%
Desired strain sensitivity (gage factor, k)	$1 < k < 2$ (all gages)
Transverse sensitivity, k_t	$k_t < 2\%$ (all gages)
Mounting configuration	Gages will be adhesively bonded directly on each strand
Logistics (installation, electrical connection, cabling requirements, etc.)	Three wire twisted, insulated cable

A set of representative hoop and vertical hairpin tendons were instrumented with gages along the length of the tendon. Five hoop tendons were instrumented: H11 near the base of the cylinder wall, H53 near the mid-height, H35 (which is deflected around the E/H and A/L penetrations), and a pair of tendons H67 and H68 halfway between the cylinder mid-height and springline, which were not equipped with the protective hardware. Three vertical tendons were also instrumented: V46, which had the shortest radius in the dome, V37, which had the largest radius in the dome, and V85, which was also deflected around the E/H penetration.

The typical arrangement of the strain gages at a measurement location is shown in Figure 3.15. This figure also illustrates the positioning of the load blocks on the tendons to protect the gages from damage. The specific arrangement of gages at a given measurement location is described in Section 3.3.

3.2.7 Visual Observations

Both video and still photography was employed inside and outside of the PCCV model at locations where large deformation or other signs of damage, such as liner tearing, concrete cracking, or crushing might be expected to occur. These observations were intended to supplement the discrete measurements obtained by the other transducers. Visually monitoring the model with live video during the test was also a safety requirement. It was important to observe various sections of the model visually to properly conduct the high-pressure test.

The video cameras were placed outside the model to monitor the overall behavior, while some were placed close to the model to monitor specific areas, such as the E/H, A/L, and wall-basemat junction. Interior video cameras monitored the liner behavior. A sketch of the video and camera layout is shown in Figure 3.16 In addition, several still cameras were placed near the outside of the model to record snap-shots at each pressure step during the test. Based on the pseudostatic nature of the pressure tests and the unlikelihood of a catastrophic rupture, the video cameras were of normal speed (30 frames/sec) and there were no requirements to use high-speed video cameras during testing.

3.2.8 Acoustic Monitoring

Acoustic monitoring was not specified in the basic instrumentation plan, but incorporated into the final instrumentation plan to allow monitoring of the entire structure and identify damage that could occur at locations not monitored via other methods. The specific goals of the acoustic monitoring system were to:

1. detect tendon wire breaks,
2. detect rebar breaks,
3. detect concrete cracking and crushing, and
4. detect liner tearing and leakage.

Acoustic monitoring of the PCCV model during both the prestressing and low and high pressure tests was performed by Pure Technologies Inc. of Calgary, Canada under a turn-key contract. Pure Technologies developed the SoundPrint® acoustic monitoring system[29] and has extensive experience in acoustically monitoring structures, especially prestressed concrete structures, such as parking garages and bridges. This system was run independently of the main data acquisition system (DAS). The system consisted of acoustic sensors, essentially piezo-electric accelerometers, bonded to the structure and connected to a separate DAS. One unique feature of this system is the capability to perform real-time data processing and analysis to identify event types and locations. Thirty-two sensors were glued to the external surface of the model and 16 sensors were placed inside the model. The sensors are shown in Figure 3.17.

[29]Pure Technologies Ltd., 705 11th Avenue SW, Calgary, AB, Canada T2R 0E3 (http://www.soundprint.com/)

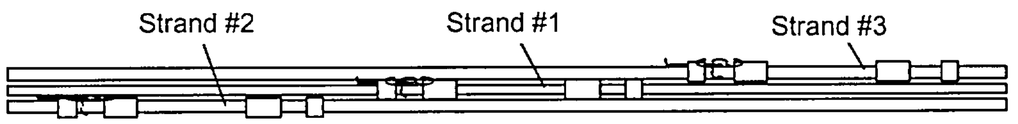

(a) Tendon Instrumentation Layout (Typical)

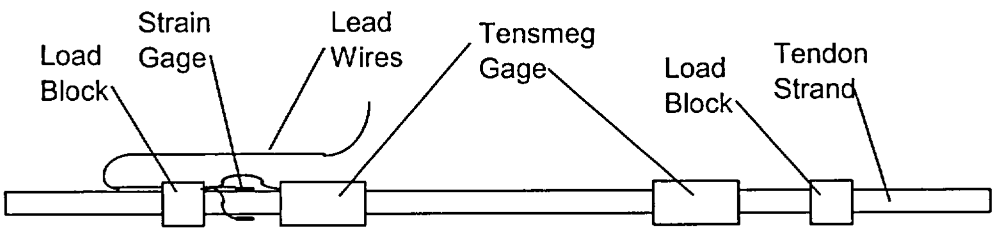

(b) Strand Instrumentation Layout (Typical)

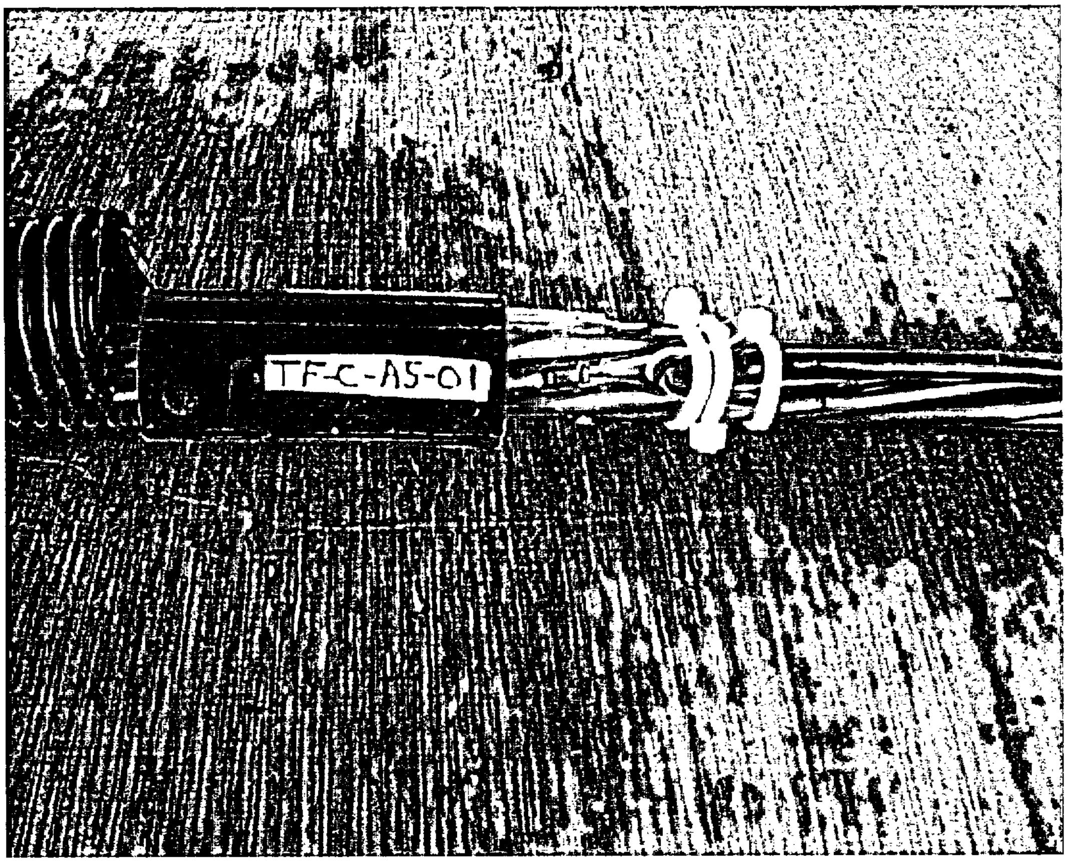

(c) Tensmeg End Block and Wire Strain Gage

Figure 3.15 Tendon Strain Instrumentation Arrangement

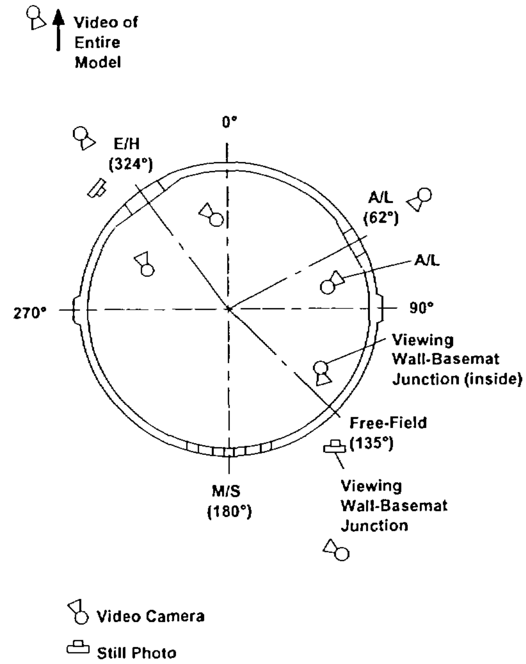

Figure 3.16 Video and Camera Layout

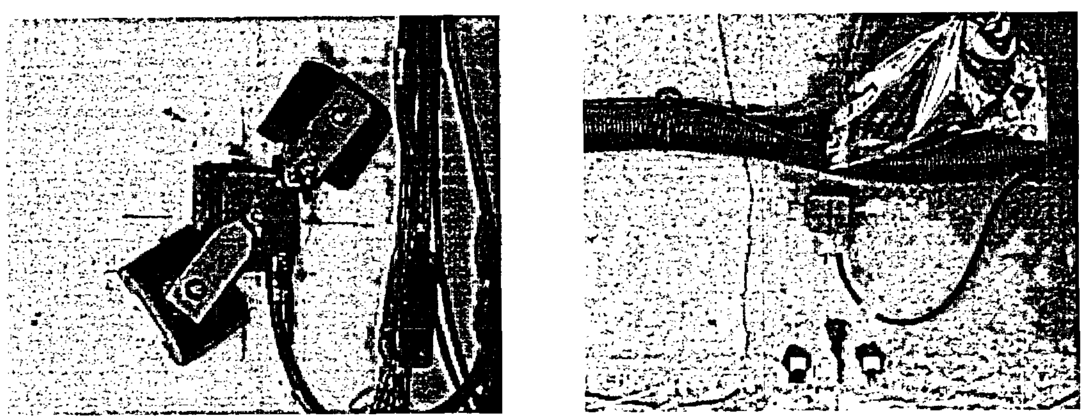

Figure 3.17 Interior and Exterior Acoustic Sensor (clamps during installation only)

3.3 Instrument Installation

3.3.1 Instrument Locations

The final list of gages installed on the PCCV model is provided in Appendix D. This list identifies every gage installed on the model and any gages that were damaged during construction or testing. The format of the tables in Appendix D is given in Table 3.14.

Because of the large number of transducers and the DAS requirement to have a unique address or label, a Gage ID scheme was developed to provide basic information about the type of gage and its orientation and location while providing each gage with a unique identity for subsequent reference and data management. A set of gage type abbreviations were developed to form the first part of the name. These abbreviations are listed in Table 3.15.

Table 3.14 Instrumentation List Format

Column	Description
1	Gage ID (name) AAA-B-CC-DD AAA Type abbreviation (Table 3.15) B Orientation (R-radial, M-meridional, C-circumferential CC General location designator (azimuth *letter*/ elevation *number* from Figure 3.1) DD Sequential numbering (for each similar type and location)
2	Azimuth
3	Vertical Elevation
4	Radial Distance (from centerline of containment)
5	Transducer Designation (for procurement)
6	Location Drawing No. (Appendix E)
7	Details Drawing No.
8	Basic Mark Number (construction designation)
9	Modified Mark Number (instrumented designation)
10	Comments
11	Calibration (pre- and post-calibration status)

Table 3.15 Gage Type Nomenclature

Type Abbreviation	Description
RS	rebar strain, single element gage
GB	gage bar, multiple elements
CE	concrete strain, embedded fiber optic gage
LSI	liner strain, single element gage, inside surface
LRI	liner strain, rosette gage, inside surface
LSO	liner strain, single element gage, outside surface
LRO	liner strain, rosette gage, outside surface
LSA	liner strain, single gage, on anchor
LRA	liner strain, rosette gage, on anchor
LSS	liner strain, single gage, on stiffener
LRS	liner strain, rosette gage, on stiffener
DL	linear variable differential transformer displacement transducer
DT	Temposonics linear displacement transducer
CP	cable potentiometer displacement transducer
IT	inclinometer displacement transducer
TC	thermocouple, embedded in concrete basemat, type K
TW	thermocouple, embedded in cylinder wall, type T
TI	thermocouple, inside liner surface, type T
RT	resistance temperature detector
PG	pressure gauge
TL	tendon load cells
TT	tendon strain, Tensmeg
TF	tendon strain, foil

The location designation is based on the cardinal azimuth and elevation lines shown in Figure 3.1. For example, gage DT-R-Z6-01 is easily recognized as a Temposonics displacement transducer (DT) measuring the radial displacement (R) at Azimuth 135 degrees (Z), Elevation 6200 (6). Since there is only one transducer at this location, it is by default number one (01). These gage IDs are used in reporting and discussing the test data in Chapter 5.

The nominal location of the gages are shown in Figures 3.18 to 3.23. A set of detailed instrumentation drawings is provided in Appendix E. The total number of each type of instrument installed on the PCCV Model is shown in Table 3.16.

Table 3.16 PCCV Instrument Summary

Instrument Type		Number of Gages
Strain	Liner	559
	Rebar	391
	Tendons (Tensmeg)	37
	Tendons (wire)	156
	Concrete	94
Displacements		101
Load Cells (1/3 of Tendons)		68
Temperature and Pressure		100
Acoustic		54
Total		**1560**

3.3.2 Quality Assurance and Control

The PCCV Instrumentation QA Task Plan [33] describes and documents the SNL process for installing instrumentation on the PCCV model. The Task Plan addresses transducer calibration, installation, and wiring to the terminal boards, instrument check-out procedures, and compliance records. In addition, personnel roles, responsibilities, and training appropriate to accomplish the PCCV instrumentation installation task are described. As-installed measurements were made and the exact location of each instrument was recorded as a permanent quality record for the experiment. The tasks, objectives, and responsible project team member described in the Task Plan are summarized in Table 3.17.

Table 3.17 PCCV Instrumentation Procedures Summary

Tasks	Objectives	Responsible Member
1. Provide Instrumentation Drawings for: Transducer Location Deliver As-Built Drawings	Assure proper sensor location to match predicted deformation analysis Assure correct channel assignment to terminal board Assure integrity of instrumentation installation	Instrumentation Engineer
2. Instrument the PCCV Model	Monitor PCCV deformation behavior	Instrumentation Leader
3. Develop/Issue Environmental Safety and Health (ES&H) Operating Procedure	Control hazardous material/processes	Test Leader
4. Install Terminal Boards/Sensor Wiring	Maintain channel assignments	Instrumentation Leader
5. Check Instrument Functionality	Assure sensor integrity	Instrumentation Leader
6. Obtain Required Transducer Calibrations	Assure data accuracy/acceptance	Instrumentation Engineer
7. Complete All Documentation	Assure integrity/traceability of acquired data	Instrumentation Engineer

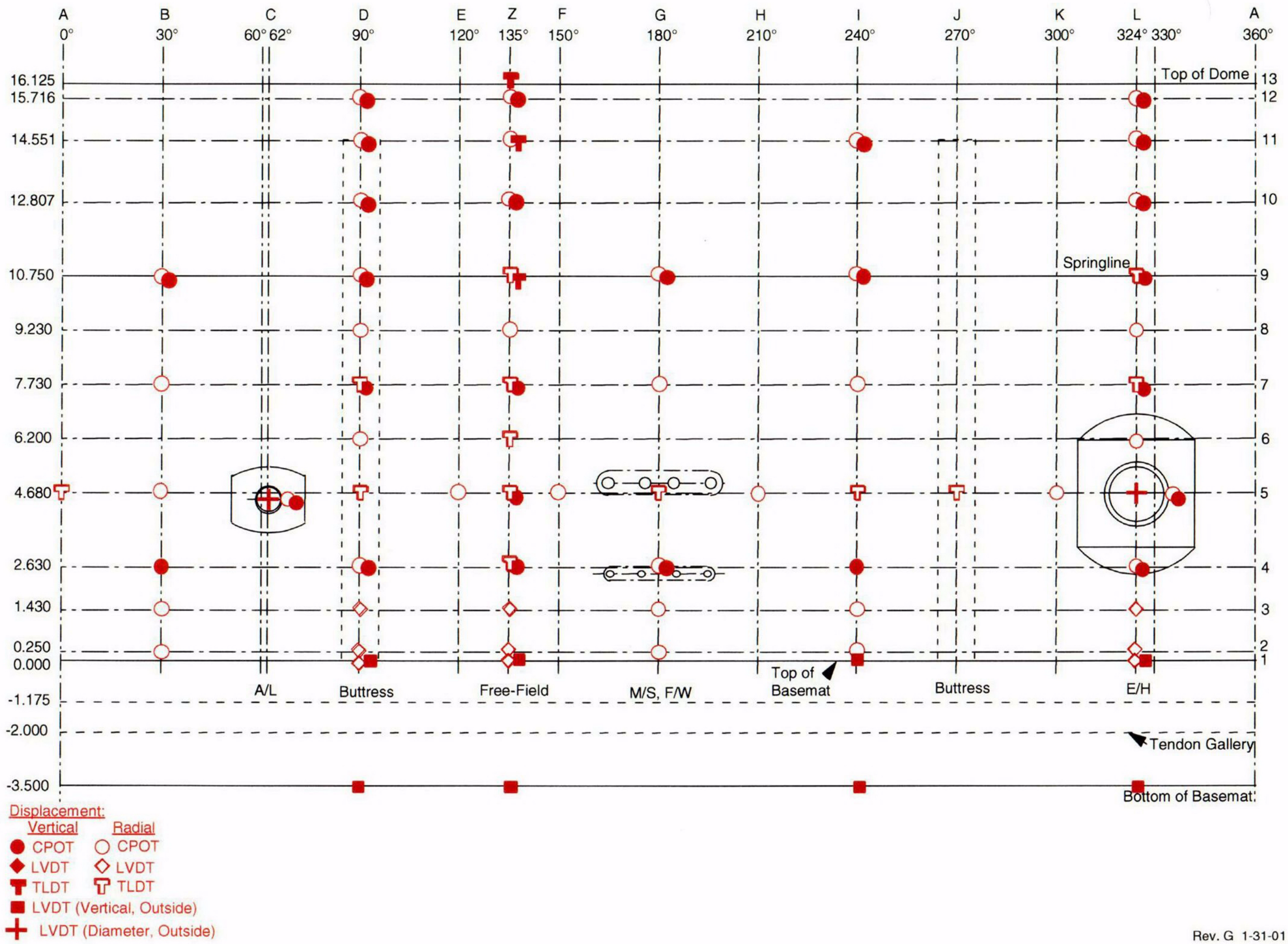

Figure 3.18. Displacement Instrumentation Locations

C11

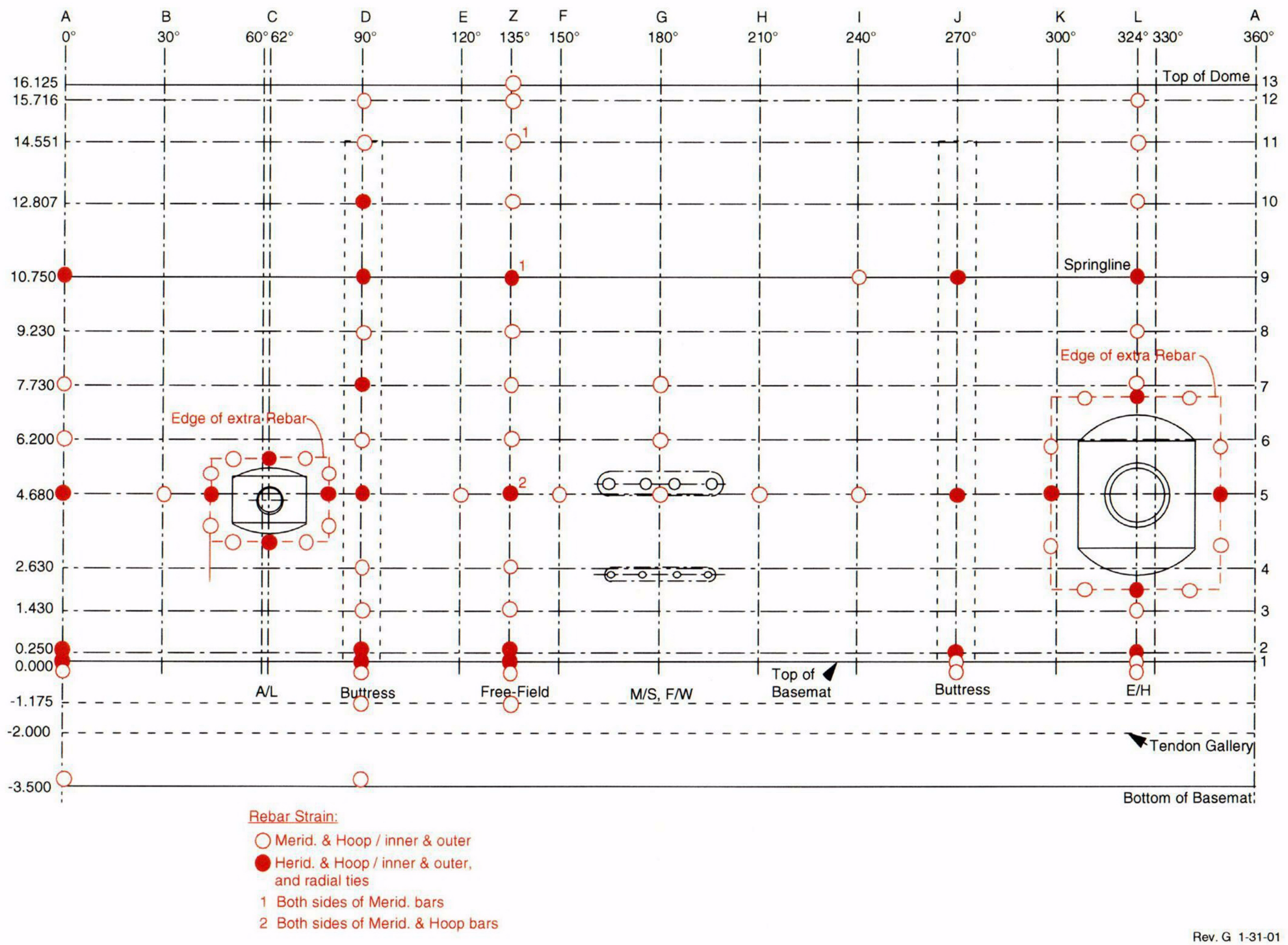

Figure 3.19. Rebar Instrumentation Locations

C12

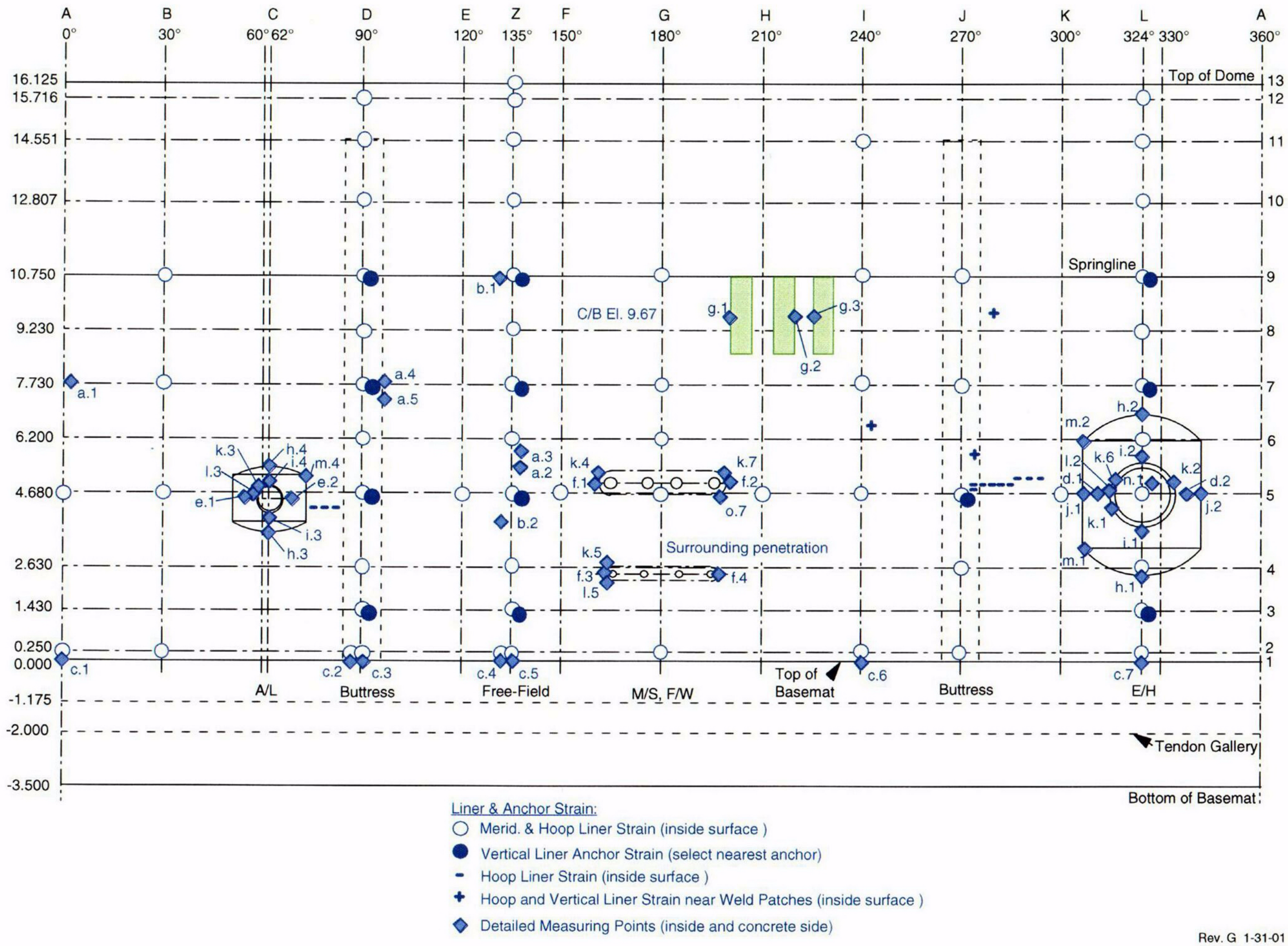

Figure 3.20. Liner and Liner Anchor Instrumentation Locations

C13

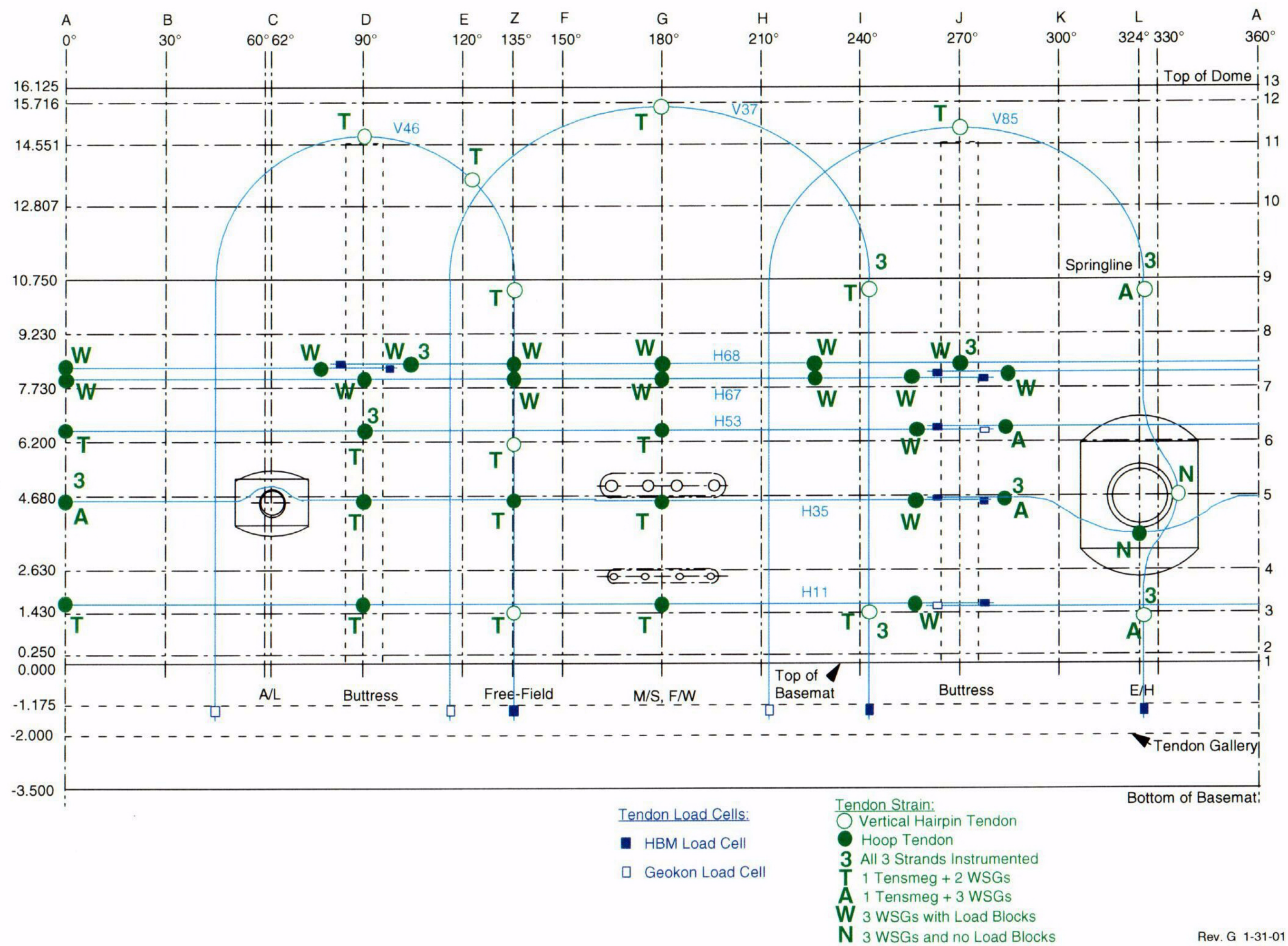

Figure 3.21. Tendon Instrumentation Locations

C14

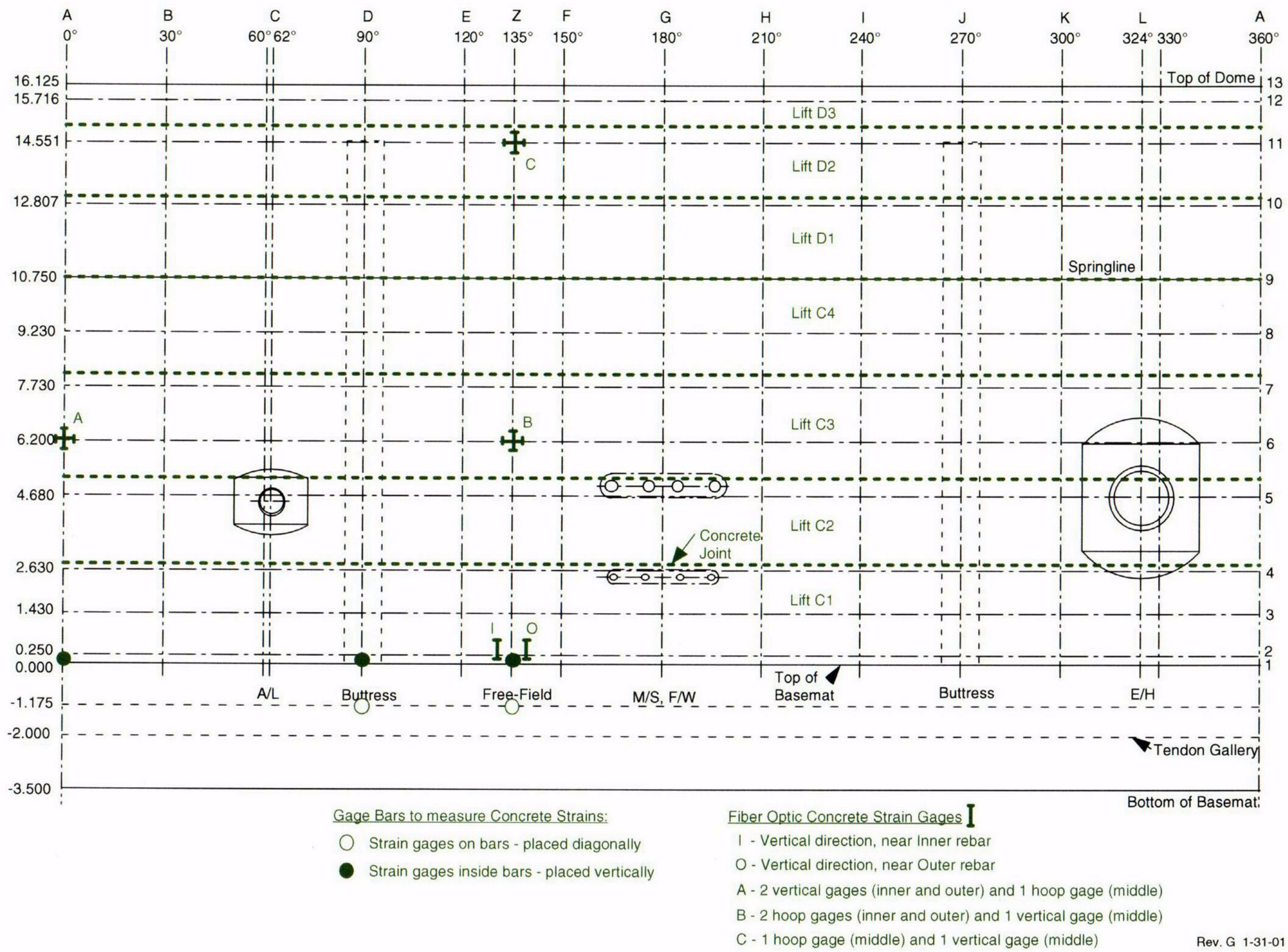

Figure 3.22. Concrete Instrumentation Locations

C15

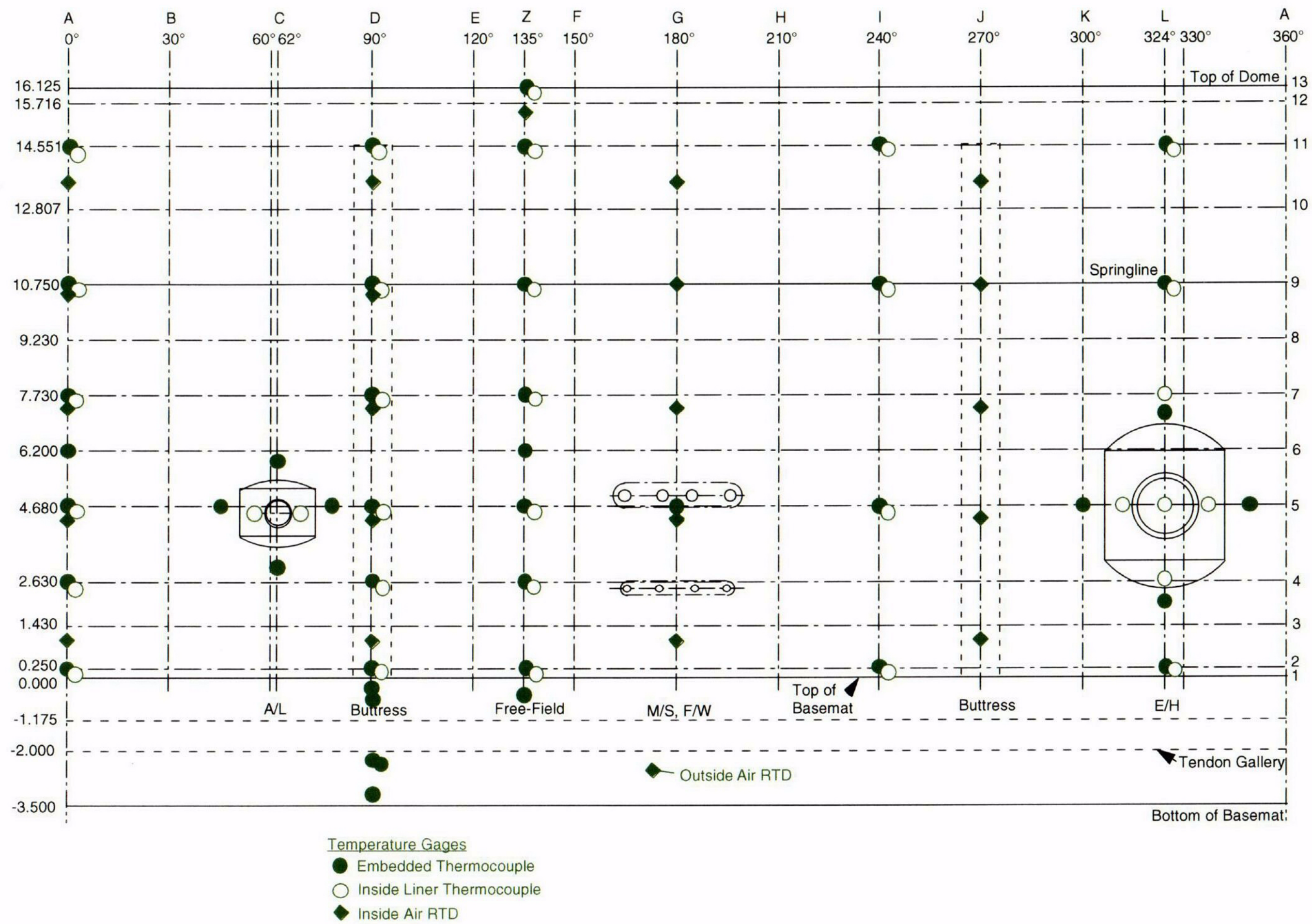

Rev. G 1-31-01

Figure 3.23. Temperature Instrumentation Locations

C16

4. DATA ACQUISITION

The DAS comprises integrated hardware and software components to acquire, interpret, record, display, correct, and archive data from the suite of transducers installed on the PCCV model. The basic data acquisition requirements were specified by NUPEC and, after discussions with the NRC and SNL, a detailed DAS Plan [29] was developed and approved. The DAS Plan specified the objectives, performance requirements, and basic architecture of the DAS. A DAS QA Task Plan [30] specified and documented the detailed procedures that guaranteed the DAS satisfied the operational specifications. The key elements of the DAS Plan and QA Task Plan are summarized in this chapter.

4.1 Objectives

The primary program objectives the DAS must satisfy included the following.

1. The DAS must be fully functional, verified, and approved at the time of model prestressing. This means that the output signal from all operational sensors can be read, that the source and location of all output signals was known with certainty, and that the output signal can be converted to accurate engineering measurement units within the tolerances specified in the Instrumentation Plan.
2. During prestressing operation, the DAS must:
   a. be capable of monitoring all instruments, including all strain gages, displacement transducers, and T/Cs, except those gages in the uncompleted portion of the basemat,
   b. provide a real-time display of selected sensor output (especially load cells and tendon gages) in engineering units to monitor prestressing operations, and
   c. retain a record of final data after prestressing as initial conditions for subsequent readings.
3. The DAS must be capable of periodic data acquisition between prestressing and testing phases.
4. During low and high pressure testing, the DAS must be capable of scanning all active sensor data and storing dynamic data and data of record (DoR) data. The DAS must be capable of providing real-time displays of any sensor output (uncorrected) in engineering units and facilitating comparison with pretest predictions to guide the conduct of the test. The DAS may also be integrated with other systems controlling and monitoring the test, such as the pressurization system, acoustic monitoring system, visual monitoring system (video and still photography), lighting systems, and audio systems.
5. The DAS must record the data in a manner that facilitates timely and accurate correction of the raw data after the test is complete.

4.2 Hardware Description

The PCCV hardware configuration for both the instrumentation system and the DAS is shown in Figure 4.1. A more detailed schematic is provided in Appendix F. This schematic not only graphically "maps" all component classifications important to the data acquisition effort, but also provides details on where documentation pertaining to each component of the system may be found. This documentation includes installation, wiring, and quality control information. For the PCCV tests, there were approximately 1500 instruments mounted on the model. Each of these gages had lead wires extending from the gage itself to a terminal board. From the terminal board, the gage's signal was carried to a specific channel on a card located in a mainframe. The channel location defined the General Purpose Interface Bus (GPIB) address for that gage. This address was used for acquisition, tracking, and recording of the gage's data. There were 13 mainframes located in a DAS trailer. From the mainframes, a fiber optic cable carried the signals from all of the gages to the data acquisition computer located in the control room (9950). The hardware from the gages to the front side of the terminal boards made up the instrumentation system. The remaining hardware (shown on the right of Figure 4.1) made up the DAS. The data acquisition computers stored the data on redundant media and also made the data available to the display computer. The display computer allowed test personnel to track the behavior of the gages in real time. The stored data were protected and used for posttest data analysis.

The primary hardware component involved in the data gathering was the Hewlett Packard 75000 Series B system, which included the HP1302A VXI Mainframe and its associated 5 ½ digit multimeter (HP1326B). Analog signals from the instruments were sent to plug-in cards installed into the mainframe housing. An analog bus jumper connected the signals to the digital multimeter where the analog-to-digital (A-D) conversion occurred.

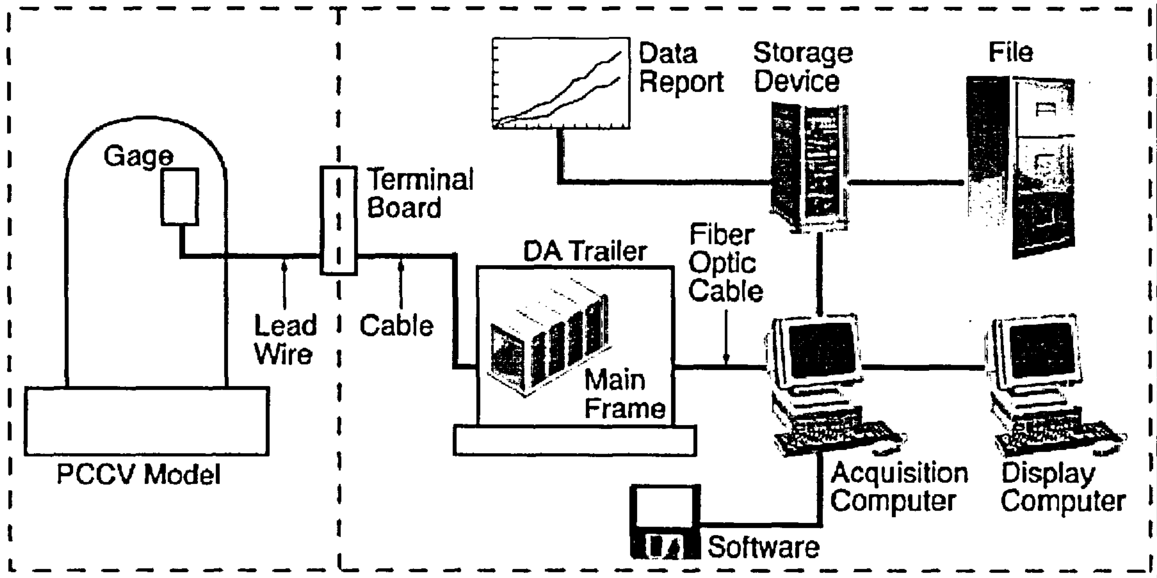

Figure 4.1 PCCV/DAS Hardware Configuration

Data were then stored in input/output (I/O) buffers dedicated to the multimeter, or in the RAM of the mainframe, for eventual transfer over a standard GPIB cable to the data acquisition computer. The mainframe was able to manage the channel switching and data transfer operations as well as respond to controller commands over the GPIB. In addition, the status of the data transfer operations was monitored.

The digital multimeter can be used as a stand-alone device through the VXI bus. However, for this test, it was connected through the analog bus jumper to a series of relay multiplexers. It measured and converted five types of input signals: DC voltage, RMS AC voltage, 2-wire resistance, 4-wire resistance, and electrically-based temperature sensing devices (T/Cs and RTDs).

The characteristics of the multiplexer cards varied based on the type of signal they carried. This experiment used three types of cards: 350 Ω and 120 Ω strain gage cards (Wheatstone quarter-bridge circuits, 8-channel capacity) and a 16-channel voltage card (i.e., non-bridged voltage producing device). To service the different types of instruments installed on the PCCV model, 137 350 Ω cards, 26 120 Ω cards, and 23 voltage cards were used. Two types of VXI mainframes were used. One accepted seven multiplexer cards, and the other type accepted 16 cards. There were no basic differences between these mainframes other than their card capacities. In order to accommodate the cards needed, 13 mainframes were utilized.

Strain gage multiplexer cards are designed to measure the voltage produced in a bridge circuit due to resistance changes in a strain gage. Consequently, these circuits require excitation voltage, which is provided by external power supplies. The strain gage multiplexer cards provide excitation and scale the output of the strain gages. The 1326B digital multimeter measures the voltage and converts the reading to strain units. Thus, the raw data received by the data acquisition computer is in strain units.

The data are held in the VXI bus buffer until the GPIB controller-in-charge (the data acquisition computers) commands a transfer. The mainframes were located in a data analysis trailer situated near the mudmat of the PCCV model and an opening to the Tendon Gallery tunnel, as well as the small penetrations that would feed all internal instrumentation cables (180 degrees). The location, near 180 degrees, was chosen as it allowed cable lengths to be as short as reasonable, thus preserving signal integrity. The data acquisition computers were located remotely at the 9950 site. Adapting the standard GPIB cable to a fiber-optic bundle minimized digital signal loss and degradation. This cable could be extended over long distances and eventually readapted to standard GPIB format for installation into GPIB cards on the DAS computer chassis.

From the perspective of the data acquisition computers, each mainframe/multimeter pair represents a single GPIB instrument. One GPIB card is capable of controlling seven GPIB instruments. For the PCCV experiment, two GPIB interface cards and two data acquisition computers were used, as more than eight GPIB instruments were needed.

The data acquisition software used for the PCCV test was designed as a general instrumentation monitoring system, with a single GPIB card and controlled by a single data acquisition computer. This implies that any computer running the acquisition software can scan any instrumentation suite with an accurate configuration file. Thus, each data acquisition computer scanned approximately half of the instruments on the model. Each data acquisition computer operated independently of the other. The display computer read data from both computers, one at a time.

The final major piece of hardware involved in the DAS was a display computer. This computer read the experimental data from the data acquisition computers upon demand and presented it in optional formats (plot form, array form, comparison form). The display computer provided the test conductor information to help make real-time decisions during the test.

The display computer had additional monitors allowing observers (located outside the test control room) to view the display.

Additionally, the DAS included two separate data storage devices (one connected to each data acquisition computer). These stored redundant copies of the data files to ensure data protection.

4.2.1 Hardware Specifications

Manuals and hardware specifications for each DAS component were included in the DAS Plan. All of the hardware chosen for the PCCV data acquisition effort was expected to meet requirements for the overall system operation.

The total time required for the actual acquisition of data from the VXI mainframes was governed by two primary factors: the switching and settling time of the on-board multiplexer and the aperture setting for each sampled channel. This statement assumes very short times for I/O from the controller to the multimeters. By far, the largest of these components is the aperture setting for a static DAS with unfiltered data signals. (The settling time for the mechanical relays in the PCCV's VXI mainframes is on the order of µseconds.) For the PCCV tests, the aperture time was set to 16.5 ms, which ensures electrical filtering of common 60 Hz noise sources. Decreasing the aperture time allows for more rapid data acquisition, but significantly increases signal noise, particularly for unfiltered data. Signal degradation is further complicated by the moderate to long cable lengths, which are necessary in a test of this sort. Therefore, the default 16.5 ms aperture for each channel was used. This setting results in a maximum possible sampling frequency of 60 Hz. This value is decreased incrementally by the relay operation and I/O to the controller.

Scan time is defined as including: 1) the time required for the GPIB-based READ command to reach the mainframe from the control computer; 2) the time for the command module in the appropriate mainframes to receive the request for data and set the multiplexer for operation; 3) the time for multiplexer switching and the multimeter aperture delay for each configured channel; and 4) the time required to transfer all the data from the controller buffer back to the DAS computers. Thus, the scan time was larger than the product of the sampling frequency multiplied by the number of gages scanned, because of the time required to transfer the large controller buffer contents via the GPIB. Scan times were slightly different for the two DAS computers, with PCCV1 requiring approximately 50 seconds and PCCV2 requiring approximately 70 seconds.

Cycle time includes the scan time plus the time to store the data on the requested storage devices. The plan was to immediately generate two copies of the data, one on an internal hard disk and one on a removable disk. The storage required the largest amount of time by far. To shorten this as much as possible, the DAS software was written to facilitate this operation (i.e., separation of data display and data acquisition computers, up-front creation and preparation of data files, use of binary high-speed I/O data file formats rather than ASCII, termination of all unnecessary processing during data storage, etc.) and the data storage hardware was chosen to minimize disk seek time, transfer rate, and access time. Cycle time was approximately 120 seconds during system checkout, a setting that was used for the remainder of the testing.

4.2.2 Gage Wiring

The criteria to determine from which opening each gage's wires left the model was based solely on the route requiring the shortest length of wire. Thus, in the majority of cases, each gage's wires exited the model from the opening closest to the gage itself. Once the wires exited the model, they went to one of several terminal boards. The wires leaving the terminal boards entered the DAS trailer and connected to the data acquisition mainframe cards.

As stated, lead wires were as short as reasonable while still enabling the needed connections. All gage/wire combinations were reviewed, and corrections to gage factors were made posttest, as per Appendix G.

4.3 Software Description

The software used to control the DAS and display the acquired data during the experiment was developed using National Instrument's Labview™ software package.[30] The basic building block of Labview™ is called the virtual instrument (VI). A VI is similar to a subprogram or a module of code.

The data acquisition program is made up of VI trees, each representing a code module with a specific purpose. Graphics objects (such as knobs, dials, switches, etc.) visible on the screen during the data acquisition process can adjust instrument and data acquisition control parameters. Users may manipulate these objects with mouse commands.

The PCCV/DAS software is separated into three major groups: the primary program group used to gather and store the data during the experiment, a secondary program group to display the data during the experiment, and a utility group of programs used either before or after the test. These utility routines were designed to accomplish several tasks:

1. Form the configuration file and channel set-up,
2. Run DAS diagnostics and self-testing,
3. Perform channel and instrument integrity evaluations,
4. Evaluate noise, and
5. Present posttest data and storage to customer-defined formats.

4.3.1 Software Structure

The software was separated into two main groups of programs and a group of utility routines. (The term "group" refers to a series of linked subprograms existing as separate files.)

The data acquisition software (the primary group) was used to both gather and store the data during each of the tests (e.g., pre-stressing, SIT, final). This program group required input in the form of configuration files and was primarily responsible for data scanning, immediate redundant data storage, and fault limit detection and announcement.

The data display software (the secondary group) used the data gathered by the primary group. The display software did not access the stored data files on the acquisition computer, but rather global variables that were shared by the acquisition and display computers. In Labview™, global variables are used to easily access a set of values from any active VI. This allows values to be shared between Labview™ programs without requiring any other connections between the programs. This software group was responsible for displaying the experimental data on demand in the form requested by the user. Several different display modes were developed to meet the need of the PCCV experiments. These included a stability review, strain and displacement distributions, and a primary graphical user interface.

The utility group provided the necessary input channel configuration information to the main group software. There were many other secondary tasks the utility group performed as needs arose.

[30] National Instruments Corporation, Austin, TX (http://amp.ni.com/niwc/labview/what.jsp?node=1381)

4.3.2 Software Module Specifics

The three PCCV DAS software groups were divided into seven main modules. Modules 1, 2, and 4a composed the main acquisition group. Module 4b was the main display software group. Modules 3, 5, 6, and 7 composed the Utility Group. Figure 4.2 shows a schematic of the modules and how they were grouped.

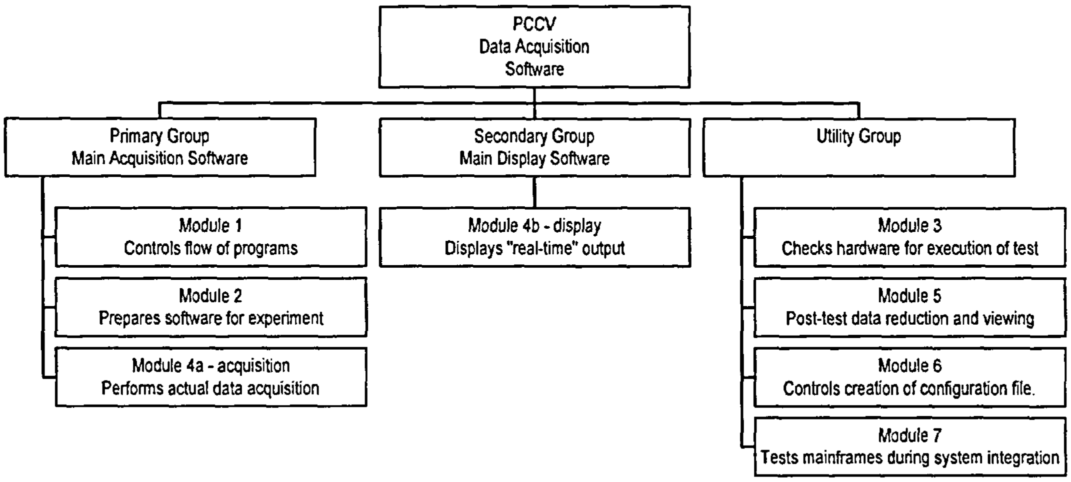

Figure 4.2. DAS Software Tree

The modules are listed below with a brief description of each.

Module 1: Controls flow of program through Modules 2, 3, and 4a.

Module 2: Prepares the software package to conduct a test including configuration information input to the acquisition software.

Module 3: Prepares the hardware for executing the test. Includes checking the GPIB bus for the configured listeners and card layouts, and diagnosing the status (electronically) of the mainframes, digital multimeters (DMMs), and any other hardware.

Module 4a: Performs the actual data acquisition, including readings during non-steady-state operation as well as the steady-state (DOR) scans. Includes writing raw data to disk as soon as possible. Provides continuous pressure information as well.

Module 4b: Allows the user to select and display the desired real-time output.

Module 5: Provides posttest data reduction and viewing.

Module 6: Simplifies creating the configuration file and putting configuration information into the configuration file to minimize errors.

Module 7: Facilitates mainframe testing during system integration. Easily configurable to rapidly indicate status of connected instruments.

4.3.3 Input/Output File Structure

4.3.3.1 File Structure Description

The two basic sets of I/O files necessary in the DAS software package were:

1. A configuration that file that provided the necessary input data to the DAS software, and
2. Data files into which the recorded data were placed.

Data File Structure

The design of the output data file structure allowed standard plotting software to select segments of data for plotting.

The output data file structure:

- Provided users with a clear map between the columns of numbers in a data file and the location and type of instrument originating the data,

- Used nomenclature for naming the files that provided the nature of the data contained and the types of instruments represented in the files,

- Generated an easily accessible set of files for archival purposes, anticipating future inquiries for analysis and presentation, and

- Facilitated rapid data correction and post-processing.

Two levels of folders below a "main" data folder were required to properly organize the data files. These levels are shown in Figure 4.3.

All data from this experiment was stored as *raw* data signals (i.e., the output of the A-D conversion step in the DAS process). Posttest data reduction converted the raw data into standard engineering units.

Table 4-1 lists the raw and reduced data units for the instruments in the PCCV experiment.

Note that the term "raw" in this table indicates the nature of the data signal after hardwired, "firmware" processing, which occurred automatically within the digital multimeter of the HP VXI Mainframe.

The data from some instruments was used to compensate or correct the raw data from other instruments. Details on this practice are found in Appendix G. Figure 4-4 illustrates the basic data flow diagram for the PCCV project.

4.4 Miscellaneous DAS Issues

4.4.1 Loss of Power

During the verification and validation testing, the results of losing electrical power to the DAS computers were determined. This determination involved actually shutting down electrical power to the computers while the DAS software was running. Several iterations of this were done, each at a different point in the acquisition process. It was necessary that data be maintained in the event of a power outage.

4.4.2 Integration of DAS with Other Systems

In general, the DAS was independent of all other systems involved in the PCCV experiments. There were two exceptions: still camera operation and the activation of redundant interior model lights. It was possible from the main data acquisition screen to operate the still cameras positioned throughout the PCCV model. Similarly, the interior model lighting was controlled from the main data acquisition screen. It was possible to turn the redundant lights on or off from the DAS computer.

The Soundprint acoustic monitoring system and the SOFO fiber-optic gages were equipped with their own independent DASs, also located in the data acquisition trailer. The only interface between these systems and the main DAS was manual synchronization of clock time. This provided the correlation between gage output and pressure subsequently used to analyze the test data.

Table 4.1. Description of Raw and Reduced Data for the PCCV Test

Instrument Type	Raw Data Units	Reduced Data Units
Strain gage (includes Tensmegs gages)	strain or microstrain (depending on gage factor format)	Strain
Cable-type displacement transducer	DC volts	Displacement (mm)
LVDT	DC volts	Displacement (mm)
Temposonic	DC volts	Displacement (mm)
Inclinometer-type displacement transducer	DC volts	Tilt angle (degrees)
Thermocouple	temperature (°C)	Same as raw
RTD	temperature (°C)	Same as raw
Pressure gage	DC volts	Pressure (MPa)
Load cells	DC volts	Load (Newtons)
Power supplies	DC volts	Same as raw (data used to reduce instrument voltages to CPOT distances)

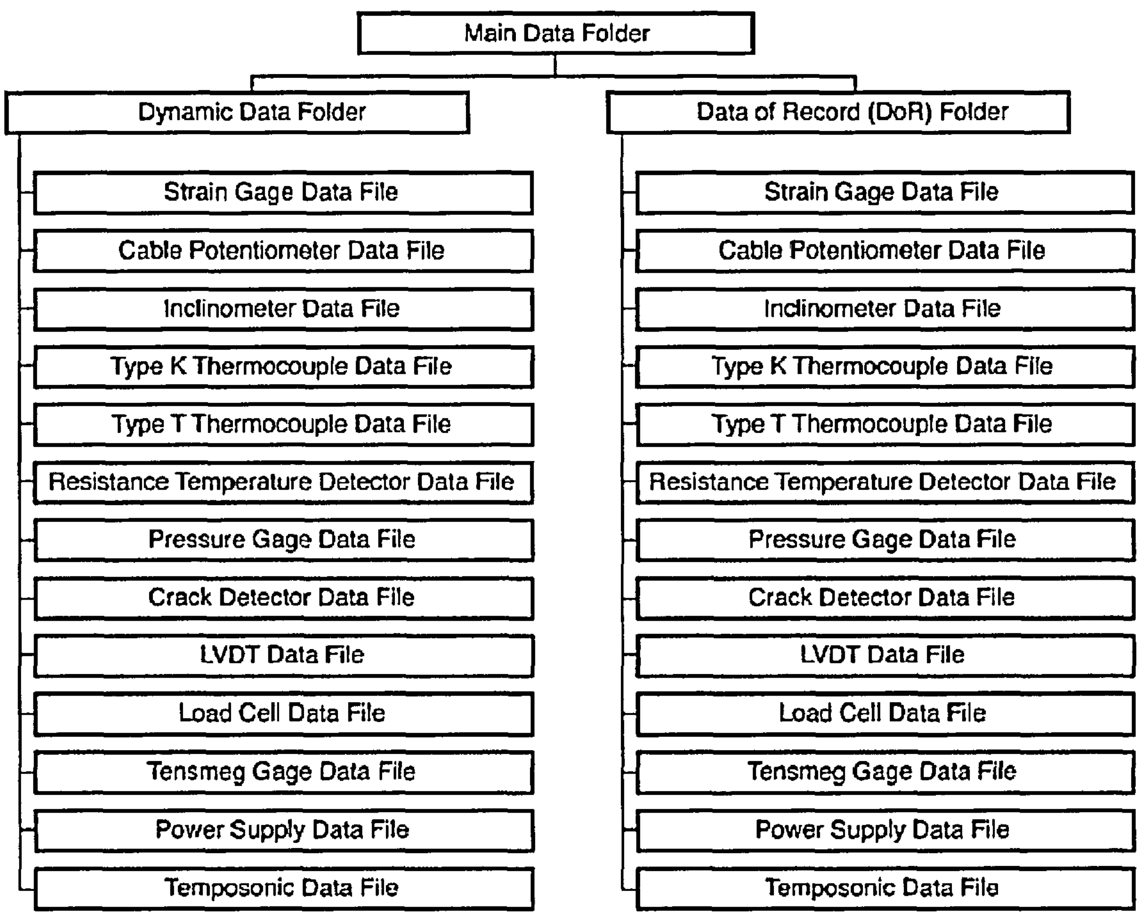

Figure 4.3 Top-Down Data File Folder Structure

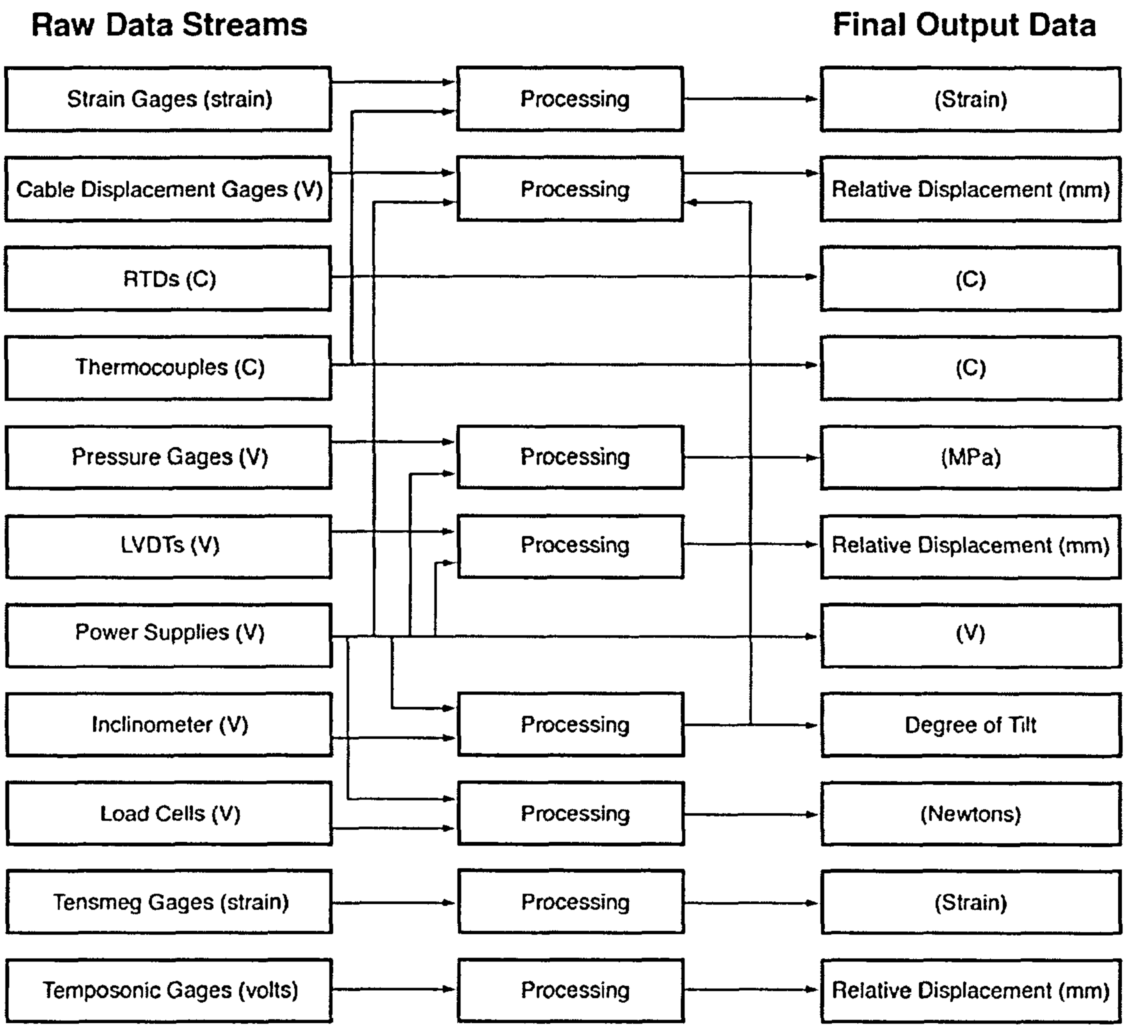

Figure 4.4 Basic PCCV Data Flow Diagram